CONCEPTUAL CONSIDERATIONS OF THE YUCCA MOUNTAIN GROUNDWATER SYSTEM WITH SPECIAL EMPHASIS ON THE ADEQUACY OF THIS SYSTEM TO ACCOMMODATE A HIGH-LEVEL NUCLEAR WASTE REPOSITORY

PREPARED BY:

JERRY S. SZYMANSKI
PHYSICAL SCIENTIST
U.S. DEPARTMENT OF ENERGY
NEVADA OPERATIONS OFFICE
YUCCA MOUNTAIN PROJECT OFFICE

LAS VEGAS, NEVADA
JULY 26, 1989

8908030304

~~8908030303~~ part 3

Appendix A
REFERENCES

REFERENCES

Aggarwal, Y. P., L. R. Sykes, J. Armbruster, and M. L. Sbar, 1973. **Premonitory Changes in Seismic Velocities and Prediction of Earthquakes**, Nature 241.

Allan, D. W., W. B. Thompson, and N. O. Weiss, 1967. "Convection in the Earth's Mantle," **Mantles of the Earth and Terrestrial Planets**, Interscience Publishers, S. K. Runcorn, (ed).

Allmendinger, R. W., T. A. Hauge, E. C. Hauser, C. J. Potter, S. L. Klemperer, K. D. Nelson, P. Kneupfer, and J. Oliver, 1987. **Overview of the COCORP 40°N Transect, Western United States: The Fabric of an Orogenic Belt**, Geological Society of America Bulletin, Vol. 98.

Anderson, L. A., 1981. **Rock Property Analysis of Core Samples from the Yucca Mountain UE-25a-1 Borehole, Nevada Test Site, Nevada**, USGS Open-file Report 81-1338, the United States Geological Survey, Denver, CO.

Anderson, R. N., 1980. "1980 Update of Heat Flow in the East and Southeast Asian Seas," **The Tectonic and Geologic Evolution of Southeast Asian Seas and Islands**, Geophysical Monograph 23, American Geophysical Union, D. E. Hayes, (ed).

Artyushkov, E. V., and Y. A. Mescherikov, 1969. "Recent Movements of the Earth's Crust and Isostatic Compensation," **The Earth's Crust and Upper Mantle**, Geophysical Monograh 13, American Geophysical Union, Pembroke J. Hart, (ed).

Atwater, T., 1970. **Implications of Plate Tectonics for the Cenozoic Tectonic Evolution of Western North America**, Geological Society of America Bulletin, Vol. 81.

Baker, D. W., and N. L. Carter, 1972. "Seismic Velocity Anisotropy Calculated for Ultramafic Minerals and Aggregates," **Flow and Fracture of Rocks**, Geophysical Monograph 16, American Geophysical Union.

Barton, N., S. Bandis, and K. Bakhter, 1985. **Strength, Deformation and Conductivity Coupling of Rock Joints**, Int. J. Rock Mech. Min. Sci. and Geomech. Abstract 22,3.

Beck, J. L., 1972. **Convection in a Box of Porous Material Saturated with Fluid**, Phys. Fluids, 15.

Beloussov, V. V., 1969. "Continental Rifts," **The Earth's Crust and Upper Mantle**, Geophysical Monograph 13, Pembroke J. Hart, (ed).

Beloussov, V. V., 1969. "Interrelations Between the Earth's Crust and Upper Mantle," **The Earth's Crust and Upper Mantle**, Geophysical Monograph 13, American Geophysical Union, Pembroke J. Hart, (ed).

Bentley, C. B., 1984. **Geohydrologic Data for Test Well USW G-4, Yucca Mountain Area, Nye County, Nevada**, USGS-OFR-84-063, Open-file Report, the United States Geological Survey, Denver, CO.

Bentley, C. B., J. H. Robison, and R. W. Spengler, 1983. **Geohydrologic Data for Test Well USW H-5, Yucca Mountain Area, Nye County, Nevada**, USGS-OFR-83-853, Open-file Report, the United States Geological Survey, Denver CO.

Bernal, J. D., 1961. "Continental and Oceanic Differentation," **Nature 192**.

Berry, M. J., and L. Knopoff, 1967. **Structure of the Upper Mantle Under the Western Mediterranean**, J. Geophys. Res., 72(14).

Biot, M. A., 1941. **Theory of Elasticity and Consolidation for a Porous Isotropic Solid**, J. Appl. Phys., 12.

Biot, M. A., 1961. **Theory of Folding of Stratified Viscoelastic Media and its Implications in Tectonics and Orogenesis**, Geological Society of America Bulletin, 72.

Birch, F., 1969. "Density and Composition of the Upper Mantle: First Approximation as an Olivine Layer," **The Earth's Crust and Upper Mantle**, Geophysical Monograph 13, Pembroke J. Hart, (ed).

Birdwell, R. J., 1978. "The Rio Grande Rift and a Diapiric Mechanism for Continental Rifting," **Tectonics and Geophysics of Continental Rifts**, I. B. Ramberg and E. R. Neumann, (eds).

Birdwell, R. J., and C. Potzick, 1981. **Thermal Regimes, Mantle Diapirs and Crustal Stresses of Continental Rifts**, Tectonophysics, 73.

Blankenagel, R. K., and J. E. Weir, Jr., 1973. **Geohydrology of the Eastern Part of Pahute Mesa, Nevada Test Site, Nye County, Nevada**, USGS Professional Paper 712-B, the United States Geological Survey, Washington, DC.

Borg, I. Y., R. Stone, H. B. Levy, and L. D. Ramspott, 1976. **Information Pertinent to the Migration of Radionuclides in Ground Water at the Nevada Test Site**, UCRL-52-078, Lawrence Livermore National Laboratory, Livermore, CA.

Brace, W. F., 1972. "Pore Pressure in Geophysics," **Flow and Fracture of Rocks**, Geophysical Monograph 16, American Geophysical Union.

Bredehoeft, J. D., 1987. "Letter to M. D. Carr," USGS Water Resources Division, Western Region, the United Geological Survey, Menlo Park, CA.

Bucknam, R. C., and D. D. Dickey, 1971. "Ground Deformation Measurements," **Geologic and Hydrologic Effects of the Handley Event, Pahute Mesa, Nevada Test Site**, USGS-474-95, the United States Geological Survey, Denver, CO.

Caltagirone, J. P., 1975. **Thermoconvective Instabilities in a Horizontal Porous Layer**, J. Fluid Mech., 72.

Carr, W. J., 1984. **Regional Structural Setting of Yucca Mountain, Southwestern Nevada, and Late Cenozoic Rates of Tectonic Activity in Part of the Southwestern Basin, Nevada and California**, USGS-OFR-86-175, Open-file Report, the United States Geological Survey, Menlo Park, CA.

Carr, M. D., S. J. Waddell, G. S. Vick, J. M. Stock, S. A. Monsen, A. G. Harris, B. W. Cork, and F. M. Byers, Jr., 1986. **Geology of Drill Hole UE25p 1: A Test Hole into Pre-Tertiary Rocks near Yucca Mountain, Southern Nevada**, USGS-OFR-86-175, Open-file Report, the United States Geological Survey, Menlo Park, CA.

Carter, N. L., D. W. Baker, and R. P. George, 1972. "Seismic Anisotropy, Flow, and Constitution of the Upper Mantle," **Flow and Fracture of Rocks**, Geophysical Monograph 16, American Geophysical Union.

Cathles, L. M., 1975. **The Viscosity of the Earth's Mantle**, Princeton University Press, Princeton, NJ.

Christiansen, R. L., and E. H. McKee, 1978. **Late Cenozoic Volcanic and Tectonic Evolution of the Great Basin and Columbia Intermontane Regions**, Geological Society of America Memoir 152.

Clebsch, A. J., 1960. **Tritium Age of Ground Water at the Nevada Test Site, Nye County, Nevada**, USGS Professional Paper 424-C, the United States Geologic Survey, Denver, CO.

Corchary, G. S., and G. A. Dinwiddie, 1976. **Field Trip to Nevada Test Site**, the United States Geological Survey, Denver, CO.

Craig, R. W., R. L. Reed, and R. W. Spengler, 1983. **Geohydrologic Data for Test Well USW H-6 Yucca Mountain Area, Nye County, Nevada**, USGS-OFR-83-856, Open-file Report, the United States Geological Survey, Denver, CO.

Craig, R. W., and J. H. Robison, 1984. **Geohydrology of Rocks Penetrated by Test Well UE-25p#1, Yucca Mountain Area, Nye County, Nevada**, USGS-WRI-84-4248, Water Resources Investigations Report, the United States Geological Survey, Denver, CO.

Craig, R. W., and R. L. Reed, 1987. **Geohydrology of Rocks Penetrated by Test Well USW H-6, Yucca Mountain Area, Nye County, Nevada**, USGS Water Resources Investigations Report, the United States Geological Survey, Denver, CO.

Craig, R. W., and K. A. Johnson, 1984. **Geohydrologic Data for Test Well UE25p#1, Yucca Mountain Area, Nye County, Nevada**, USGS Open-file Report 84-450, the United States Geological Survey, Denver, CO.

Creveling, J. B., F. S. Shuri, K. M. Foster, and S. V. Mills, 1984. **In Situ Stress Measurements at the Spent Fuel Test, Climax Facility**, UCRL-15-628, Lawrence Livermore National Laboratory, Livermore, CA.

Crowe, B. M., and D. T. Vaniman, (Comps.), 1985. **Research and Development Related to the Nevada Nuclear Waste Storage Investigations, January 1 - March 31, 1984**, LA-10154-PR, Los Alamos National Laboratory, Los Alamos, NM.

Crowe, B. M., K. H. Wohletz, D. T. Vaniman, E. Gladney, and N. Bower, 1986. **Status of Volcanic Hazard Studies for the Nevada Nuclear Waste Storage Investigations**, LA-9325-MS, Vol. II, Los Alamos National Laboratory, Los Alamos, NM.

Czarnecki, J. B., 1987. **Should the Furnace Creek Ranch-Franklin Lake Playa Ground-Water Subbasin Simply Be the Franklin Lake Playa Ground-Water Subbasin?**, American Geophysical Union, Abstract.

Czarnecki, J. B., and R. K. Waddell, 1984. **Finite-element Simulation of Ground-Water Flow in the Vicinity of Yucca Mountain, Nevada-California**, USGS-WRI-84-4349, Water Resources Investigations Report, the United States Geological Survey, Denver, CO.

DeBoer, J., 1967. **Paleomagnetic Tectonic Study of Mesozoic Dike Swarm in the Appalachians**, Journ. Geophys. Res., Vol. 72, No. 8.

DOE (U. S. Department of Energy), 1984. **Draft Environmental Assessment, Yucca Mountain Site, Nevada Research and Development Area, Nevada**, DOE/RW-0012, Washington, DC.

DOE (U. S. Department of Energy), 1986. **Environmental Assessment, Yucca Mountain Site, Nevada Research and Development Area, Nevada**, DOE/RW-0073, Washington, DC.

DOE (U. S. Department of Energy), 1988. **Site Characterization Plan, Yucca Mountain Site, Nevada Research and Development Area, Nevada**, the U. S. Department of Energy, Office of Civilian Radioactive Waste Management, Washington, DC.

Donaldson, I. G., 1962. **Temperature Gradients in the Upper Layers of the Earth's Crust Due to Convective Water Flows**, J. Geophys. Res. 67.

Donath, F., 1982. **The Isolation of High-Level Nuclear Wastes in a Geologic Repository**, Radiation Research, 91.

Domenico, P. A., 1972. "Concepts and Models in Groundwater Hydrology," **Earth and Planetary Sciences**, McGraw-Hill International Series.

Dudley, W. W., L. E. Wollitz, Jr., D. A. Baldwin, and H. C. Claassen, 1971. **Geologic and Hydrologic Effects of the Handley Event, Pahute Mesa, Nevada Test Site (Effects on Wells and Aquifers)**, USGS-474-95, the United States Geological Survey, Denver, CO.

Eakin, T. E., S. L. Schoff, P. Cohen, 1963. **Regional Hydrology of a Part of Southern Nevada: A Reconnaissance**, USGS-TEI-833, Trace Elements Investigations Report, the United States Geological Survey, Denver, CO.

Eakin, T. E., 1963. **Ground-water Appraisal of Pahranagat and Pehroc Valleys, Lincoln and Nye Counties, Nevada**, Nevada Dept. Conserv. and Nat. Resources Ground-Water Resources-Reconn. Ser. Rept. 21.

Eaton, G. P., R. R. Wahl, H. J. Prostka, D. R. Mabey, and M. D. Kleinkopf, 1978. **Regional Gravity and Tectonic Pattern: Their Relationship to Late Cenozoic Epeirogeny and Lateral Spreading in the Western Cordillera**, Geological Society of America Memoir 152.

Elder, J. W., 1967. **Steady Free Convection in a Porous Medium Heated from Below**, J. Fluid Mech., 27.

Ellis, W. L., and J. E. Magner, 1982. **Determination of the In Situ State of Stress at the Spent Fuel Test, Climax Site, Climax Stock, Nevada Test Site**, USGS Open-file Report, the United States Geological Survey, Denver, CO.

Ellis, W. L., and J. E. Magner, 1980. **Compilation of Results of Three-Dimensional Stress Determinations Made in Rainier and Aqueduct Mesas, Nevada Test Site, Nevada**, USGS-OFR-80-1098, Open-file Report, the United States Geological Survey, Reston, VA.

Ellis, W. L., and J. R. Ege, 1976. **Determination of In-Situ Stress in U12g Tunnel, Rainier Mesa, Nevada Test Site, Nevada**, USGS-474-219, the United States Geological Survey, Denver, CO.

Fenske, P. R., and R. L. Charnell, 1971. **Infill of Nuclear Rubble Chimneys by Ground-Water**, Teledyne Isotopes, NVO-1229-171, Palo Alto, CA.

Frank, F. C., 1965. **On Dilatancy in Relation to Seismic Sources**, Rev. Geophys. 3,484-503.

Friedman, I., 1970. **Some Investigations of the Deposition of Travertine from Hot Springs-I. The Isotopic Composition of a Travertine-Depositing Spring**, Geochemical et. Cosmochimica Acta, Vol. 34.

Garber, M. S., 1963. **Large Rise and Following Decline of Water Level in Well 7, Area 3, Nevada Test Site, An Effect from the Aardvark Underground Nuclear Explosion,** USGS Technical Letter Yucca-48, the United States Geological Survey, Denver, CO.

Garber, M. S., 1971. **Hydraulic Test and Quality of Water Data from Hole U-3cr PS#2, Bilby Site, Nevada Test Site**, USGS-474-105, the United States Geological Survey, Denver, CO.

Germain, L. S., and J. S. Kahn, 1969. "Phenomenology and Containment of Underground Nuclear Explosions," **Technical Discussions of Offsite Safety Programs for Underground Nuclear Detonations**, the U. S. Atomic Energy Commission, Nevada Operations Office, NVO-40, Las Vegas, NV.

Green, H. W., and S. V. Radcliffe, 1972. "Deformation Processes in the Upper Mantle," **Flow and Fracture of Rocks**, Geophysical Monograph 16, American Geophysical Union.

Greensfelder, R. W., F. C. Kintzer, and M. R. Somerville, 1980. **Seismotectonic Regionalization of the Great Basin and Comparison of Moment Rates Computed from Holocene Strain and Historic Seismicity**, Geological Society of America Bulletin Part II, Vol. 91, pp. 2039-2111.

Haimson, B. C., 1983. **A Comparative Study of Deep Hydrofracturing and Overcoring Stress Measurements at Six Locations with Particular Interest to the Nevada Test Site**, U. S. National Committee for Rock Mechanics, National Academy of Sciences.

Haimson, B. C., J. Lacoumb, A. H. Jones, and S. J. Green, 1974. **Deep Stress Measurements in Tuff at the Nevada Test Site**, Advances in Rock Mechanics, Vol. IIa, National Academy of Sciences.

Haimson, B. C., and C. Fairhurst, 1967. **Initiation and Extension of Hydraulic Fractures in Rocks**, J. Soc. Petro. Engineers, Vol. 7.

Hale, W. E., I. J. Winograd, and M. S. Garber, 1963. **Preliminary Appraisal of Close-In Aquifer Response to the Bilby Event, Yucca Flat, Nevada**, USGS Technical Letter, NTS-63, the United States Geological Survey, Denver, CO.

Hamilton, R. M., and J. H. Healy, 1969. **Aftershocks of the Benham Nuclear Explosion**, Seismological Society of America Bulletin, Vol. 59, No. 6.

Hanson, G. N., V. R. Baker, P. M. Bethke, P. J. Hudleston, and G. R. Roguemore, 1987. "Report of the Peer Review Panel on the Proposed Program of Studies of the Calcite and Opaline-Silica Deposits in the Yucca Mountain Area, Nevada."

Harper, T. R., and N. C. Last, 1987. **Numerical Modeling of Fracture System Hydraulic Conductivity Changes During Fluid Injection**, workshop on forced fluid flow through "strong" fractured rock masses, for submission to Annales Geophysicae; now - Koninklijake/Shell Exploratie en Productie Laboratorium, Gerchy, France.

Harper, T. R., and J. S. Szymanski, 1982. "Complex Geologic Characterization of the Repository Environment," **Underground Space**, Vol. 6, Pergamon Press, Ltd.

Harper, T. R., and J. S. Szymanski, 1980. "A Perspective of Geological Characterizations Required for Subsurface Nuclear Waste Disposal," **Subsurface Space**, Proceedings of the International Symposium (Rockstore '80), M. Bergman, (ed), Stockholm, Sweden.

Hay, R. L., R. E. Pexton, T. T. Teague, and T. K. Kyser, 1986. **Spring-Related Carbonate Rocks, Mg Clays, and Associated Minerals in Pliocene Deposits of the Amargosa Desert, Nevada and California**, Geological Society of America Bulletin, 97.

Heath, R. C., 1984. **Ground-water Regions of the United States**, USGS Water Supply Paper 2242, the United States Geological Survey, Washington, DC.

Henne, M. S., 1982. **The Dissolution of Rainier Mesa Tuffs, and its Application to the Analysis of the Ground-Water Environment**, M.S., University of Nevada-Reno, Reno, NV.

Herrin, E., 1969. "Regional Variations of P-Wave Velocity in the Upper Mantle Beneath North America," **The Earth's Crust and Upper Mantle**, Geophysical Monograph 13, Pembroke J. Hart, (ed).

Homsy, G. M., and A. E. Sherwood, 1976. **Convective Instabilities in Porous Media with Through Flow**, AIChE Journal, Vol. 22, No. 1.

Hoover, D. L., 1968. **Genesis of Zeolites, Nevada Test Site**, Geological Society of America Memoir 110, E. B. Eckel, (ed).

Hoover, D. L., W. C. Swadley, and A. J. Gordon, 1981. **Correlation Characteristics of Surficial Deposits with a Description of Surficial Stratigraphy in the Nevada Test Site Region**, USGS-OFR-81-512, Open-file Report, the United States Geological Survey, Denver, CO.

Hubbert, M. K., and D. G. Willis, 1957. **Mechanics of Hydraulic Fracturing**, J. Petro. Tech., Vol. 9.

Isherwood, D., J. Harrar, and E. Raber, 1982. **Characterization of Climax Granite Ground Water**, UCRL-53-309, Lawrence Livermore National Laboratory, Livermore, CA.

Jeffrys, H., 1930. **The Instability of a Compressible Fluid Heat Below**, Proc. Cambridge Philosophical Society, Vol. 26.

Keen, C. E., and D. L. Barrett, 1971. **A Measurement of Seismic Anisotropy in the Northeast Pacific**, Can. J. Earth Sci., 8.

Keller, G. V., 1960. **Physical Properties of the Oak Spring Formation, Nevada**, USGS Professional Paper 400-B, the United States Geological Survey, Denver, CO.

Keller, G. V., 1962. **Electrical Resistivity of Rocks in the Area 12 Tunnels, Nevada Test Site, Nye County, Nevada**, Geophysics, Vol. 27, No. 2.

Kerrisk, J. G., 1987. **Groundwater Chemistry at Yucca Mountain, Nevada, and Vicinity**, LA-10929-MS, Los Alamos National Laboratory, Los Alamos, NM.

Knauss, K. G., 1981. **Dating Fault Associated Quaternary Material from the Nevada Test Site Using Uranium-Series Methods**, UCRL-53231, Lawrence Livermore National Laboratory, Livermore, CA.

Knopoff, L., 1964. **The Convection Current Hypothesis**, Rev. Geophysics, 2.

Knopoff, L., 1967. "Thermal Convection in the Earth's Mantle," **The Earth's Mantle**, Academic Press, T. F. Gaskell, (ed).

Knox, J. B., D. E. Rawson, and J. A. Korver, 1965. **Analysis of a Groundwater Anomaly Created by an Underground Nuclear Explosion**, J. Geophys. Res. 70(4).

Lahoud, R. G., D. H. Lobmeyer, and M. S. Whitfield, Jr., 1984. **Geohydrology of Volcanic Tuff Penetrated by Test Well UE-25b-1, Yucca Mountain, Nye County, Nevada**, USGS-WRI-84-4253, Water Resources Investigations Report, the United States Geological Survey, Denver, CO.

Lee, W. H. K., and S. Uyeda, 1965. **Terrestrial Heat Flow**, Geophysical Monograph 8, American Geophysical Union, W.H.K. Lee, (ed).

Lobmeyer, D. H., M. S. Whitfield, R. R. Lahoud, and L. Bruckheimer, 1983. **Geohydrologic Data for Test Well US-25b#1, Nevada Test Site, Nye County, Nevada**, USGS-OFR-83-855, Open-file Report, the United States Geological Survey, Denver, CO.

Lomnitz, C., 1974. "Global Tectonics and Earthquake Risk," **Developments in Geotectonics 5**, Elsevier Scientific Publishing Company.

Lowell, R. P., 1977. **Convection and Thermoelastic Effects in Narrow, Vertical Fracture Spaces**, Technical Letter Report 1, School of Geophysical Science, Georgia Institute of Technology, Atlanta, GA.

Lubimova, E. A., and B. G. Polyak, 1969. "Heat Flow Map of Eurasia," **The Earth's Crust and Upper Mantle**, Geophysical Monograph 13, American Geophysical Union, Pembroke J. Hart, (ed).

Lyustikh, E. N., 1969. "Problem of Convection in the Earth's Mantle," **The Earth's Crust and Upper Mantle**, Geophysical Monograph 13, American Geophysical Union, Pembroke J. Hart, (ed).

Magnitsky, V. A., and V. N. Zharkov, 1969. "Low-Velocity Layers in the Upper Mantle," **The Earth's Crust and Upper Mantle**, Geophysical Monograph 13, American Geophysical Union, Pembroke J. Hart, (ed).

Maldonado, F., 1985. **Geologic Map of the Jackass Flats Area, Nye County, Nevada**, Miscellaneous Investigations Series Map I-1519, the United States Geological Survey, Denver, CO.

McCaig, A. M., 1988. **Deep Fluid Circulation in Fault Zones**, Geology, Vol. 16.

Miller, C. H., D. R. Miller, W. L. Ellis, and J. R. Ege, 1975. **Determination of In Situ Stress at U12e-18 Working Point, Rainier Mesa, Nevada Test Site**, USGS-474-217, the United States Geological Survey, Denver, CO.

Monfort, M. E., and J. R. Evans, 1982. **Three-Dimensional Modeling of the Nevada Test Site and Vicinity From Teleseismic P-Wave Residuals**, USGS-OFR-82-409, the United States Geological Survey, Menlo Park, CA.

Moody, J. D., and M. J. Hill, 1956. **Wrench-Fault Tectonics**, Geological Society of America Bulletin, Vol. 67, No. 9.

Morris, G. B., R. W. Raitt, and G. G. Shor, 1969. **Velocity Anisotropy and Delay-Time Maps of the Mantle Near Hawaii**, J. Geophys. Res., 74.

Morris, R. H., 1971. "Geologic and Hydrologic Effects of the Handley Event, Pahute Mesa, Nevada Test Site," **Geologic Effects**, USGS-474-95, the United States Geological Survey, Denver, CO

Murphy, H. D., 1979. **Convective Instabilities in Vertical Fractures and Faults**, J. Geophys. Res., 84.

Murray, W. A. 1981. **Geohydrology of the Climax Stock Granite and the Surrounding Rock Formations, Nevada Test Site**, UCRL-53-138, Lawrence Livermore National Laboratory, Livermore, CA.

Norris, A. E., K. Wolfsberg, and S. K. Gifford, 1985. **^{36}CL Measurements of the Unsaturated Zone Flux at Yucca Mountain**, LA-UR 85-2408, Los Alamos National Laboratory, Los Alamos, NM.

Norris, A. E., 1989. **Analyses of ^{36}CL in Samples of Tuff from the Yucca Mountain Project**, Abstract for Invited Seminar, Nuclear Structure Research Laboratory, University of Rochester, Los Alamos National Laboratory, Los Alamos, NM.

Nur, A., 1972. **Dilatancy, Pore Fluids and Premonitory Variations of ts/tp Travel Times**, Bulletin. Seismal. Society of America 62.

O'Neil, J. R., 1984. "Letter Report from J. R. O'Neil (USGS) to D. Vaniman (LANL), December 19, 1984, regarding stable isotope analyses of three samples from Yucca Mountain."

O'Neil, J. R., 1985. "Letter Report from J. R. O'Neil (USGS) to S. Levy (LANL), April 29, 1985, regarding stable isotope analysis and oxygen isotope temperatures of samples."

O'Neil, J. R., R. N. Clayton, and T. K. Mayeda, 1969. **Oxygen Isotope Fractionation in Divalent Metal Carbonates**, Journal Chemistry Physics, Vol. 51.

Palm, E., J. E. Weber, and O. Kvernvold, 1972. **On Steady Convection in a Porous Medium**, J. Fluid Mech., 54.

Panek, L. A., 1966. **Calculation of the Average Ground Stress Components from Measurements of the Diametral Deformation of a Drill Hole**, U. S. Bureau of Mines, Washington, DC.

Peters, R. R., E. A. Klavetter, I. J. Hall, S. C. Blair, P. R. Heller, and G. W. Gee, 1984. **Fracture and Matrix Hydrologic Characteristics of Tuffaceous Materials from Yucca Mountain, Nye County, Nevada**, SAND84-1471, Sandia National Laboratories, Albuquerque, NM.

Porath, H., 1971. **Magnetic Variation Anomalies and Seismic Low Velocity Zone in the Western United States**, J. Geophys. Res., Vol. 76.

Prats, M., 1982. **Thermal Recovery**, Soc. Pet. Engineers of AIME, Monograph Vol. 7, Henry L. Doherty Series.

Raitt, R. W., G. G. Shor, and T. J. Francis, 1969. **Anisotropy of the Pacific Upper Mantle**, J. Geophys. Res., 74.

Raleigh, C. B., and S. H. Kirby, 1970. **Creep in the Upper Mantle**, Mineralogical Society of America Special Paper 3.

Ramberg, H., 1981. **Gravity, Deformation, and the Earth's Crust**, Academic Press, 2nd Edition.

Ramsay, J. G., 1967. **Folding and Fracturing of Rocks**, McGraw-Hill Book Company.

Rayleigh, Lord, 1916. **On Convection Currents in a Horizontal Layer of Fluid When the Higher Temperature is on the Underside**, Phil. Mag., Ser. 6, Vol. 32.

Reed, W. E., 1970. **Transport of Water Away from a Buried Heat Source with Special Reference to Hydrologic Phenomena Observed at Aardvark Nuclear Detonation**, J. Geophys. Res. 75.

Reheis, M., 1986. **Preliminary Study of Quaternary Faulting on the East Side of Bare Mountain, Nye County, Nevada**, USGS-OFR-86-576, Open-file Report, the United States Geological Survey, Denver, CO.

Ringwood, A. E., 1969. "Composition and Evaluation of the Upper Mantle," **The Earth's Crust and Upper Mantle**, Geophysical Monograph 13, Pembroke J. Hart, (ed).

Robison, J. H., D. M. Stephens, R. R. Luckey, and D. A. Baldwin, 1988. **Water Levels in Periodically Measured Wells in the Yucca Mountain Area, Nevada, 1981-87**, USGS Open-file Report, the United States Geological Survey, Denver, CO.

Robison, J. H., 1984. **Ground-Water Level Data and Preliminary Potentiometric-Surface Maps, Yucca Mountain and Vicinity, Nye County, Nevada**, USGS-WRI-84-4197, Water Resources Investigations Report, the United States Geological Survey, Lakewood, CO.

Rogers, A. M., S. C. Harmsen, W. J. Carr, and W. Spence, 1983. **Southern Great Basin Seismological Data Report for 1981 and Preliminary Data Analysis**, USGS-OFR-83-669, Open-file Report, the United States Geological Survey, Denver, CO.

Rogers, A. M., S. C. Harmsen, and M. Meremonte, 1987. **Evaluation of the Seismicity of the Southern Great Basin and Its Relationship to the Tectonic Framework of the Region**, USGS-OFR-87, Open-file Report, the United States Geological Survey, Denver, CO.

Ross, B., 1984. **A Conceptual Model of Deep Unsaturated Zones with Negligible Recharge**, Water Resources Research, Vol. 20, No. 11.

Roy, R. G., D. D. Blackwell, and F. Birch, 1968. **Heat Generation of Plutonic Rock and Continental Heat Flow Provinces**, Earth Planetary Scientific Letter 5.

Runcorn, S. K., 1962. **Convection Currents in the Earth's Mantle**, Nature, 195.

Runcorn, S. K., 1969. "Convection in the Mantle," **The Earth's Crust and Upper Mantle**, Geophysical Monograph 13, American Geophysical Union, Pembroke J. Hart, (ed).

Rush, F. E., W. Thordarson, and L. Bruckheimer, 1983. **Geohydrologic and Drill-Hole Data for Test Well USW H-1, Adjacent to Nevada Test Site, Nye County, Nevada**, USGS-OFR-83-141, Open-file Report, the United States Geological Survey, Denver, CO.

Rush, F. E., W. Thordarson, and D. G. Pyles, 1984. **Geohydrology of Test Well USW H-1, Yucca Mountain, Nye County, Nevada**, Investigations Report USGS-WRI-84-4032, the United States Geological Survey, Denver, CO.

Russell, C. E., 1987. **Hydrogeologic Investigations of Flow in Fractured Tuffs, Rainier Mesa, Nevada Test Site**, M.S. Thesis, University of Nevada-Reno, Reno, NV.

Sadovsky, M. A., I. L. Nersesow, S. K. Nigmatullaev, L. A. Latynina, A. A. Lukk, A. N. Semenov, I. G. Simbireva, and R. I. Vlomov, 1972. **The Process Preceding Strong Earthquakes in Some Regions of Middle Asia**, Tectonophysics, 14.

SAIC (Science Applications International Corporation), 1985. **Tectonic Stability and Expected Ground Motion at Yucca Mountain, Report of a Workshop at SAIC - LaJolla, August 7-8, 1984 and January 25-26, 1985**, DOE/NV/10270-2(Rev. 1).

Sass, J. H., and H. Lachenbruch, 1982. **Preliminary Interpretation of Thermal Data from the Nevada Test Site**, USGS-OFR-82-973, Open-file Report, the United States Geological Survey, Denver, CO.

Sass, J. H., A. H. Lachenbruch, R. J. Munroe, G. W. Greene, and T. H. Moses, Jr., 1971. **Heat Flow in the Western United States**, Journal of Geophysical Research, Vol. 76, No. 26, pp. 6376-6413.

Sass, J. H., W. H. Diment, A. H. Lachenbruch, B. V. Marshall, R. J. Munroe, T. H. Moses, Jr., and T. C. Urban, 1976. **A New Heat-Flow Contour Map of the Conterminous United States**, USGS-OFR-76-756, Open-file Report, the United States Geological Survey, Denver, CO.

Sass, J. H., H. A. Lachenbruch, and E. W. Mase, 1980. **Analysis of Thermal Data from Drill Holes UE-24a3 and UE-25a-1, Calico Hills and Yucca Mountain, Nevada Test Site**, USGS-OFR-80-826, Open-file Report, the United States Geological Survey, Denver, CO.

Sass, J. H., A. H. Lachenbruch, H. Grubb, and T. H. Moses, 1983. **Status of Thermal Observations at Yucca Mountain, Nevada**, Letter Report.

Sass, J. H., A. H. Lachenbruch, W. W. Dudley, S. S. Priest, and R. J. Munroe, 1987. **Temperature, Thermal Conductivity, and Heat Flow near Yucca Mountain, Nevada: Some Tectonic and Hydrologic Implications**, USGS Open-file Report, the United States Geological Survey, Denver, CO.

Schoff, S. L., and J. E. Moore, (Comps.), 1964. **Chemistry and Movement of Ground Water, Nevada Test Site**, USGS-TEI-838, the United States Geological Survey, Denver, CO.

Schoff, S. L., and I. J. Winograd, 1961. **Hydrologic Significance of Six Core Holes in Carbonate Rocks of the Nevada Test Site**, USGS Open-file Report TEI-787, the United States Geological Survey, Denver, CO.

Scholz, C. H., and R. Kranz, 1974. **Notes on Dilatancy Recovery**, Journal Geophys. Res. 79, No. 14.

Scholz, C. H., L. R. Sykes, and Y. P. Aggarwal, 1973. **The Physical Basis for Earthquake Prediction**, Science 181, No. 4102.

Scholz, C. H., M. Barazengi, and M. L. Sbar, 1971. **Late Cenozoic Evolution of the Great Basin, Western United States, as an Ensialic Interarc Basin,** Geological Society of America Bulletin, Vol. 82.

Scott, R. B., 1984. **Internal Deformation of Blocks Bounded by Basin- and Range-Style Faults**, Geological Society of America, Abstracts with Programs, Vol. 16, No. 6, p. 649.

Scott, R. B., 1986. **Extensional Tectonics at Yucca Mountain, Southern Nevada**, Geological Society of America, Abstracts with Programs, 1986, Rocky Mountain Section, Vol. 18, No. 5, p. 411, April 30-May 2, 1986, Flagstaff, AZ.

Scott, R. B., and J. Bonk, 1984. **Preliminary Geologic Map of Yucca Mountain, Nye County, Nevada, with Geologic Sections**, USGS-OFR-84-494, Open-file Report, the United States Geological Survey, Denver, CO.

Scott, R. B., and J. G. Rosenbaum, 1986. **Evidence of Rotation about a Vertical Axis during Extension at Yucca Mountain, Southern Nevada**, Transactions, American Geophysical Union, EOS, Vol. 67, No. 16, p. 358.

Scott, J. H., R. D. Carroll, and D. R. Cunningham, 1964. **Interpretation of Electrical Resistivity and Self-Potential Measurements, Bilby Event, Yucca Flat, Nevada**, USGS Technical Letter NTS-67, the United States Geological Survey, Denver, CO.

Semenov, A. M., 1969. **Variations in Travel Time of Transverse and Longitudinal Waves Before Violent Eqrthquakes**, Isv. Earth Physics, 4.

Semken, S. C., 1984. **A Neodymium and Strontium Isotopic Study of Late Cenozoic Basaltic Volcanism in the Southwestern Basin and Range Province**, M.S. Thesis, University of California-Los Angeles, Los Angeles, CA.

Sibson, R. H., J. McM. Moore, and A. H. Rankin, 1975. **Seismic Pumping - a Hydrothermal Fluid Transport Mechanism**, Journal Geological Society of London, Vol. 131.

Smith, S. W., and R. Kind, 1972. **Regional Secular Strain Fields in Southern Nevada**, Tectonophysics, 14.

Smith, W. C., W. C. Vollendorf, and W. E. Warren, 1980. **In-Situ Stress from Hydraulic Fracture Measurements in G Tunnel, Nevada Test Site**, SAND 80-1138, Sandia National Laboratories Report, Albuquerque, NM.

Spencer, J. E., and C. G. Chase, 1989. **Role of Crustal Flexure in Initiation of Low-Angle Normal Faults and Implications for Structural Evolution of the Basin and Range Province**, J. Geophys. Res., Vol. 94.

Stead, F. W., 1969. "Geologic Considerations," **Technical Discussions of Offsite Safety Programs for Underground Nuclear Detonations**, U. S. Atomic Energy Commission, Nevada Operations Office, NVO-40, Las Vegas, NV.

Stewart, J. H., 1967. **Possible Large Right-Lateral Displacement Along Fault and Shear Zones in the Death Valley-Las Vegas Area, California and Nevada**, Geological Society of America Bulletin, Vol. 82.

Stewart, J. H., J. P. Albers, and F. G. Poole, 1968. **Summary of Regional Evidence for Right-Lateral Displacement in the Western Great Basin**, Geological Society of America Bulletin, Vol. 79, No. 10, pp. 1407-1414.

Stewart, J. H., 1985. **East-Trending Dextral Faults in the Western Great Basin: An Explanation for Anomalous Trends of Pre-Cenozoic Strata and Cenozoic Faults**, Tectonics, Vol. 4, No. 6, pp. 546-564.

Stock, J. M., J. H. Healy, S. H. Hickman, and M. D. Zoback, 1985. **Hydraulic Fracturing Stress Measurements at Yucca Mountain, Nevada, and Relationship to the Regional Stress Field**, Journal of Geophysical Research, Vol. 90, No. B10, pp. 8691-8706.

Stock, J. M., J. H. Healy, J. Svitek, and L. Mastin, 1986. **Report on Televiewer Log and Stress Measurements in Holes USW G-3 and UE-25p#1, Yucca Mountain, Nye County, Nevada**, USGS-OFR-86-369, Open-file Report, the United States Geological Survey, Denver, CO.

Strauss, J. M., 1974. **Large Amplitude Convection in Porous Media**, J. Fluid Mech., 64.

Swadley, W. C., D. L. Hoover, and J. N. Rosholt, 1984. **Preliminary Report on Late Cenozoic Faulting and Stratigraphy in the Vicinity of Yucca Mountain, Nye County, Nevada**, USGS-OFR-84-788, Open-file Report, the United States Geological Survey, Denver, CO.

Swanberg, C. A., and P. Morgen, 1978. **The Linear Relation Between Temperatures Based on the Silica Content of Groundwater and Regional Heat Flow: A New Heat Flow Map of the United States**, Pure Applied Geophysics, 117.

Sutton, J. M., 1970. "Onset of Convection in a Porous Channel with Net Through Flow," **The Physics of Fluids**, Vol. 13, No. 8.

Szabo, B. J., 1984. **Uranium-Series Dating of Fault-Related Fracture and Cavity-Filling Calcite and Opal in Drill Cores from Yucca Mountain, Southern Nevada**, Geological Society of America, Abstracts with Programs, Vol. k16, No. 6, pp. 672-673, Annual Meeting, November 5-8, 1984, Reno, NV.

Szabo, B. J., and T. K. Kyser, 1985. **Uranium, Thorium Isotopic Analyses and Uranium-Series Ages of Calcite and Opal, and Stable Isotopic Compositions of Calcite from Drill Cores UE-25a 1, USW G-2, and USW G-3/GU3, Yucca Mountain Nevada**, USGS-OFR-85-224, Open-file Report, the United States Geological Survey, Denver, CO.

Szabo, B. J., W. J.Carr, and W. C. Gottschall, 1981. **Uranium-Thorium Dating of Quaternary Carbonate Accumulations in the Nevada Test Site Region, Southern Nevada**, USGS-OFR-81-119, Open-file Report, the United States Geological Survey, Denver, CO.

Szymanski, J. S., and T. R. Harper, 1980. **Assessment of the Future Evolution of Geologic Systems Intended for the Development of a Nuclear Waste Repository**, M. Bergman, (ed), Proceedings of the International Symposium (Rockstore '80), Stockholm, Sweden.

Tatel, H. E., and M. A. Tuve, 1955. "Seismic Exploration of a Continental Crust," **The Crust of the Earth**, Geological Society of America Special Paper 62.

Thompson, G. A., and D. B. Burke, 1974. **Regional Geophysics of the Basin and Range Province**, Ann. Rev. Earth Plan. Sci., Vol. 2.

Thordarson, W., 1983. **Geohydrologic Data and Test Results from Well J-13, Nevada Test Site, Nye County, Nevada**, USGS Water Resources Investigations Report, WRI-83-4171, the United States Geological Survey, Denver, CO.

Thordarson, W., F. E. Rush, and S. J. Waddell, 1985. **Geohydrology of Test Well USW H-3, Yucca Mountain, Nye County, Nevada**, USGS-WRI-84-4272, Water Resources Investigations Report, the United States Geological Survey, Lakewood, CO.

Thordarson, W., and B. P. Robison, 1971. **Wells and Springs in California and Nevada Within 100 Miles of the Point 37 deg. 15 min. N., 116 deg., 25 min. W., on Nevada Test Site**, USGS-474-85, the United States Geological Survey, Denver, CO.

Thordarson, W., 1965. **Perched Ground Water in Zeolitized-Bedded Tuff, Rainier Mesa and Vicinity, Nevada Test Site**, USGS TEI 862, the United States Geological Survey, Denver, CO.

Thunvik, R., and C. Braester, 1982. "Hydrothermal Conditions Around a Radioactive Waste Repository," **Scientific Basis for Nuclear Waste Management** V. W. Lutze, (ed), Materials Research Society Symposia Proceedings, Vol. II.

Tozer, D. C., 1965. "Heat Transfer and Convection Currents," **A Symposium on Continental Drift**, P. M. S. Blackett, E. Bullard, and S. K. Runcorn, (eds), Philosophical Transactions Royal Society.

Turcotte, D. L. and G. Schubert, 1982. **Geodynamics: Applications of Continuum Physics to Geological Problems**, John Wiley, New York, NY.

Van Bemmelen, R. W., 1961. **The Scientific Character of Geology**, J. Geol., 69(4).

Van Bemmelen, R. W., 1972. **Geodynamic Models - An Evolution and Synthesis**, Elsevier Publishing Company.

Vaniman, D. T., D. L. Bish, and S. Chipera, 1988. **A Preliminary Comparison of Mineral Deposits in Faults near Yucca Mountain, Nevada, with Possible Analogs**, LA-11289-MS, Los Alamos National Laboratory, Los Alamos, NM.

Vaniman, D. T., and B. M. Crowe, 1981. **Geology and Petrology of the Basalts of Crater Flat: Applications to Volcanic Risk Assessment for the Nevada Nuclear Waste Storage Investigations**, LA-8845-MS, Los Alamos National Laboratory, Los Alamos, NM.

Vaniman, D. T., B. M. Crowe, and E. S. Cladney, 1982. **Petrology and Geochemistry of Hawaiite Lavas from Crater Flat, Nevada**, Contributions to Mineralogy and Petrology, Vol. 80, Springer-Verlag.

Vening Meinesz, F. A., 1964. **The Earth's Crust and Mantle**, Elsevier Publishing Company.

Verhoogen, J., 1965. "Phase Changes and Convection in the Earth's Mantle," **A Symposium on Continental Drift**, Philosophical Transactions Royal Society, Soc., P. M. S. Blackett, E. Bullard, and S. K. Runcorn, (eds).

Von Herzen, R. P., and W. H. K. Lee, 1969. "Heat Flow in Oceanic Regions," **The Earth's Crust and Upper Mantle**, Geophysical Monograph 13, Pembroke J. Hart, (ed).

Waddell, R. K., 1982. **Two-Dimensional, Steady-State Model of Ground-Water Flow, Nevada Test Site and Vicinity, Nevada-California**, USGS-WRI-82-4085, Water Resources Investigations Report, the United States Geological Survey, Denver, CO.

Waddell, R. K., 1984. **Solute-Transport Characteristics of Fractured Tuffs at Yucca Mountain, Nevada Test Site-A Preliminary Assessment**, Geological Society of America, Abstracts with Programs, Vol. 16, No. 6, p. 684.

Walker, G. E., 1962. **Ground Water in the Climax Stock, Nevada Test Site, Nye County, Nevada**, USGS Report TEI-813, the United States Geological Survey, Denver, CO.

Walsh, J. B., 1981. **Effect of Pore Pressure and Confining Pressure on Fracture Permeability**, Int. J. Rock Mech., Min. Sci. Geomech. Abstract, 18.

Walsh, J. B., and E. R. Decker, 1966. **Effect of Pressure and Saturating Fluids on the Thermal Conductivity of Compact Rock**, J. Geophys. Res., 71.

Weart, W., 1969. "Earthquakes and Aftershocks Related to Nuclear Detonations," **Technical Discussions of Offsite Safety Programs for Underground Nuclear Detonations**, U. S. Atomic Energy Commission, Nevada Operations Office, NVO-40, Las Vegas, NV.

Weertman, J., 1970. **The Creep Strength of the Earth's Mantle**, Rev. Geophys. Space Phys., 8.

Wernicke, B., J. E. Spencer, B. C. Burchfiel, and P. L. Guth, 1982. **Magnitude of Crustal Extension in the Southern Great Basin**, Geology, Vol. 10.

Whitcomb, J. A., J. D. Garmany, and D. L. Anderson, 1973. **Earthquake Prediction: Variation of Seismic Velocities Before the San Fernando Earthquake**, Science, 180.

White, A. F., 1979. **Geochemistry of Ground Water Associated with Tuffaceous Rocks, Oasis Valley, Nevada**, USGS Professional Paper 712-E, the United States Geological Survey, Washington, DC.

White, A. G., H. C. Claassen, and L. V. Benson, 1980. **The Effect of Dissolution of Volcanic Glass on the Water Chemistry in a Tuffaceous Aquifer, Rainier Mesa, Nevada**, USGS-WSP1536-Q, Water Supply Paper, the United States Geological Survey, Washington, DC.

Whitfield, M. S., Jr., E. P. Eshom, W. Thordarson, and D. H. Schaefer, 1985. **Geohydrology of Rocks Penetrated by Test Well USW H-4, Yucca Mountain, Nye County, Nevada**, USGS-WRI-85-4030, Water Resources Investigations Report, the United States Geological Survey, Denver, CO.

Whitney, J. W., R. R. Shroba, F. W. Simonds, and S. T. Harding, 1986. **Recurrent Quaternary Movement on the Windy Wash Fault, Nye County, Nevada**, Geological Society of America, Abstracts with Programs, p.787.

Wilcox, R. E., T. P. Harding, and D. R. Seeley, 1973. **Basic Wrench Tectonics**, A.A.P.G. Bulletin, Vol. 57, No. 1.

Winograd, I. J., B. J. Szabo, A. C. Riggs, and P. T. Kolesar, 1985. **Two-Million-Year Record of Dueterium Depletion in Great Basin Ground Water**, Science, Vol. 227.

Winograd, I. J., and G. C. Doty, 1980. **Paleohydrology of the Southern Great Basin, with Special Reference to Water Table Fluctuations Beneath the Nevada Test Site During the Late (?) Pleistocene**, USGS-OFR-80-569, Open-file Report, the United States Geological Survey, Reston, VA.

Winograd, I. J., and W. Thordarson, 1975. **Hydrogeologic and Hydrochemical Framework, South-Central Great Basin, Nevada-California, with Special Reference to the Nevada Test Site**, USGS Professional Paper 712-C, pp. Cl-C126, Washington, DC.

Wood, S. H., 1985. **Regional Increase in Groundwater Discharge after the 1983 Idaho Earthquake; Coseismic Strain Release, Tectonic and Natural Hydraulic Fracturing**, USGS-OFR-85-290, the United States Geological Survey, Denver, CO.

Wooding, R. A., 1957. **Steady State Free Convection of Liquid in a Saturated Permeable Medium**, J. Fluid Mech., 2.

Woollard, G. P., 1969. "Regional Variations in Gravity," **The Earth's Crust and Upper Mantle**, Geophysical Monograph 13, Pembroke J. Hart, (ed).

Zebib, A., and D. R. Kassoy, 1977. **Onset of Natural Convection in a Box of Water-Saturated Porous Media with Large Temperature Variation**, Phys. Fluids, 20.

Appendix B
PLATES

LIST OF PLATES

Plate	Title
	SECTION 2.0
2.2-1	Mathematical model of "simple" groundwater system.
2.2-2	Laplace's equation.
2.2-3	Poisson's equation.
2.2-4	Transient flow equation.
2.2-5	Explanation of mathematical notations.
2.2-6	Flow equations written in a form allowing for consideration of aquifer heterogeneity and anisotropy.
2.3-1	Role of mathematical and conceptual models.
2.3-2	Interdependence of conceptual models.
2.3-3	Conceptual model of a groundwater system.
2.3-4	Importance of conceptual models.
	SECTION 3.0
3.1-1	Location of the Death Valley groundwater system within the Great Basin.
3.1-2	Simplified isostatic anomaly map of the United States.
3.1-3	Configuration of the crust in north-central Great Basin. Based on CO-CORP 40° N transect.
3.1-4	Estimated P-wave velocity in the upper mantle of the continental United States, based on deep seismic soundings, nuclear explosions, and earthquakes.
3.1-5	Intensity of heat flow in the Great Basin.
3.1-6	Schematic representation of conceptual understanding of tectonophysical character of the Great Basin.
3.2-1	Numerical analysis of a process of upwelling of asthenospheric materials into the lithosphere for the Rio Grande Rift.
3.2-2	Effect of a mantle upwelling on the lithospheric structure.
3.2-3	Surface heat flow and shear stresses in the upper mantle and lower crust resulting from convective flow of heat and mass in the upper mantle.
3.2-4	Continuum crustal stresses and surface uplift resulting from convective flow of heat and mass in the upper mantle.

3.2-5	Failure-surface trajectory diagram for the upper crust overlying convective system in the upper mantle.
3.2-6	Contour diagram of shear stress magnitude in units of maximum base normal stress. Upper crust overlying convective system in the upper mantle.
3.2-7	Idealization of the conceptual linkage between an extension dominated tectonic enviroment and a groundwater system operating in the upper crust.
3.3.1-1	The Walker Lane shear belt and major associated faults.
3.3.1-2	Major late Pliocene and Quaternary faults in the Nevada Test Site region, their relation to the Death Valley-Pancake Volcanic Zone.
3.3.1-3	Quaternary faults near proposed repository.
3.3.1-4	Quaternary faults near proposed repository.
3.3.1-5	Seismicity of the southern Great Basin. Period August 1, 1978 through December 31, 1983.
3.3.1-6	Strain changes in the vicinity of the Nevada Test Site during a two-month period.
3.3.2.1-1	Summary of strain rates and of accumulated shear strain for the region of the Yucca Mountain groundwater system.
3.3.2.3-1	Division of deformation area into strain domains.
3.3.2.2-2	Idealization of tectonic cycle for a strain domain.
3.3.2.2-3	Idealization of changes in stress field during a tectonic cycle.
3.3.2.2-4	The dilatancy/fluid diffusion model of an earthquake nucleation process.
3.3.2.2-5	Idealized response of a fractured medium during uniform extension.
3.3.2.2-6	Idealized response of a dilated fractured medium to sudden changes in pore pressure.
3.3.2.3-1	Schematic illustration of: a) division of the strain domain into the upper and lower parts with different in situ stress conditions; and b) division of the lower part of the strain domain into the dilatant zone and the "outside zone."
3.3.2.3-2	Schematic representation of strain accumulation within a single strain domain during three cycles of deformation.
3.3.2.3-3	Schematic representation of changes in the in situ stress conditions occurring near the ground surface in a cyclically deforming fractured medium.
3.3.2.3-4	Location of faults containing calcite-silica veins of Quaternary age in the Yucca Mountain area.

3.3.2.3-5	Geologic section across Yucca Mountain showing location and thickness of mosaic breccias.
3.3.3.1-1	Stress on a fracture as a function of magnitude and orientation of principal stresses.
3.3.3.2-1	Mohr's representation of stresses in two dimensions and combined Griffith/Navier-Coulomb failure envelope.
3.3.3.2-2	Assumed initial in situ stresses around a deforming fracture.
3.3.3.2-3	Idealization of changes in stresses and displacements occurring along a deforming fracture as a function of depth and time.
3.3.3.2-4	Idealization of changes in stresses and displacements occurring along a strike of a deforming fracture.
3.3.3.2-5	In situ stress states around a deforming fracture.
3.3.3.3-1	Conceptual model of conductive aperture of fractures.
3.3.3.3-2	Relationships between time and hydraulic properties for decreasing σ_{nfeff}.
3.3.3.3-3	Idealized joint response during shear displacement.
3.3.3.3-4	Relationship between time and hydraulic properties for increasing τ_f.
3.3.3.3-5	Time-dependence of S_f and K_f around a segment of a deforming fracture at a const. depth.
3.3.3.3-6	Time-dependence of vertical extent of a segment of a deforming fracture and time-dependence of the total enhancement of the conducting aperture.
3.3.3.3-7	Schematic representation of changes in : a) the in situ stress conditions; and b) the hydraulic conductivity structure, occurring near the ground surface in a cyclically deforming fractured medium.
3.3.4-1	Conceptual model of groundwater flow in a deforming fractured medium.
3.3.4-2	Deforming fractured medium-idealized history of changes in hydraulic potential.
3.3.4-3	Deforming fractured medium-idealized history of changes in hydraulic potential.
3.3.4-4	Deforming fractured medium-idealized history of changes in hydraulic potential.
3.3.4-5	Deforming fractured medium-idealized history of changes in hydraulic potential.
3.3.4-6	Idealized history of the position of the water table for a single point $P_{(x,y)}$.

3.3.4-7	Non-homogeneous strain-its relationship to configuration of the water table.
3.3.5-1	Repeated temperature profiles from Well UE-25a7.
3.3.5-2	Maximum rise of the water table at point $P_{(x,y)}$ caused by changes in the in situ stress conditions.
3.4.1-1	Generalized geologic map of the Death Valley Pancake Range Volcanic Zone and of the Death Valley groundwater system.
3.4.1-2	Location of seismic monitoring stations used for detailed analyses of the P-wave residuals.
3.4.1-3	Seismic velocity structure of the upper crust from teleseismic P-wave residuals for the region of Death Valley groundwater system.
3.4.1-4	Seismic velocity structure of the lower crust from teleseismic P-wave residuals for the region of Death Valley groundwater system.
3.4.1-5	Seismic velocity structure of the upper mantle from teleseismic P-wave residuals for the region of Death Valley groundwater system.
3.4.1-6	Seismic velocity structure of the mantle (depth 81-131 km) from teleseismic P-wave residuals for the region of Death Valley groundwater system.
3.4.1-7	Seismic velocity structure of the mantle (depth 131-231 km) from teleseismic P-wave residuals for the region of Death Valley groundwater system.
3.4.1-8	Regional heat flow values within and adjacent to the Nevada Test Site.
3.4.1-9	Intensities of heat flow at the Nevada Test Site.
3.4.1-10	Map of western United States showing intensities of heat flow.
3.4.1-11	Terrestrial temperature - a perspective.
3.4.1-12	Terrestrial heat flow - a perspective.
3.4.2-1	Total hydraulic gradient combines buoyancy and hydraulic head gradient.
3.4.2-2	Mathematical model for a simultaneous flow of heat and fluid.
3.4.2-3	Governing equations in the Galerkin finite element method.
3.4.2-4	Explanation of symbols used on Plate 3.4.2-2 and 3.4.2-3.
3.4.3.1-1	Explanation of mathematical notations used in Section 3.4.3.
3.4.3.2-1	Requirements for the onset of thermal convection in a porous medium.
3.4.3.2-2	Requirements for the onset of thermal convection in a porous medium with consideration of through-flow.

3.4.3.3-1	The stability limit (the critical Rayleigh number at neutral stability) for the onset of thermal convection in faults and fractures as a function of the aspect ratio and the heat transfer grouping.
3.4.3.3-2	The perturbation growth rate for convection in fractures.
3.4.4-1	Conceptual model of a flow system in fractured medium and influenced by terrestrial heat.
3.4.4-2	Location of a selected part of the flow system considered on Plates 3.4.4-3 through 3.4.4-6.
3.4.4-3	Change in boundary conditions for an arbitrary plane -Za caused by convection of fluids in the selected part of the flow system.
3.4.4-4	Amount of fluid in transit (storage) through the selected part of the flow system prior and during convection.
3.4.4-5	Changes introduced into the selected part of the flow system by thermal convection.
3.4.4-6	Maximum rise of water table at $P_{(x,y)}$ caused by thermal convection.
3.4.4-7	Changes introduced into flow field by thermal convection.
3.4.4-7a	Changes introduced into flow field by thermal convection-formation of perched waters.
3.4.4-7b	Changes introduced into flow field by thermal convection-formation of perched waters.
3.4.4-7c	Changes introduced into flow field by thermal convection-formation of perched waters.
3.5.2-1	Time-dependence of thermal properties (K_h and D) around a segment of a deforming fracture at a const. depth.
3.5.2-2	Time-dependence of the vertical extent of the in situ stress enhancement of thermal properties (K_h and D) and time-dependence of the value of this enhancement.
3.5.2-3	Schematic representation of changes in: a) the in situ stress conditions; and b) the thermal properties. A cyclically deforming fractured medium, near the ground surface.
3.5.2-4	Conceptual model of a "simple" flow of heat through a deforming fractured medium.
3.5.2-5	Main characteristics of the geothermal field developed in a deforming fractured medium.
3.5.3-1	Conceptual model of a heat-fluid coupled groundwater system developed in a deforming fractured medium.
3.5.3-2	Conceptual model of flow in the vadose zone of a coupled heat-fluid flow field developed in a deforming fractured medium.

3.5.3-3 Evolution of a coupled heat-fluid flow system developed in a deforming fractured medium and operating near the ground surface.

SECTION 4.0

4.1-1 Location of the Death Valley groundwater system.

4.1-2 Subdivision of the Death Valley groundwater system.

4.1-3 Precipitation, recharge, and discharge areas for the Death Valley groundwater system.

4.2.2-1 Results of laboratory measurements of the saturated matrix hydraulic conductivity. Tuff "pile"-Yucca Mountain.

4.2.2-2 Laboratory values of saturated matrix hydraulic conductivity as a function of stratigraphic depth. Tuff "pile"-Yucca Mountain.

4.2.2-3 Pumping test data for carbonate aquifers at the Nevada Test Site and vicinity.

4.2.2-4 Pumping test data for tuff "pile" at the Nevada Test Site and vicinity.

4.2.2-5 Comparison of values of hydraulic conductivity in carbonates with values of hydraulic conductivity in tuff "pile". All conductivity data are based on pumping tests.

4.2.2-6 Well H-1 - Hydraulic conductivity data based on Cooper-Brederhoeft injection tests and pumping tests.

4.2.2-6a Well H-1 - Hydraulic conductivity data based on Cooper-Brederhoeft injection tests and pumping tests.

4.2.2-7 Well H-3 - Hydraulic conductivity data based on Cooper-Brederhoeft injection tests, pumping tests, and swabbing tests.

4.2.2-8 Well H-4 - Hydraulic conductivity data based on pumping tests.

4.2.2-8a Well H-4 - Hydraulic conductivity data based on pumping tests.

4.2.2-9 Well H-6 - Hydraulic conductivity data based on Cooper-Brederhoeft injection tests and pumping tests.

4.2.2-9a Well H-6 - Hydraulic conductivity data based on Cooper-Brederhoeft injection tests and pumping tests.

4.2.2-10 Well UE-25b#1 - Hydraulic conductivity data based on Cooper-Brederhoeft injection tests and pumping tests.

4.2.2-11 Well UE-25p#1 - Hydraulic conductivity data based on Cooper-Brederhoeft injection tests and pumping tests.

4.2.2-11a Well UE-25p#1 - Hydraulic conductivity data based on Cooper-Brederhoeft injection tests and pumping tests.

4.2.2-11b	Well UE-25p#1 - Hydraulic conductivity data based on Cooper-Brederhoeft injection tests and pumping tests.
4.2.2-11c	Well UE-25p#1 - Hydraulic conductivity data based on Cooper-Brederhoeft injection tests and pumping tests.
4.2.2-12	Location map for hydraulic conductivity cross-sections.
4.2.2-13	Hydraulic conductivity structure. E-W cross-section. Yucca Mountain.
4.2.2-14	Hydraulic conductivity structure. NW-SE cross-section. Yucca Mountain.
4.2.2-15	Conceptual understanding of the "three" layer hydraulic conductivity structure at Yucca Mountain.
4.2.3-1	Degree of saturation above and below the water table.
4.2.3-2	Configuration of the water table in the Death Valley groundwater system.
4.2.3-3	Configuration of the water table in Pahute Mesa recharge area of the Death Valley groundwater system.
4.2.3-4	Configuration of the water table in Amargosa Desert discharge area of the Death Valley groundwater system.
4.2.3-4a	Explanation of symbols used on Plate 4.2.3-4.
4.2.3-5	Configuration of the water table at Yucca Montain.
4.2.3-6	Configuration of the water table in Yucca Flat and Emigrant Valley.
4.2.3-6a	Explanation of symbols used on Plate 4.2.3-6.
4.2.3-7	Configuration of the water table in southern Indian Springs Valley.
4.2.3-7a	Explanation of symbols used on Plate 4.2.3-7.
4.2.3-8	Configuration of the water table in Yucca Flat.
4.2.4.2-1	General hydrology of Yucca Flat.
4.2.4.2-2	Generalized topographic map of the Rainier Mesa quadrangle, showing locations of wells: U12e.03-1; U12e.M-S; Hagestad #1; and Test Well #1.
4.2.4.2-3	Vertical hydraulic gradients in four test wells from the area of Rainier Mesa.
4.2.4.2-4	Idealized changes in pore pressure with depth. Rainier Mesa and Yucca Flat.
4.2.4.3-1	Vertical components of flow in the area of Pahute Mesa.
4.2.4.3-2	Results of downhole measurements of distribution of hydraulic potentials, Pahute Mesa.
4.2.4.3-3	Idealized changes in hydraulic potentials in Pahute Mesa.

4.2.4.3-4	Water chemistry map for Pahute Mesa.
4.2.4.3-5	Results of chemical analyses of water samples from Pahute Mesa.
4.2.4.3-5a	Results of chemical analyses of water samples from Pahute Mesa (continued).
4.2.4.3-6	Downhole temperatures in three boreholes in Pahute Mesa.
4.2.4.4-1	Location map for deep wells at Yucca Mountain.
4.2.4.4-2	Water levels - Yucca Mountain.
4.2.4.4-2a	Water levels - Yucca Mountain (continued).
4.2.4.4-3	Idealized changes of pore pressure with depth at Yucca Mountain.
4.2.4.4-4	Schematic representation of depth-dependence of: a) pore pressure; b) temporal behavior of hydraulic potentials; c) in situ stress state; and d) conducting aperture for a single borehole penetrating the deforming fractured medium.
4.2.4.4-5	Map showing location of wells from which hydrographs shown on Plates 4.2.4.4-6 through 4.2.4.4-21 were obtained.
4.2.4.4-6	Hydrograph-Well USW WT-1.
4.2.4.4-7	Hydrograph-Well USW WT-2.
4.2.4.4-8	Hydrograph-Well UE-25 WT-3.
4.2.4.4-9	Hydrograph-Well WT-11.
4.2.4.4-10	Hydrograph-Well UE-25 WT#16.
4.2.4.4-11	Hydrograph-Well UE-25 WT#17.
4.2.4.4-12	Hydrograph-Well USW H-1.
4.2.4.4-12a	Hydrograph-Well USW H-1.
4.2.4.4-13	Hydrograph-Well USW H-3.
4.2.4.4-14	Hydrograph-Well USW H-5.
4.2.4.4-15	Hydrograph-Well USW H-6.
4.2.4.4-16	Hydrograph-Well USW G-3.
4.2.4.4-17	Hydrograph-Well USW H-1.
4.2.4.4-17a	Hydrograph-Well USW H-1.
4.2.4.4-18	Hydrograph-Well USW H-3.
4.2.4.4-19	Hydrograph-Well UE-25p#1.

4.2.4.4-20	Hydrograph-Well UE-25 WT#6.
4.2.4.4-21	Hydrograph-Well USW H-6.
4.2.4.4-22	Temperature logs obtained during and shortly after completion of borehole UE-25p#1 in the vicinity of fault contact between the Paleozoic carbonates and the tuff "pile."
4.2.4.4-23	Comparison of the results of chemical analyses of water samples from the tuff "pile" and from the Paleozoic carbonates.
4.2.4.4-24	Borehole temperature log-Well UE-25p#1.
4.2.5.2-1	Location map and geohydrologic setting. Climax Stock.
4.2.5.2-2	State of in situ stress. South heater drift, STC-C. Climax Stock.
4.2.5.2-3	Graphical representation of principal stresses. South heater drift. Climax Stock.
4.2.5.2-4	State of in situ stress. Hard hat tunnel. Climax Stock.
4.2.5.2-5	Mohr representation of in situ stress. South heater drift, STC-C. Climax Stock.
4.2.5.2-6	Mohr representation of in situ stress. Hard hat tunnel. Climax Stock.
4.2.5.2-7	State of in situ stress (USBM gauge). Spent fuel test facility. Boreholes ISS-8, 9, 10, and 11. Climax Stock.
4.2.5.2-8	State of in situ stress (CSIRO cell). Spent fuel test facility. Borehole ISS-8. Climax Stock.
4.2.5.2-9	State of in situ stress (CSIRO cell). Spent fuel test facility. Borehole ISS-9. Climax Stock.
4.2.5.2-10	State of in situ stress (CSIRO cell). Spent fuel test facility. Borehole ISS-10. Climax Stock.
4.2.5.2-11	State of in situ stress (CSIRO cell). Spent fuel test facility. Borehole ISS-11. Climax Stock.
4.2.5.2-12	Mohr representation of in situ stress. Spent fuel test facility. Boreholes ISS-8, 9, 10, borehole depth > 60 feet. Climax Stock.
4.2.5.2-13	Mohr representation of in situ stress. Spent fuel test facility. Boreholes ISS-8, 9, 11, borehole depth > 60 feet. Climax Stock.
4.2.5.2-14	Mohr representation of in situ stress. Spent fuel test facility. Boreholes ISS-8, 9, 10, 11, borehole depth > 60 feet. Climax Stock.
4.2.5.2-15	Mohr representation of in situ stress. Spent fuel test facility. Borehole ISS-8, borehole depth 67.8 feet. Climax Stock.
4.2.5.2-16	Mohr representation of in situ stress. Spent fuel test facility. Borehole ISS-8, borehole depth 81 feet. Climax Stock.

4.2.5.2-17 Mohr representation of in situ stress. Spent fuel test facility. Borehole ISS-8, borehole depth 96.7 feet. Climax Stock.

4.2.5.2-18 Mohr representation of in situ stress. Spent fuel test facility. Borehole ISS-8, borehole depth 109.4 feet. Climax Stock.

4.2.5.2-19 Mohr representation of in situ stress. Spent fuel test facility. Borehole ISS-9, borehole depth 39.1 feet. Climax Stock.

4.2.5.2-20 Mohr representation of in situ stress. Spent fuel test facility. Borehole ISS-9, borehole depth 42.6 feet. Climax Stock.

4.2.5.2-21 Mohr representation of in situ stress. Spent fuel test facility. Borehole ISS-9, borehole depth 46.9 feet. Climax Stock.

4.2.5.2-22 Mohr representation of in situ stress. Spent fuel test facility. Borehole ISS-9, borehole depth 50.5 feet. Climax Stock.

4.2.5.2-23 Mohr representation of in situ stress. Spent fuel test facility. Borehole ISS-9, borehole depth 59.2 feet. Climax Stock.

4.2.5.2-24 Mohr representation of in situ stress. Spent fuel test facility. Borehole ISS-10, borehole depth 64.4 feet. Climax Stock.

4.2.5.2-25 Mohr representation of in situ stress. Spent fuel test facility. Borehole ISS-10, borehole depth 67.8 feet. Climax Stock.

4.2.5.2-26 Mohr representation of in situ stress. Spent fuel test facility. Borehole ISS-10, borehole depth 73.1 feet. Climax Stock.

4.2.5.2-27 Mohr representation of in situ stress. Spent fuel test facility. Borehole ISS-10, borehole depth 80.4 feet. Climax Stock.

4.2.5.2-28 Mohr representation of in situ stress. Spent fuel test facility. Borehole ISS-11, borehole depth 70.6 feet. Climax Stock.

4.2.5.2-29 Mohr representation of in situ stress. Spent fuel test facility. Borehole ISS-11, borehole depth 75.5 feet. Climax Stock.

4.2.5.2-30 Mohr representation of in situ stress. Spent fuel test facility. Borehole ISS-11, borehole depth 84.3 feet. Climax Stock.

4.2.5.2-31 Mohr representation of in situ stress. Spent fuel test facility. Borehole ISS-11, borehole depth 89.4 feet. Climax Stock.

4.2.5.2-32 Mohr representation of in situ stress. Spent fuel test facility. Borehole ISS-11, borehole depth 94.5 feet. Climax Stock.

4.2.5.2-33 State of in situ stress. Summary. Climax Stock.

4.2.5.3-1 Geologic map of the Nevada Test Site showing location of Rainier Mesa and Aqueduct Mesa.

4.2.5.3-2 State of in situ stress. U12g tunnel, main drift bypass. Rainier Mesa.

4.2.5.3-3 Graphical representation of principal stresses. U12g tunnel, main drift bypass. Rainier Mesa.

4.2.5.3-4	State of in situ stress. U12e.06 drift. Rainier Mesa.
4.2.5.3-5	State of in situ stress. U12e.18 working point. Rainier Mesa.
4.2.5.3-6	Graphical representation of principal stresses. U12e tunnel complex. Rainier Mesa.
4.2.5.3-7	State of in situ stress. U12n.07 drift. Rainier Mesa.
4.2.5.3-8	State of in situ stress. U12n.10 working point. Rainier Mesa.
4.2.5.3-9	State of in situ stress. U12n.10A working point. Rainier Mesa.
4.2.5.3-10	State of in situ stress. U12n.10B structures drift. Rainier Mesa.
4.2.5.3-11	Graphical representation of principal stress, U12n tunnel complex. Rainier Mesa.
4.2.5.3-12	State of in situ stress. U12t.02 SRI alcove. Aqueduct Mesa.
4.2.5.3-13	State of in situ stress. U12t.03 working point. Aqueduct Mesa.
4.2.5.3-14	Graphical representation of prinicpal stresses. U12t tunnel complex. Aqueduct Mesa.
4.2.5.3-15	State of in situ stress. U12n tunnel. Rainier Mesa.
4.2.5.3-16	State of in situ stress. U12n and U12g tunnels. Rainier Mesa.
4.2.5.3-17	Mohr representation of in situ stress. U12g tunnel, main drift bypass. Rainier Mesa, Aqueduct Mesa.
4.2.5.3-18	Mohr representation of in situ stress. U12e.06 drift. Rainier Mesa, Aqueduct Mesa.
4.2.5.3-19	Mohr representation of in situ stress. U12e working point. Rainier Mesa, Aqueduct Mesa.
4.2.5.3-20	Mohr representation of in situ stress. U12n.07 drift. Rainier Mesa, Aqueduct Mesa.
4.2.5.3-21	Mohr representation of in situ stress. U12n.10 working point. Rainier Mesa, Aqueduct Mesa.
4.2.5.3-22	Mohr representation of in situ stress. U12n.10A working point. Rainier Mesa, Aqueduct Mesa.
4.2.5.3-23	Mohr representation of in situ stress. U12n.10B structures drift. Rainier Mesa, Aqueduct Mesa.
4.2.5.3-24	Mohr representation of in situ stress. U12t.02 SRI alcove. Rainier Mesa, Aqueduct Mesa.
4.2.5.3-25	Mohr representation of in situ stress. U12t.03 working point. Rainier Mesa, Aqueduct Mesa.
4.2.5.3-26	Mohr representation of in situ stress. U12n tunnel. Rainier Mesa, Aqueduct Mesa.

4.2.5.3-27	Mohr representation of in situ stress. U12n tunnel. Rainier Mesa, Aqueduct Mesa.
4.2.5.3-28	Mohr representation of in situ stress. U12n tunnel. Rainier Mesa, Aqueduct Mesa.
4.2.5.3-29	Mohr representation of in situ stress. U12n tunnel. Rainier Mesa, Aqueduct Mesa.
4.2.5.3-30	Mohr representation of in situ stress. U12n tunnel. Rainier Mesa, Aqueduct Mesa.
4.2.5.3-31	Mohr representation of in situ stress. U12n tunnel. Rainier Mesa, Aqueduct Mesa.
4.2.5.3-32	Mohr representation of in situ stress. U12n tunnel. Rainier Mesa, Aqueduct Mesa.
4.2.5.3-33	Mohr representation of in situ stress. U12n tunnel. Rainier Mesa, Aqueduct Mesa.
4.2.5.3-34	Mohr representation of in situ stress. U12n tunnel. Rainier Mesa, Aqueduct Mesa.
4.2.5.3-35	Mohr representation of in situ stress. U12n tunnel. Rainier Mesa, Aqueduct Mesa.
4.2.5.3-36	Mohr representation of in situ stress. U12n tunnel. Rainier Mesa, Aqueduct Mesa.
4.2.5.3-37	Mohr representation of in situ stress. U12n tunnel. Rainier Mesa, Aqueduct Mesa.
4.2.5.3-38	Mohr representation of in situ stress. U12n tunnel. Rainier Mesa, Aqueduct Mesa.
4.2.5.3-39	State of in situ stress. Summary. Rainier Mesa and Aqueduct Mesa.
4.2.5.4-1	Map showing location of hydrofracture wells in the area of Yucca Mountain.
4.2.5.4-2	Results of in situ stress determinations in Well USW G-1. Yucca Mountain.
4.2.5.4-3	Results of in situ stress determinations in Well USW G-2. Yucca Mountain.
4.2.5.4-4	Results of in situ stress determinations in Well USW G-3. Yucca Mountain.
4.2.5.4-5	Results of in situ stress determinations in Well UE-25p#1. Yucca Mountain.
4.2.5.4-6	Results of in situ stress determinations in Well UE-25p#1. Yucca Mountain.
4.2.5.4-7	Mohr representation of in situ stress. Borehole G-1, depth 646 m. Yucca Mountain.
4.2.5.4-8	Mohr representation of in situ stress. Borehole G-1, depth 792 m. Yucca Mountain.

4.2.5.4-9 Mohr representation of in situ stress. Borehole G-1, depth 945 m. Yucca Mountain.

4.2.5.4-10 Mohr representation of in situ stress. Borehole G-1, depth 1038 m. Yucca Mountain.

4.2.5.4-11 Mohr representation of in situ stress. Borehole G-1, depth 1218 m. Yucca Mountain.

4.2.5.4-12 Mohr representation of in situ stress. Borehole G-1, depth 1288 m. Yucca Mountain.

4.2.5.4-13 Mohr representation of in situ stress. Borehole G-2, depth 295 m. Yucca Mountain.

4.2.5.4-14 Mohr representation of in situ stress. Borehole G-2, depth 418 m. Yucca Mountain.

4.2.5.4-15 Mohr representation of in situ stress. Borehole G-2, depth 432 m. Yucca Mountain.

4.2.5.4-16 Mohr representation of in situ stress. Borehole G-2, depth 1026 m. Yucca Mountain.

4.2.5.4-17 Mohr representation of in situ stress. Borehole G-2, depth 1209 m. Yucca Mountain.

4.2.5.4-18 Mohr representation of in situ stress. Borehole G-3, depth 1074 m. Yucca Mountain.

4.2.5.4-19 Mohr representation of in situ stress. Borehole G-3, depth 1338 m. Yucca Mountain.

4.2.5.4-20 Mohr representation of in situ stress. Borehole G-3, depth 1356 m. Yucca Mountain.

4.2.5.4-21 Mohr representation of in situ stress. Borehole UE-25p#1, depth 731 m. Yucca Mountain.

4.2.5.4-22 Mohr representation of in situ stress. Borehole UE-25p#1, depth 1001 m. Yucca Mountain.

4.2.5.4-23 Mohr representation of in situ stress. Borehole UE-25p#1, depth 1131 m. Yucca Mountain.

4.2.5.4-24 Mohr representation of in situ stress. Borehole UE-25p#1, depth 1564 m. Yucca Mountain.

4.2.5.4-25 Mohr representation of in situ stress. Borehole UE-25p#1, depth 1573 m. Yucca Mountain.

4.2.5.4-26 Mohr representation of in situ stress. Borehole UE-25p#1, depth 1693 m. Yucca Mountain.

4.2.5.4-27 Interpretation key for the Cooper-Bredehoeft injection tests performed in the Yucca Mountain area.

4.2.5.4-28 Location of wells where the Cooper-Bredehoeft injection tests were performed.

4.2.5.4-29 Results of the Cooper-Bredehoeft injection tests in Well USW H-1.
4.2.5.4-30 Results of the Cooper-Bredehoeft injection tests in Well USW H-1.
4.2.5.4-31 Results of the Cooper-Bredehoeft injection tests in Well USW H-1.
4.2.5.4-32 Results of the Cooper-Bredehoeft injection tests in Well USW H-6.
4.2.5.4-33 Results of the Cooper-Bredehoeft injection tests in Well USW H-6.
4.2.5.4-34 Results of the Cooper-Bredehoeft injection tests in Well UE-25b#1.
4.2.5.4-35 Results of the Cooper-Bredehoeft injection tests in Well USW H-1.
4.2.5.4-36 Results of the Cooper-Bredehoeft injection tests in Well USW H-3.
4.2.5.4-37 Results of the Cooper-Bredehoeft injection tests in Well USW H-3.
4.2.5.4-38 Results of the Cooper-Bredehoeft injection tests in Well USW H-3.
4.2.5.4-39 Results of the Cooper-Bredehoeft injection tests in Well USW H-4.
4.2.5.4-40 Results of the Cooper-Bredehoeft injection tests in Well USW H-5.
4.2.5.4-41 Results of the Cooper-Bredehoeft injection tests in Well USW H-5.
4.2.5.4-42 Results of the Cooper-Bredehoeft injection tests in Well USW H-5.
4.2.5.4-43 Results of the Cooper-Bredehoeft injection tests in Well USW H-5.
4.2.5.4-44 Results of the Cooper-Bredehoeft injection tests in Well USW H-6.
4.2.5.4-45 Results of the Cooper-Bredehoeft injection tests in Well USW H-6.
4.2.5.4-46 Results of the Cooper-Bredehoeft injection tests in Well UE-25b#1.
4.2.5.4-47 Results of the Cooper-Bredehoeft injection tests in Well UE-25b#1.
4.2.5.4-48 Results of the Cooper-Bredehoeft injection tests in Well USW G-4.
4.2.5.4-49 Results of the Cooper-Bredehoeft injection tests in Well USW H-3.
4.2.5.4-50 Results of the Cooper-Bredehoeft injection tests in Well USW H-4.
4.2.5.4-51 Results of the Cooper-Bredehoeft injection tests in Well USW H-4.
4.2.5.4-52 Results of the Cooper-Bredehoeft injection tests in Well USW H-4.
4.2.5.4-53 Results of the Cooper-Bredehoeft injection tests in Well USW H-4.
4.2.5.4-54 Results of the Cooper-Bredehoeft injection tests in Well USW H-4.
4.2.5.4-55 Results of the Cooper-Bredehoeft injection tests in Well USW H-4.
4.2.5.4-56 Results of the Cooper-Bredehoeft injection tests in Well USW H-4.
4.2.5.4-57 Results of the Cooper-Bredehoeft injection tests in Well USW H-5.
4.2.5.4-58 Results of the Cooper-Bredehoeft injection tests in Well USW H-5.

4.2.5.4-59 Results of the Cooper-Bredehoeft injection tests in Well USW H-5.
4.2.5.4-60 Results of the Cooper-Bredehoeft injection tests in Well USW H-6.
4.2.5.4-61 Results of the Cooper-Bredehoeft injection tests in Well USW H-6.
4.2.5.4-62 Results of the Cooper-Bredehoeft injection tests in Well UE-25b#1.
4.2.5.4-63 Results of the Cooper-Bredehoeft injection tests in Well UE-25b#1.
4.2.5.4-64 Results of the Cooper-Bredehoeft injection tests in Well UE-25b#1.
4.2.5.4-65 Results of the Cooper-Bredehoeft injection tests in Well UE-25b#1.
4.2.5.4-66 Results of the Cooper-Bredehoeft injection tests in Well UE-25p#1.
4.2.5.4-67 Results of the Cooper-Bredehoeft injection tests in Well UE-25p#1.
4.2.5.4-68 Results of the Cooper-Bredehoeft injection tests in Well USW G-4.
4.2.5.4-69 Results of the Cooper-Bredehoeft injection tests in Well USW G-4.
4.2.5.4-70 Results of the Cooper-Bredehoeft injection tests in Well USW G-4.
4.2.5.4-71 Results of the Cooper-Bredehoeft injection tests in Well USW H-4.
4.2.5.4-72 Results of the Cooper-Bredehoeft injection tests in Well USW H-5.
4.2.5.4-73 Results of the Cooper-Bredehoeft injection tests in Well USW H-5.
4.2.5.4-74 Results of the Cooper-Bredehoeft injection tests in Well USW H-6.
4.2.5.4-75 Results of the Cooper-Bredehoeft injection tests in Well USW H-6.
4.2.5.4-76 Results of the Cooper-Bredehoeft injection tests in Well USW H-6.
4.2.5.4-77 Results of the Cooper-Bredehoeft injection tests in Well UE-25b#1.
4.2.5.4-78 Results of the Cooper-Bredehoeft injection tests in Well UE-25b#1.
4.2.5.4-79 Results of the Cooper-Bredehoeft injection tests in Well UE-25b#1.
4.2.5.4-80 Results of the Cooper-Bredehoeft injection tests in Well UE-25p#1.
4.2.5.4-81 Results of the Cooper-Bredehoeft injection tests in Well UE-25p#1.
4.2.5.4-82 Results of the Cooper-Bredehoeft injection tests in Well UE-25p#1.
4.2.5.4-83 Results of the Cooper-Bredehoeft injection tests in Well UE-25p#1.
4.2.5.4-84 Results of the Cooper-Bredehoeft injection tests in Well UE-25p#1.
4.2.5.4-85 Results of the Cooper-Bredehoeft injection tests in Well UE-25p#1.
4.2.5.4-86 Results of the Cooper-Bredehoeft injection tests in Well UE-25p#1.

4.2.5.4-87	Results of the Cooper-Bredehoeft injection tests in Well UE-25p#1.
4.2.5.4-88	Results of the Cooper-Bredehoeft injection tests in Well UE-25p#1.
4.2.5.4-89	Results of the Cooper-Bredehoeft injection tests in Well UE-25p#1.
4.2.5.4-90	Results of the Cooper-Bredehoeft injection tests in Well UE-25p#1.
4.2.5.4-91	Results of the Cooper-Bredehoeft injection tests in Well USW G-4.
4.2.5.4-92	Results of the Cooper-Bredehoeft injection tests in Well USW G-4.
4.2.5.4-93	Results of the Cooper-Bredehoeft injection tests in Well USW G-4.
4.2.5.4-94	Results of the Cooper-Bredehoeft injection tests in Well USW G-4.
4.2.5.4-95	State of in situ stress. Summary. Yucca Mountain.
4.2.5.4-96	State of in situ stress. Summary. Yucca Mountain.
4.2.5.4-97	Location map for in situ stress cross-sections. Yucca Mountain.
4.2.5.4-98	In situ stress field. NW-SE cross-section. Yucca Mountain.
4.2.5.4-99	In situ stress field. W-E cross-section. Yucca Mountain.
4.3.2-1	Location of wells in which temperature measurements were made.
4.3.2-2	Composite temperature profile. Pahute Mesa.
4.3.2-3	Composite temperature profile for Rainier Mesa and environments.
4.3.2-4	Composite temperature profile for Yucca Flat area.
4.3.2-5	Composite plot of temperatures below 100 m. Syncline Ridge area.
4.3.2-6	Composite temperature profile for the southern NTS.
4.3.2-7	Temperatures in wells deeper than 600 m. Yucca Mountain.
4.3.2-8	Downhole in situ temperatures at a depth of 500 m. Nevada Test Site.
4.3.2-9	Distribution of in situ temperature at a depth of 500 m. Nevada Test Site.
4.3.3-1	Location map-thermal data. Yucca Mountain.
4.3.3-2	Location map-thermal data. Yucca Mountain.
4.3.3-3	Well J-13. Temperature profile.
4.3.3-4	Well UE-25a. Temperature profile.
4.3.3-5	Well UE-25b. Temperature profile.
4.3.3-6	Well UE-25p#1. Temperature profile.
4.3.3-7	Well USW VH-1. Temperature profile.
4.3.3-8	Well USW VH-2. Temperature profile.

4.3.3-9 Well USW G-1. Temperature profile.
4.3.3-10 Well USW G-2. Temperature profile.
4.3.3-11 Well USW G-3. Temperature profile.
4.3.3-12 Well USW G-4. Temperature profile.
4.3.3-13 Well USW H-1. Temperature profile.
4.3.3-14 Well USW H-3. Temperature profile.
4.3.3-15 Well USW H-4. Temperature profile.
4.3.3-16 Well USW H-5. Temperature profile.
4.3.3-17 Well USW H-6. Temperature profile.
4.3.3-18 Well UE-25a No. 4. Temperature profile.
4.3.3-19 Well UE-25a No. 5. Temperature profile.
4.3.3-20 Well UE-25a No. 6. Temperature profile.
4.3.3-21 Well UE-25a No. 7. Temperature profile.
4.3.3-22 Well UZ-1. Temperature profile.
4.3.3-23 Well USW WT-1. Temperature profile.
4.3.3-24 Well USW WT-2. Temperature profile.
4.3.3-25 Well UE-25 WT-3. Temperature profile.
4.3.3-26 Well UE-25 WT-4. Temperature profile.
4.3.3-27 Well UE-25 WT-5. Temperature profile.
4.3.3-28 Well UE-25 WT-6. Temperature profile.
4.3.3-29 Well USW WT-7. Temperature profile.
4.3.3-30 Well USW WT-10. Temperature profile.
4.3.3-31 Well USW WT-11. Temperature profile.
4.3.3-32 Well UE-25 WT-12. Temperature profile.
4.3.3-33 Well UE-25 WT-13. Temperature profile.
4.3.3-34 Well UE-25 WT-14. Temperature profile.
4.3.3-35 Well UE-25 WT-15. Temperature profile.
4.3.3-36 Well UE-25 WT-16. Temperature profile.
4.3.3-37 Well UE-25 WT-17. Temperature profile.
4.3.3-38 Well UE-25 WT-18. Temperature profile.
4.3.3-39 Thermal conductivities from the Tertiary tuff "pile" in Well USW G-1.

4.3.3-39a	Thermal conductivities from the Tertiary tuff "pile" in Well USW G-1.
4.3.3-39b	Thermal conductivities from the Tertiary tuff "pile" in Well USW G-1.
4.3.3-40	Thermal conductivities from the Tertiary tuff "pile" in Well USW G-2.
4.3.3-40a	Thermal conductivities from the Tertiary tuff "pile" in Well USW G-2.
4.3.3-40b	Thermal conductivities from the Tertiary tuff "pile" in Well USW G-2.
4.3.3-41	Thermal conductivities from the Tertiary tuff "pile" in Well USW G-3.
4.3.3-41a	Thermal conductivities from the Tertiary tuff "pile" in Well USW G-3.
4.3.3-41b	Thermal conductivities from the Tertiary tuff "pile" in Well USW G-3.
4.3.3-42	Thermal conductivities from the Tertiary tuff "pile" in Well USW G-4.
4.3.3-42a	Thermal conductivities from the Tertiary tuff "pile" in Well USW G-4.
4.3.3-43	Thermal conductivities from Paleozoic carbonates.
4.3.3-44	Location map. Thermal cross-sections for Yucca Moutnain.
4.3.3-45	Location map. Thermal cross-sections for Yucca Mountain.
4.3.3-46	Summary of thermal data. NNW-SSE cross-section. Yucca Mountain.
4.3.3-46a	NNW-SSE thermal cross-section. Yucca Mountain.
4.3.3-47	Summary of thermal data. NW-SE cross-section. Yucca Mountain.
4.3.3-47a	NW-SE thermal cross-section. Yucca Mountain.
4.3.3-48	Summary of thermal data. E-W cross-section. Yucca Mountain.
4.3.3-48a	E-W thermal cross-section. Yucca Mountain.
4.3.3-49	Temperature profiles. Vadose zone at Yucca Mountain.
4.3.3-50	In situ temperatures at a depth of 350 m. Yucca Mountain-vadose zone.
4.3.3-51	Histogram of thermal conductivities from the Tertiary tuff "pile." Yucca Mountain.
4.3.3-52	Average thermal conductivities. Yucca Mountain.
4.3.3-53	Estimates of heat flow. Yucca Mountain.
4.3.3-54	$\partial^{13}C$ ratios and calcite saturation indexes for water samples from Yucca Mountain.
4.3.4-1	Location of boreholes where calcite samples from Yucca Mountain were collected.
4.3.4-2	Analytical data from fracture filling calcites from Yucca Mountain.
4.3.4-2a	Analytical data from fracture filling calcites from Yucca Mountain (continued).

4.3.4-3 Calculated uranium series ages of fracture filling calcite from Yucca Mountain.

4.3.4-4 $\partial^{18}O$ versus $\partial^{13}C$ ratios for calcites from Yucca Mountain.

4.3.4-5 Estimate of paleo-temperatures based on stable isotope content of calcites from Yucca Mountain.

4.3.4-6 Comparison of contemporary and Late Quaternary in situ temperatures at Yucca Mountain.

4.4.1-1 Potential increase of pore pressure caused by vibratory ground motion.

4.4.1-2 Location of geodetic survey networks. Handley event, Pahute Mesa.

4.4.1-3 Location of leveling lines. Handley event, Pahute Mesa.

4.4.1-4 Vertical displacements produced by Handley event.

4.4.1-5 Principal horizontal displacements produced by Handley event within triangulation network B.

4.4.1-6 Principal horizontal strains produced by Handley event within quadrilateral networks P and G.

4.4.2-1 Location of detonation site of the Aardvark event.

4.4.2-2 Observed and calculated histories of groundwater levels in test Well #7. Aardvark event.

4.4.2-3 Calculated configuration of the groundwater mound produced by the Aardvark event as a function of time.

4.4.3-1 Location of detonation site of the Bilby nuclear device.

4.4.3-2 Fluid overpressure caused by the Bilby event.

4.4.3-3 History of groundwater level in test Well #U-3cn-4 after the Bilby event.

4.4.3-4 History of groundwater level in Well #7 after the Bilby event.

4.4.3-5 Fluid level rise in U-3cn PS#2.

4.4.4-1 Location of detonation site of the Handley nuclear device.

4.4.4-2 Location of offsite wells monitored during the Handley event.

4.4.4-3 Dynamic fluid overpressure produced by the Handley detonation.

4.4.4-4 Pressure response observed in two wells at the Amargosa Tracer Site, at a distance of 90 km from the Handley detonation site.

4.4.4-5 Location of monitoring wells at Pahute Mesa. Handley detonation.

4.4.4-6 Hydrologic response in Pahute Mesa to the Handley detonation.

4.4.4-7 Hydrologic response to the Handley event in Well UE-20f.

4.4.4-8 Hydrologic response to the Handley event in Well UE-20p.

4.4.5-1	Increased discharge from a seep caused by the April 10, 1986 nuclear detonation.
4.4.5-2	Change in aqueous chemistry caused by the April 6, 1985 nuclear detonation.
4.4.5-3	Change in aqueous chemistry caused by the April 6, 1985 nuclear detonation.
4.4.5-4	Change in aqueous chemistry caused by the April 10, 1986 nuclear detonation.
4.4.5-5	Change in aqueous chemistry caused by the April 10, 1986 nuclear detonation.
4.4.5-6	Stiff diagram of aqueous chemistry before and after the April 6, 1985 nuclear detonation.
4.4.5-7	Stiff diagram of aqueous chemistry before and after the April 10, 1986 nuclear detonation.
4.4.5-8	Change in deuterium content caused by two nuclear detonations.
4.4.5-9	Change in oxygen-18 content caused by two nuclear detonations.
4.5.2-1	Location of hydrologic features considered in Section 4.5.2.
4.5.2.3-1	General hydrology of Yucca Flat and Frenchman Flat. Nevada Test Site.
4.5.2.3-2	Potentiometric setting of the Skull Mountain area. Nevada Test Site.
4.5.2.3-3	Local hydrologic conditions near Skull Mountain. Nevada Test Site.
4.5.2.3-3a	Explanation of symbols used on Plate 4.5.2.3-3.
4.5.2.3-4	Results of chemical analyses of water samples from Well #68-69 and Well #73-66.
4.5.2.4-1	Potentiometric setting of Rainier Mesa.
4.5.2.4-2	Schematic diagram illustrating local hydrology of Rainier Mesa.
4.5.2.4-3	Results of chemical anlayses of interstitial water. Core U12T3. Rainier Mesa.
4.5.2.4-4	Results of chemical analyses of fracture water. Tunnels in Rainier Mesa.
4.5.2.4-5	Comparison of cation ratios in fracture and interstitial waters. Rainier Mesa.
4.5.2.4-6	Comparison of anion ratios in fracture and interstitial waters. Rainier Mesa.
4.5.2.5-1	Geologic setting of the Climax Stock area.
4.5.2.5-2	Potentiometric setting of the Climax Stock area.
4.5.2.5-3	Location of exploratory boreholes. The area of Climax Stock.

4.5.2.5-4	The results of chemical and radiochemical analyses of water samples from Climax Stock.
4.5.2.5-5	Location of water samples. Climax Stock.
4.5.2.5-6	The results of chemical analyses of 5 water samples from Climax Stock.
4.5.2.5-6a	The results of chemical analyses of 5 water samples from Climax Stock.
4.5.2.5-7	The results of isotopic analyses of water samples from Climax Stock.
4.5.2.5-8	Selected mineral saturation indexes for Climax perched waters.
4.5.2.5-9	Environmental isotope data for groundwater samples from the tuff and tuffaceous valley fill aquifers in the region near Yucca Mountain.
4.5.2.5-10	Environmental isotope data for groundwater samples from the carbonate aquifer and from mixed carbonate-tuff sources.
4.5.2.5-11	Comparison of chemical composition of Climax Stock perched water with spring waters discharging from the Paleozoic carbonates.
4.5.3-1	Location of samples analyzed and dated by Szabo et al., 1981.
4.5.3-2	Location of samples analyzed and dated by Knauss, 1981.
4.5.3-3	Description of samples analyzed and dated by Szabo et al., 1981.
4.5.3-3a	Description of samples analyzed and dated by Szabo et al., 1981.
4.5.3-3b	Description of samples analyzed and dated by Szabo et al., 1981.
4.5.3-3c	Description of samples analyzed and dated by Szabo et al., 1981.
4.5.3-4	Description of samples analyzed and dated by Knauss, 1981.
4.5.3-4a	Description of samples analyzed and dated by Knauss, 1981.
4.5.3-4b	Description of samples analyzed and dated by Knauss, 1981.
4.5.3-4c	Description of samples analyzed and dated by Knauss, 1981.
4.5.3-4d	Description of samples analyzed and dated by Knauss, 1981.
4.5.3-4e	Description of samples analyzed and dated by Knauss, 1981.
4.5.3-4f	Description of samples analyzed and dated by Knauss, 1981.
4.5.3-4g	Description of samples analyzed and dated by Knauss, 1981.
4.5.3-5	Analytical data and uranium series ages of carbonates at the Nevada Test Site.
4.5.3-5a	Analytical data and uranium series ages of carbonates at the Nevada Test Site.
4.5.3-5b	Analytical data and uranium series ages of carbonates at the Nevada Test Site.

4.5.3-5c	Analytical data and uranium series ages of carbonates at the Nevada Test Site.
4.5.3-6	Analytical data for carbonates from the Nevada Test Site.
4.5.3-6a	Analytical data for carbonates from the Nevada Test Site.
4.5.3-6b	Analytical data for carbonates from the Nevada Test Site.
4.5.3-7	Ages of carbonates from the Nevada Test Site.
4.5.3-8	Idealization of contemporary and paleo-hydrologic conditions between Death Valley and Amargosa Desert.
4.5.3-9	Location of faults containing calcite-silica veins of Quaternary age. Yucca Mountain.
4.5.3-10	Geologic section across Yucca Mountain showing location and thickness of breccias.
4.5.3-11	Photograph of the calcite-silica veins emplaced in the Late Miocene bedrock. Yucca Mountain.
4.5.3-12	Photograph of the calcite-silica veins and aprons emplaced within Late Quaternary eolian sediments. Yucca Mountain area.
4.5.3-13	Comparison of stable isotope composition of three samples of calcite-silica veins with isotopic composition of calcite veins from subsurface.
4.5.3-14	Comparison of temperature of formation of calcite-silica deposits, based isotopic composition of three samples, with contemporary temperature at Yucca Mountain.

TRANSIENT OR NON-EQUILIBRIUM FLOW	STEADY STATE FLOW	GOVERNING EQUATION CONTINUITY EQUATION. LAW RELATING VELOCITY VECTOR TO THE GRADIENT OF HYDRAULIC POTENTIAL.
		BOUNDARY CONDITIONS DIRICHLET CONDITIONS; NEUMANN CONDITIONS; AND "MIXED CONDITIONS.
		INITIAL CONDITIONS SET OF HYDRAULIC POTENTIAL VALUES AT THE ONSET OF NON-EQUILIBRIUM FLOW.

Mathematical model of "simple" groundwater system.

CONTINUITY EQUATION

$$\frac{\partial q_x}{\partial x} + \frac{\partial q_y}{\partial y} + \frac{\partial q_z}{\partial z} = 0$$

DARCY'S LAW

$$q_x = -K\frac{\partial h}{\partial x}; \quad q_y = -K\frac{\partial h}{\partial y}; \quad q_z = -K\frac{\partial h}{\partial z}$$

LAPLACE'S EQUATION

$$\frac{\partial^2 h}{\partial x^2} + \frac{\partial^2 h}{\partial y^2} + \frac{\partial^2 h}{\partial z^2} = 0; \text{ or}$$

$$\nabla^2 h = 0$$

Laplace's equation.

CONTINUITY EQUATION

$$\frac{\partial q_x}{\partial x} + \frac{\partial q_y}{\partial y} + \frac{\partial q_z}{\partial z} = R_{(x,y,z)} \cdot \triangle z^{-1}$$

DARCY'S LAW

$$q_x = -K\frac{\partial h}{\partial x}; \quad q_y = -K\frac{\partial h}{\partial y}; \quad q_z = -K\frac{\partial h}{\partial z}$$

POISSON'S EQUATION

$$\frac{\partial^2 h}{\partial x^2} + \frac{\partial^2 h}{\partial y^2} + \frac{\partial^2 h}{\partial z^2} = -R_{(x,y,z)} \cdot T^{-1}; \text{ or}$$

$$\nabla^2 h = -R_{(x,y,z)} \cdot T^{-1}$$

Poisson's equation.

CONTINUITY EQUATION

$$\frac{\partial q_x}{\partial x} + \frac{\partial q_y}{\partial y} + \frac{\partial q_z}{\partial z} = R_{(x,y,z,t)} \cdot \triangle z^{-1} - S \cdot \triangle z^{-1} \frac{\partial h}{\partial t}$$

DARCY'S LAW

$$q_x = -K \frac{\partial h}{\partial x}; \quad q_y = -K \frac{\partial h}{\partial y}; \quad q_z = -K \frac{\partial h}{\partial z}$$

TRANSIENT FLOW EQUATION

$$\frac{\partial^2 h}{\partial x^2} + \frac{\partial^2 h}{\partial y^2} + \frac{\partial^2 h}{\partial z^2} = S \cdot T^{-1} \frac{\partial h}{\partial t} - R_{(x,y,z,t)} \cdot T^{-1}; \text{ or}$$

$$\nabla^2 h = S \cdot T^{-1} \frac{\partial h}{\partial t} - R_{(x,y,z,t)} \cdot T^{-1}$$

Transient flow equation.

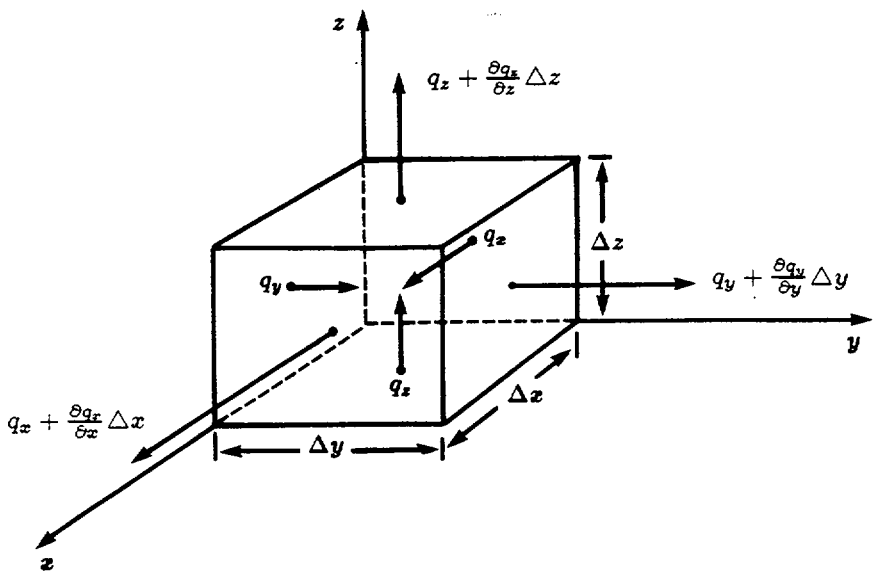

$\Delta V = \Delta x \Delta y \Delta z$ - VOLUME;

$\frac{\partial q_x}{\partial x}\Delta V$ - NET CHANGE IN THE DISCHARGE RATE IN x DIRECTION;

$\frac{\partial q_y}{\partial y}\Delta V$ - NET CHANGE IN THE DISCHARGE RATE IN y DIRECTION;

$\frac{\partial q_z}{\partial z}\Delta V$ - NET CHANGE IN THE DISCHARGE RATE IN z DIRECTION;

$R_{(x,y,z)}$ - VOLUME OF WATER ADDED PER UNIT TIME PER UNIT AQUIFER VOLUME TO THE INFINITESIMAL VOLUME AROUND A POINT $P_{(x,y,z)}$;

$S = \frac{-\Delta V w}{\Delta x \Delta y \Delta h}$ - STORATIVITY, REPRESENTS VOLUME OF WATER RELEASED FROM STORAGE PER UNIT AREA OF AQUIFER PER UNIT DECLINE IN HEAD;

$\frac{\Delta V w}{\Delta t} = -S\frac{\partial h}{\partial t}\Delta x \Delta y$ - RATE OF FLUID RELEASE FROM STORAGE;

T - TRANSMISSIVITY.

Explanation of mathematical notations.

LAPLACE'S EQUATION

$$\frac{\partial}{\partial x}(K_x \frac{\partial h}{\partial x}) + \frac{\partial}{\partial y}(K_y \frac{\partial h}{\partial y}) + \frac{\partial}{\partial z}(K_z \frac{\partial h}{\partial z}) = 0$$

POISSON'S EQUATION

$$\frac{\partial}{\partial x}(T_x \frac{\partial h}{\partial x}) + \frac{\partial}{\partial y}(T_y \frac{\partial h}{\partial y}) + \frac{\partial}{\partial z}(T_z \frac{\partial h}{\partial z}) = -R_{(x,y,z)}$$

TRANSIENT FLOW EQUATION

$$\frac{\partial}{\partial x}(T_x \frac{\partial h}{\partial x}) + \frac{\partial}{\partial y}(T_y \frac{\partial h}{\partial y}) + \frac{\partial}{\partial z}(T_z \frac{\partial h}{\partial z}) = S\frac{\partial h}{\partial t} - R_{(x,y,z,t)}$$

Flow equations written in a form allowing for consideration of aquifer heterogeneity and anisotropy.

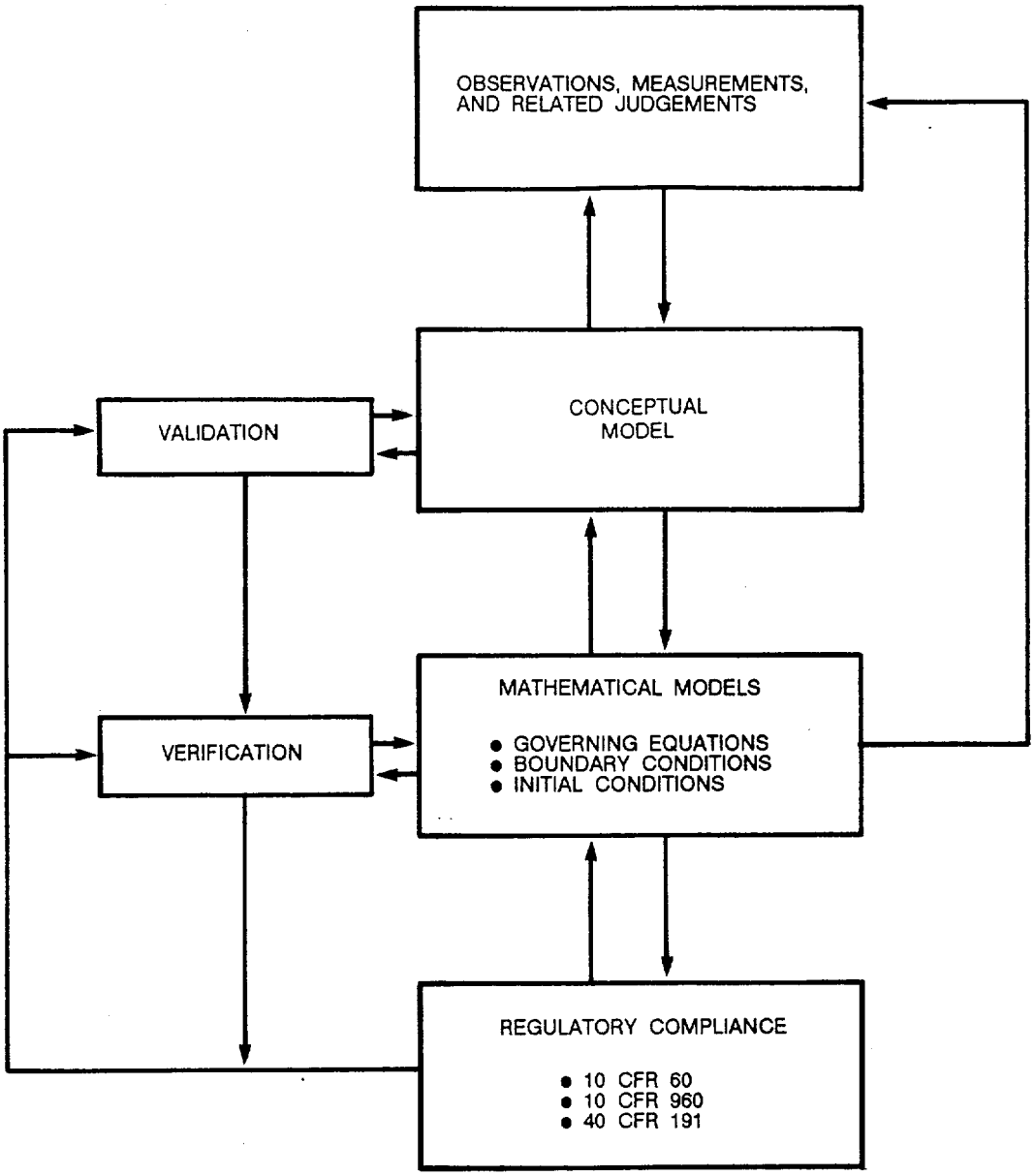

Role of mathematical and conceptual models.

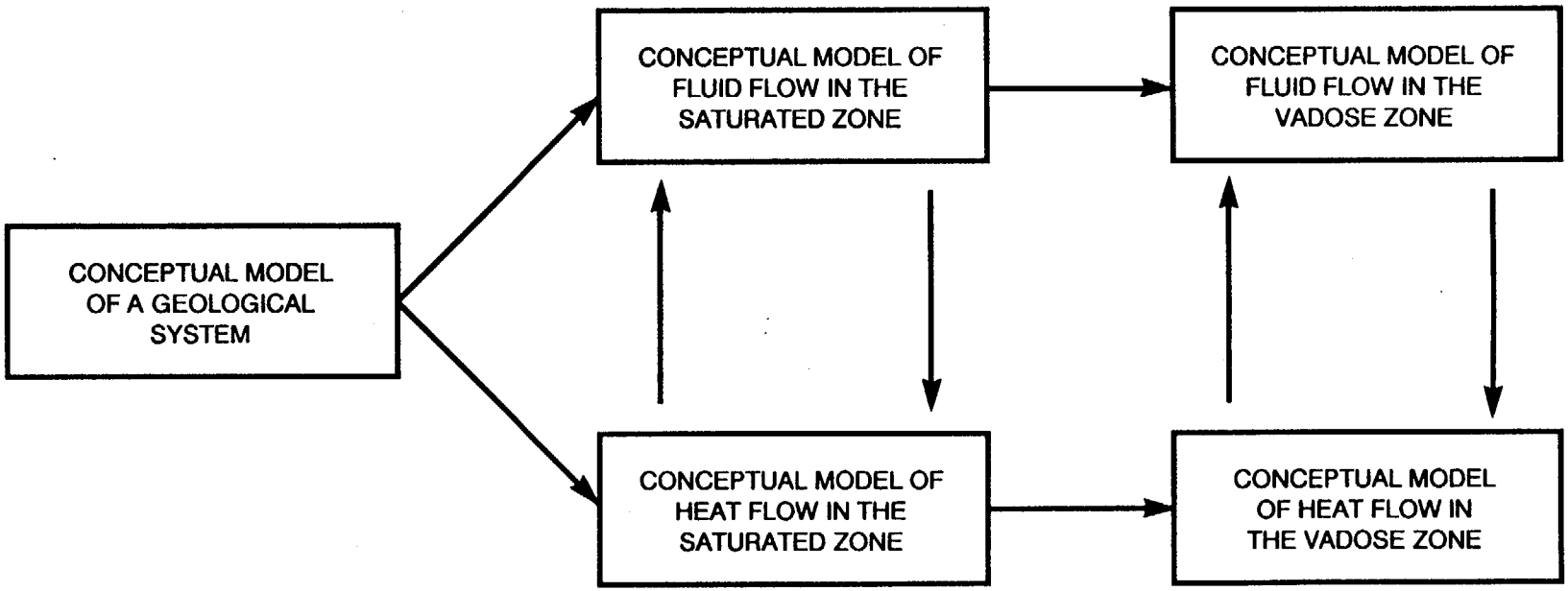

NOTE: CONCEPTUAL MODEL OF A SUBSYSTEM MUST NOT BE TREATED IN ISOLATION FROM THE GEOLOGICAL SYSTEM OF WHICH IT IS ONLY A PART.

Interdependence of conceptual models.

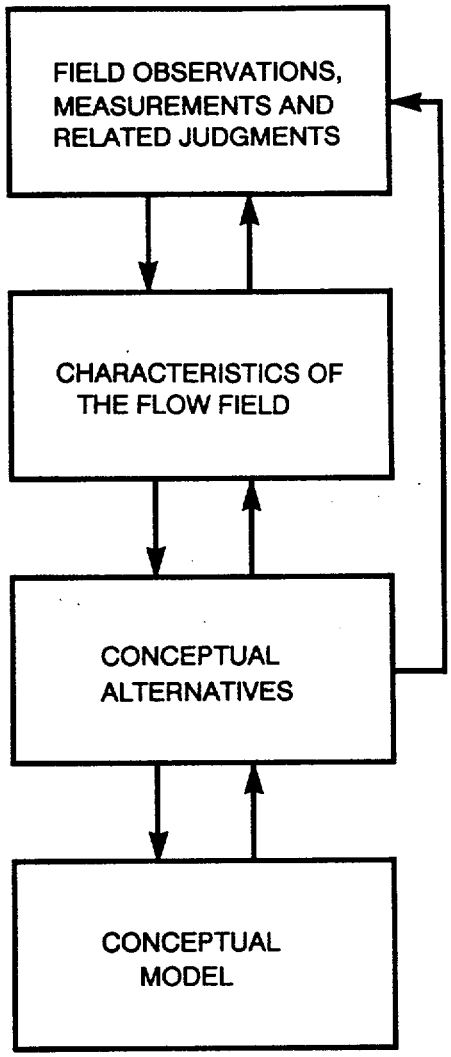

Conceptual model of a groundwater system.

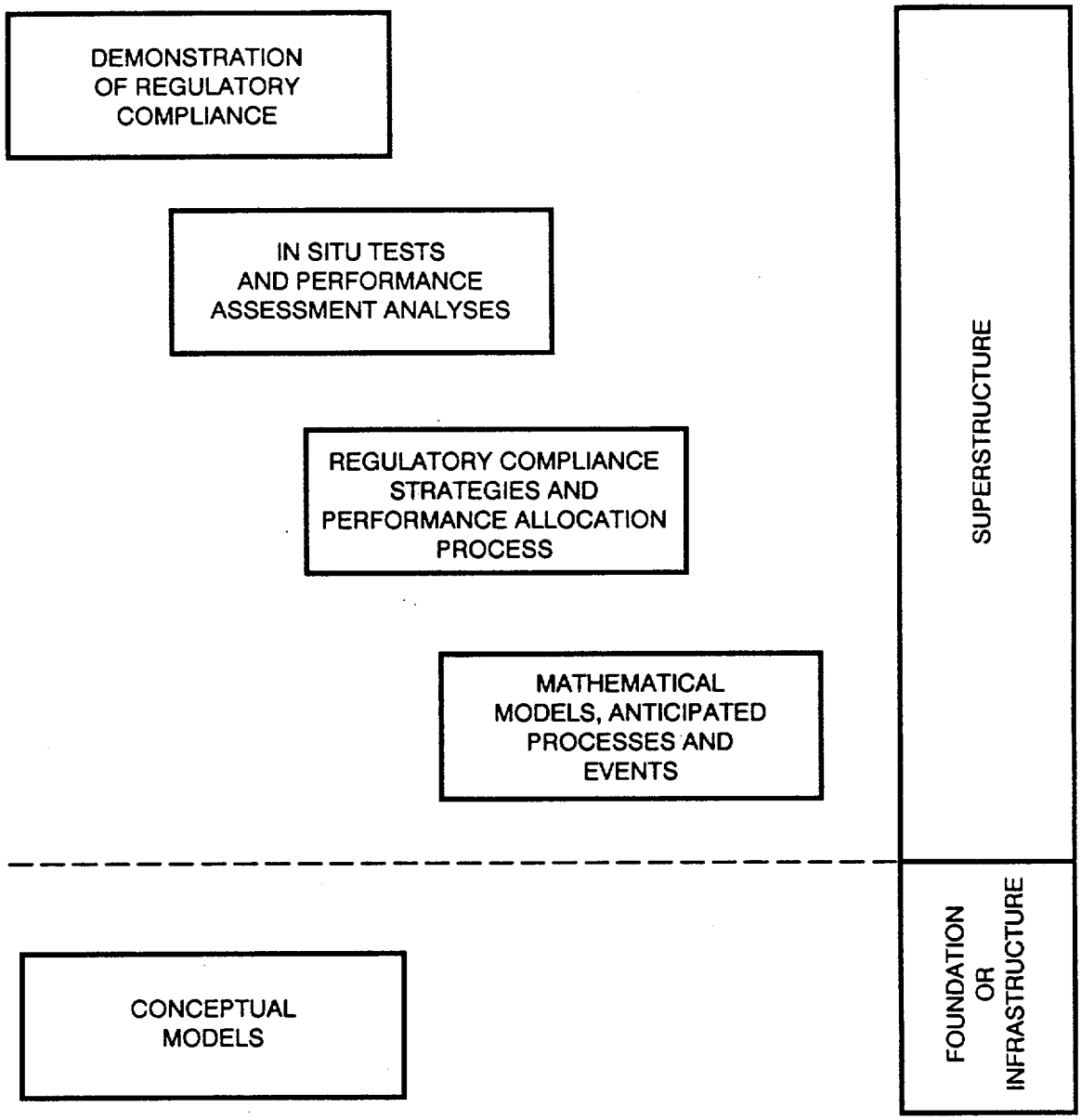

Importance of conceptual models.

plate 2.3.-4

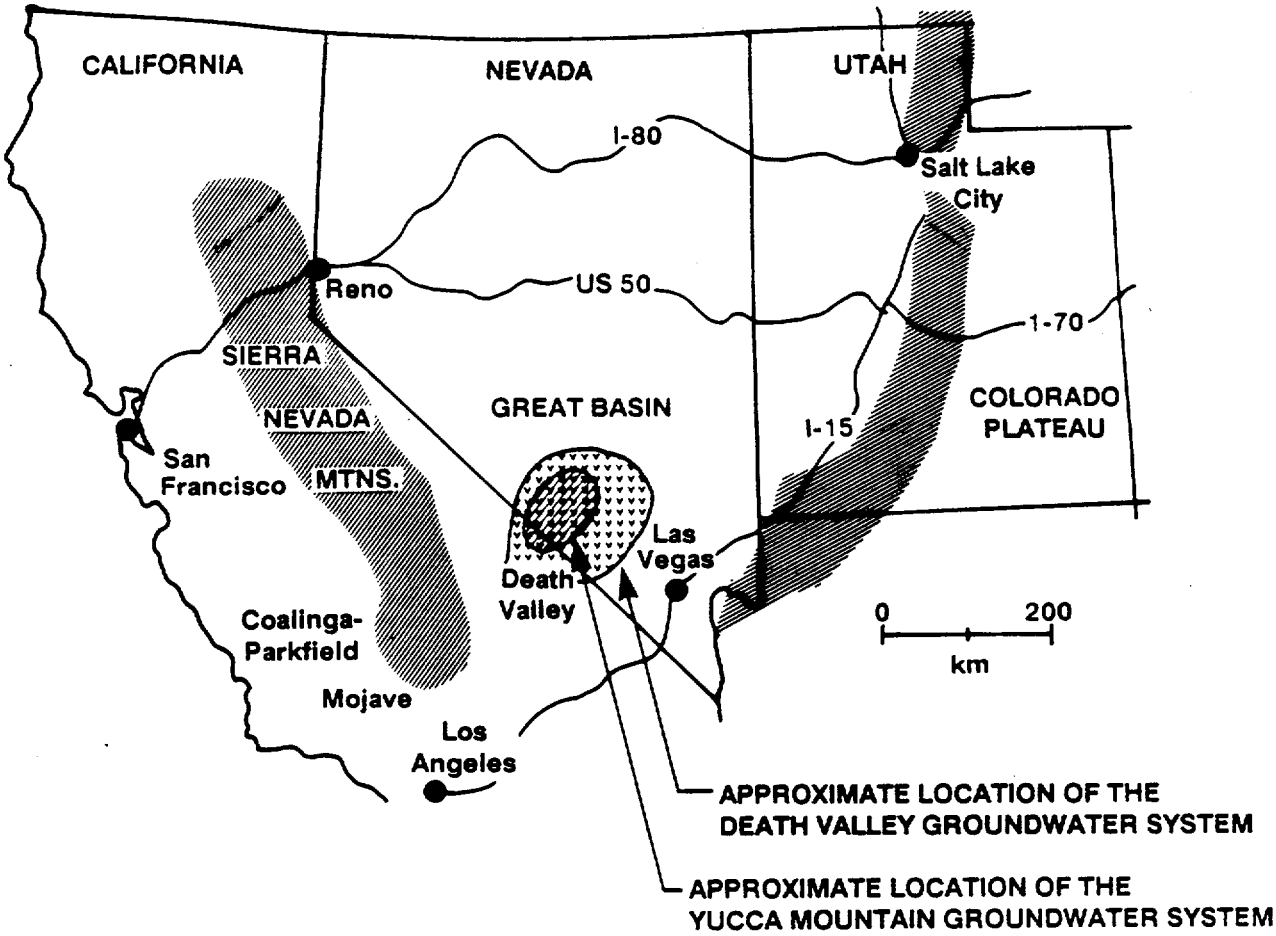

Location of the Death Valley groundwater system within the Great Basin.

plate 3.1-1

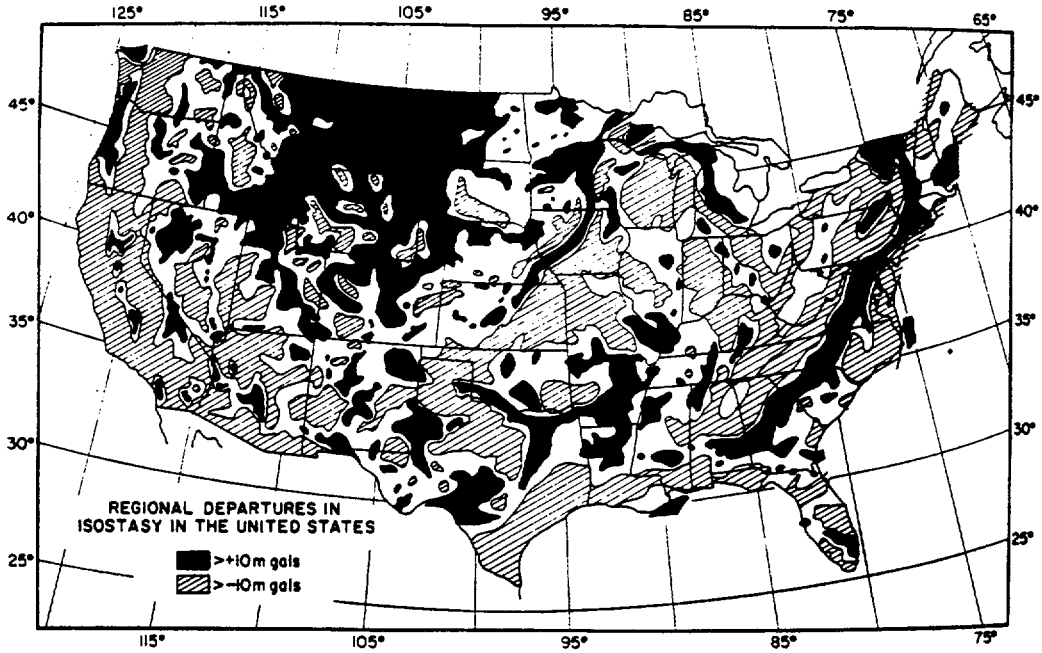

NOTE:
MASS DEFICIENCY IN THE AREA OF SOUTH CENTRAL GREAT BASIN CAN BE ACCOUNTED FOR BY ASSUMING THAT ISOSTATIC COMPENSATION IS ACHIEVED EITHER BY THE AIRY-HEISKANEN MECHANISM OR BY THE PRATT-HAYFORD MECHANISM.

Simplified isostatic anomaly map of the United States. From Woolard, 1969.

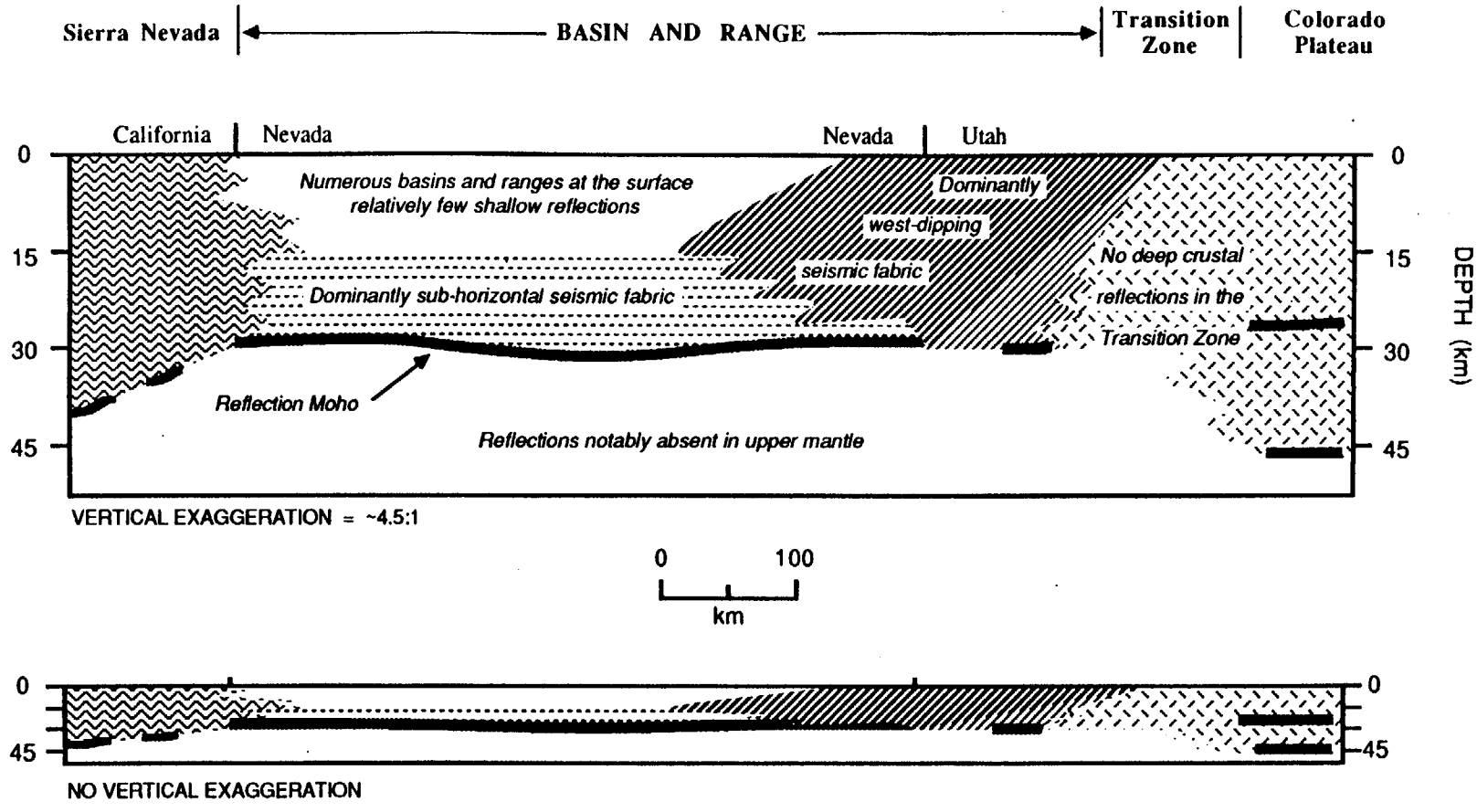

Configuration of the crust in north-central Great Basin. Based on COCORP 40° N transect. From Allmendinger, et al., 1987.

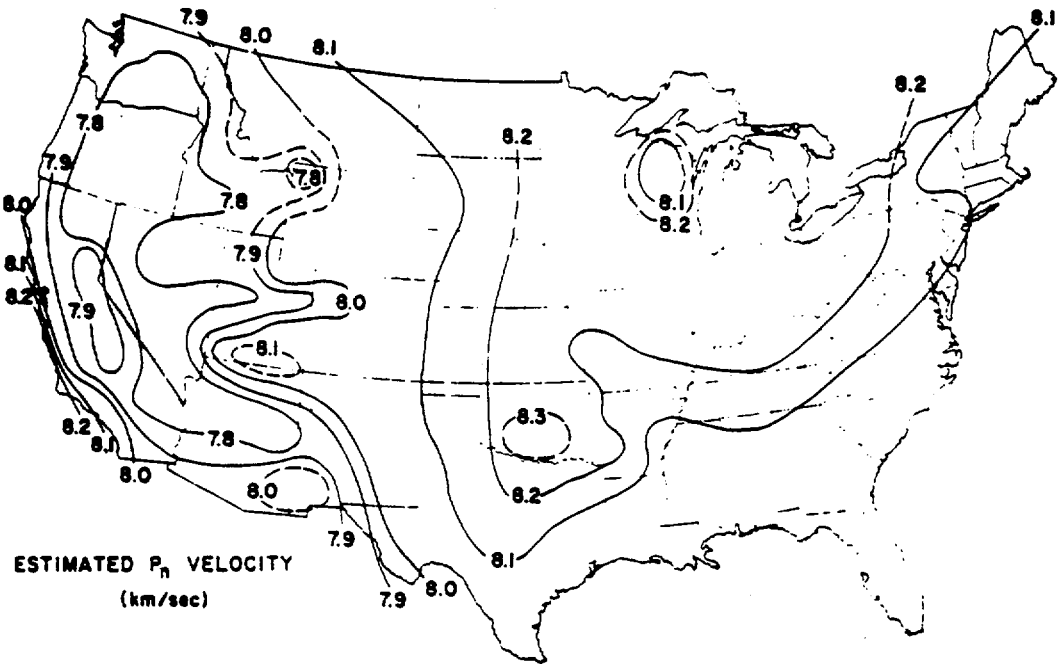

Estimated P-wave velocity in the upper mantle of the continental United States, based on deep seismic soundings, nuclear explosions, and earthquakes. From E. Herrin, 1969.

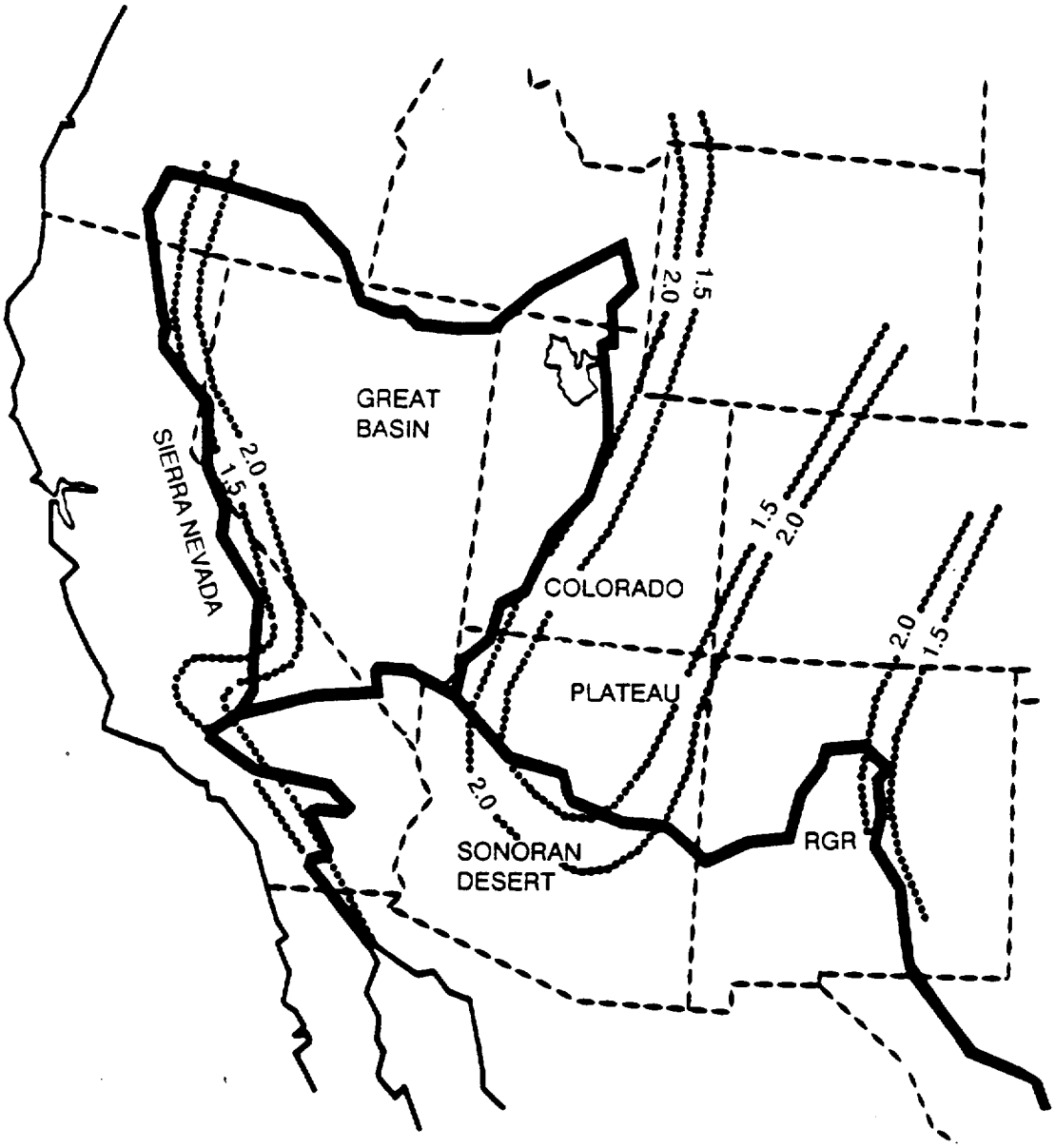

EXPLANATION:

- BOUNDARY OF PHYSIOGRAPHIC PROVINCES. FROM FENNEMAN (1931)
- • • • 2.0 • • • - CONTOURS OF INTENSITY OF HEAT FLOW IN HFU. FROM THOMPSON AND BURKE (1974)

Intensity of heat flow in the Great Basin. From Semken, 1984.

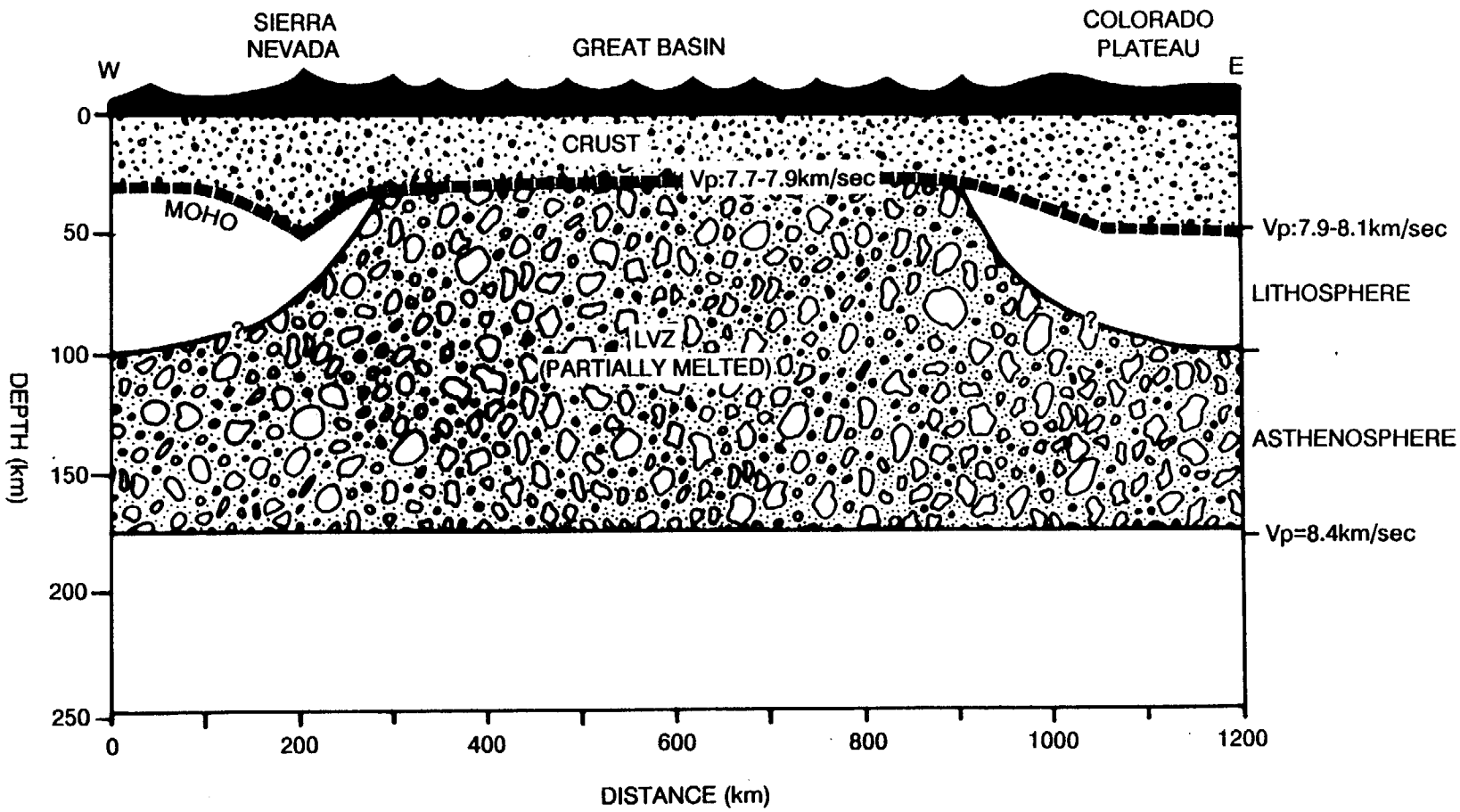

Schematic representation of conceptual understanding of tectonophysical character of the Great Basin, based on Scholz et al., 1971. From Semken , 1984.

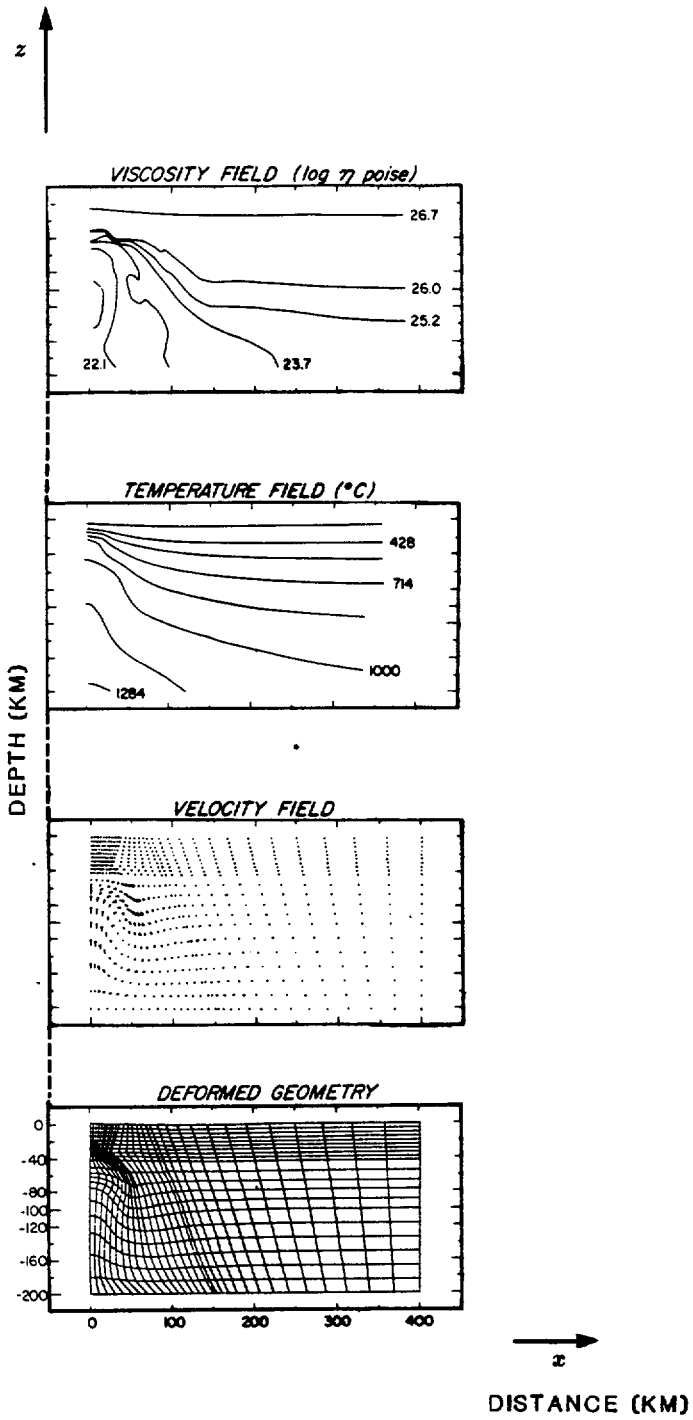

Numerical analysis of a process of upwelling of asthenospheric materials into the lithosphere for the Rio Grande Rift. From Bridwell and Potzick, 1981.

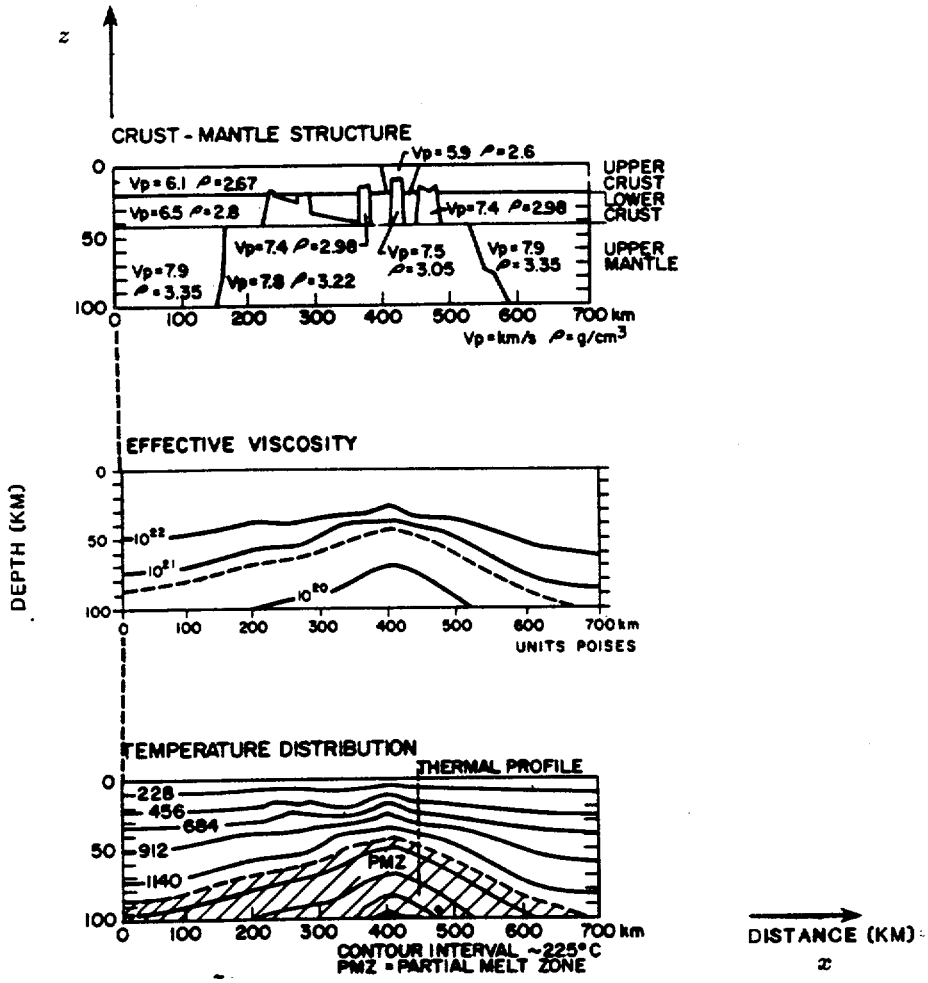

Effect of mantle upwelling on lithospheric structure. From Bridwell, 1978.

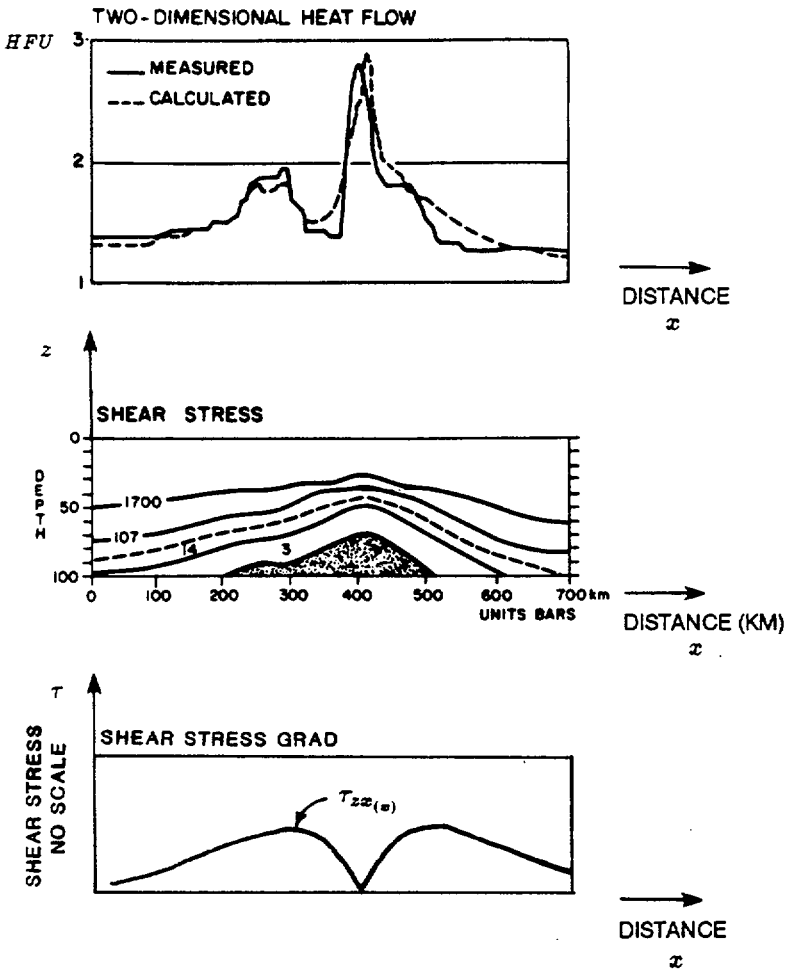

Surface heat flow and shear stresses in upper mantle and lower crust resulting from convective flow of heat and mass in the upper mantle. From Bridwell, 1978.

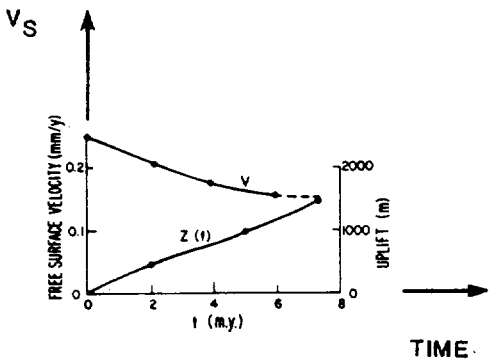

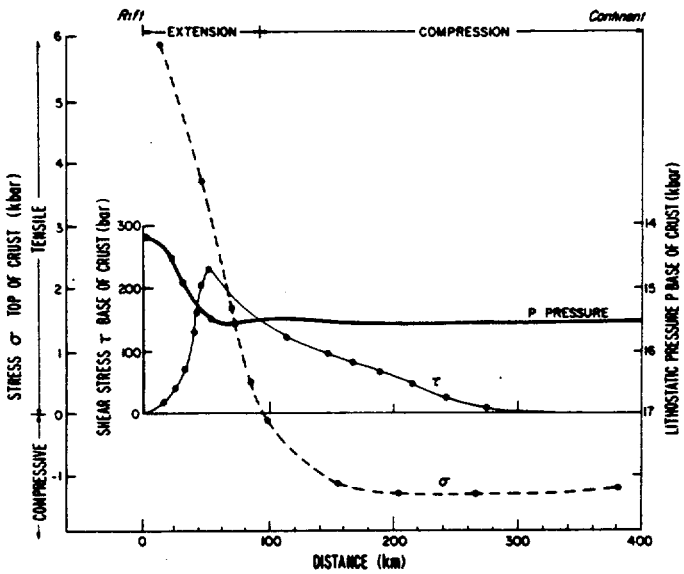

Continuum crustal stresses and surface uplift resulting from convective flow of heat and mass in the upper mantle. From Bridwell and Potzick, 1981.

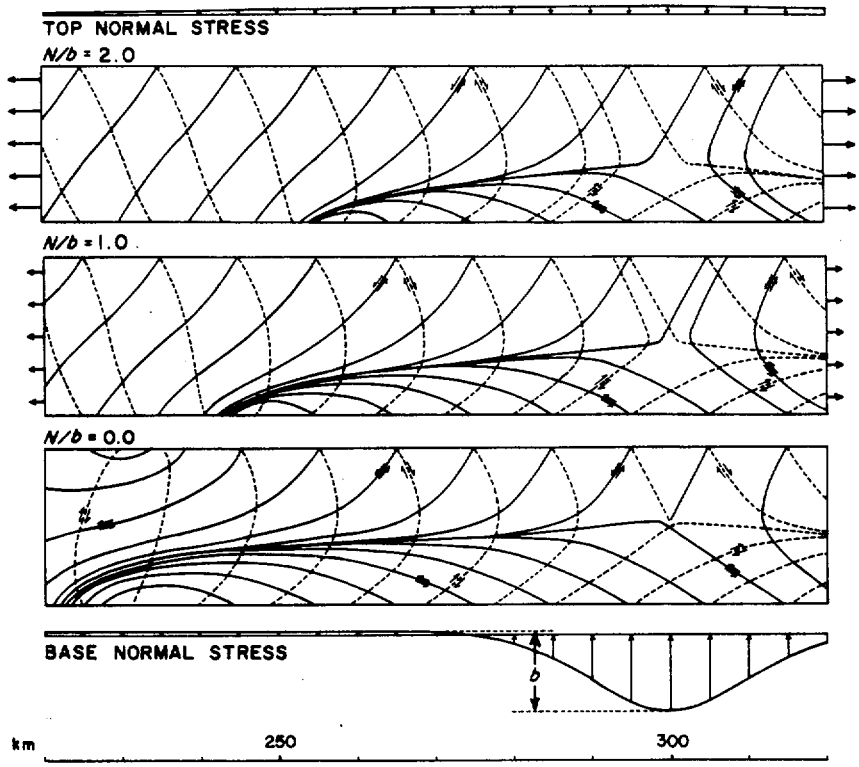

Failure - surface trajectory diagram for the upper crust overlying convective system in the upper mantle. From Spencer and Chase, 1989.

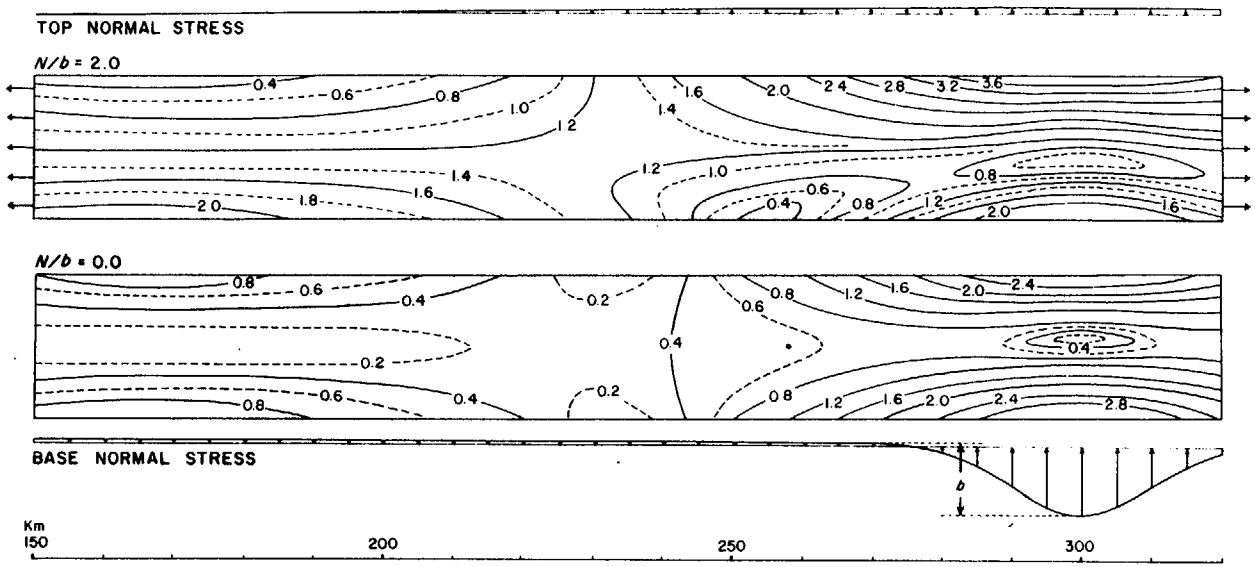

Contour diagram of shear stress magnitude in units of maximum base normal stress. Upper crust overlying convective system in the upper mantle. From Spencer and Chase, 1989.

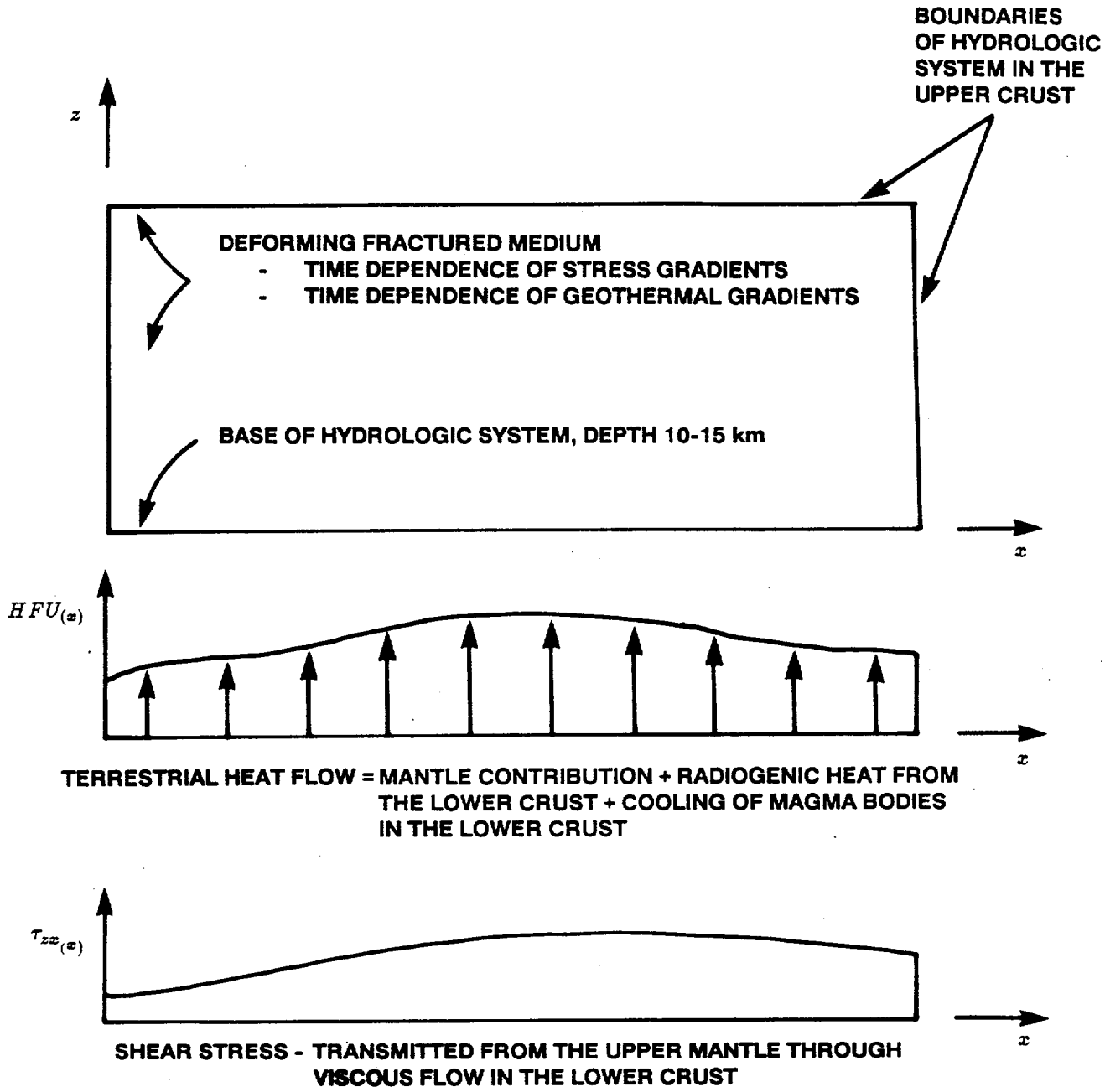

Idealization of the conceptual linkage between an extension dominated tectonic environment and a groundwater system operating in the upper crust.

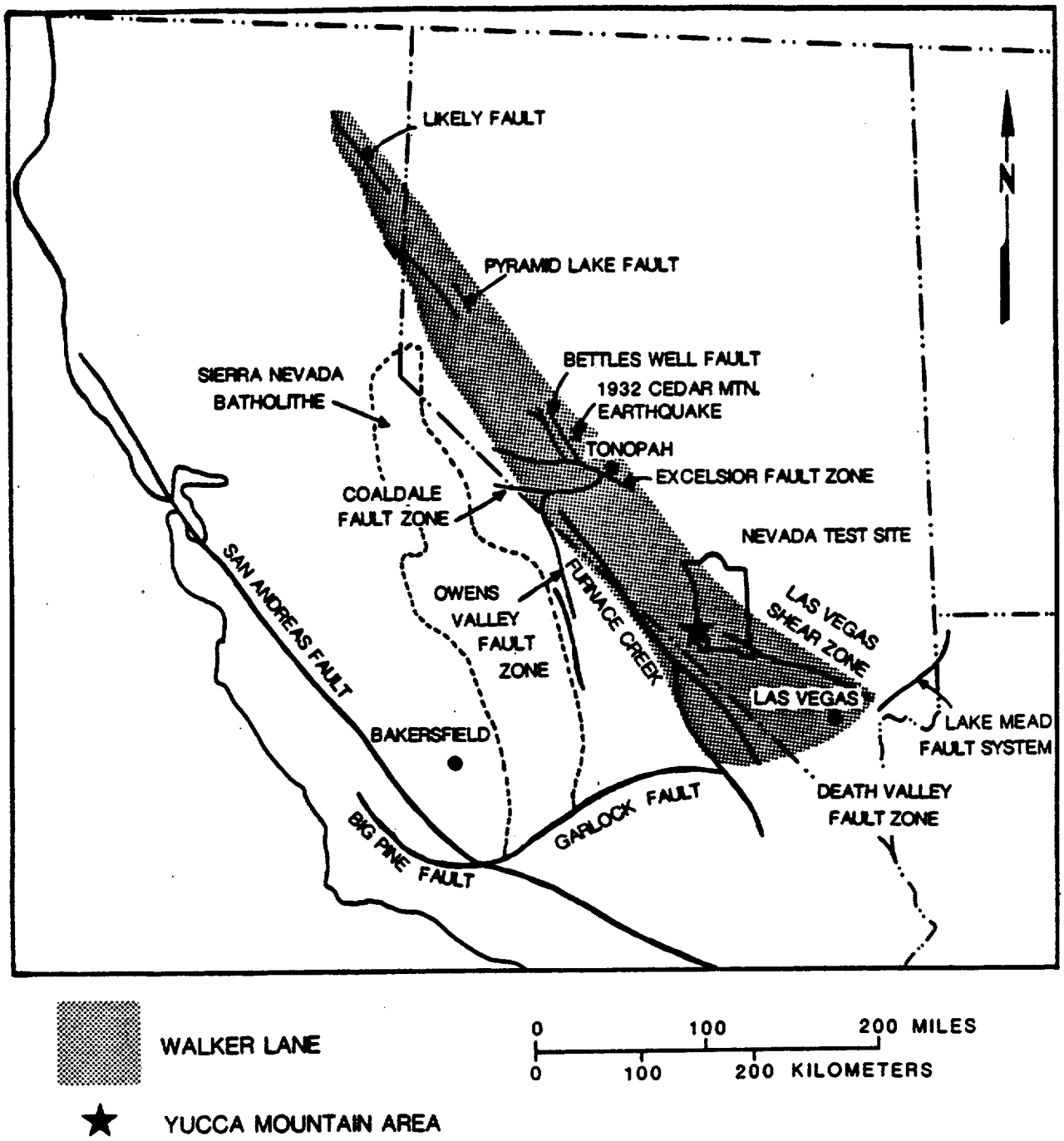

The Walker Lane shear belt and major associated faults. Modified from Stewart, 1985.

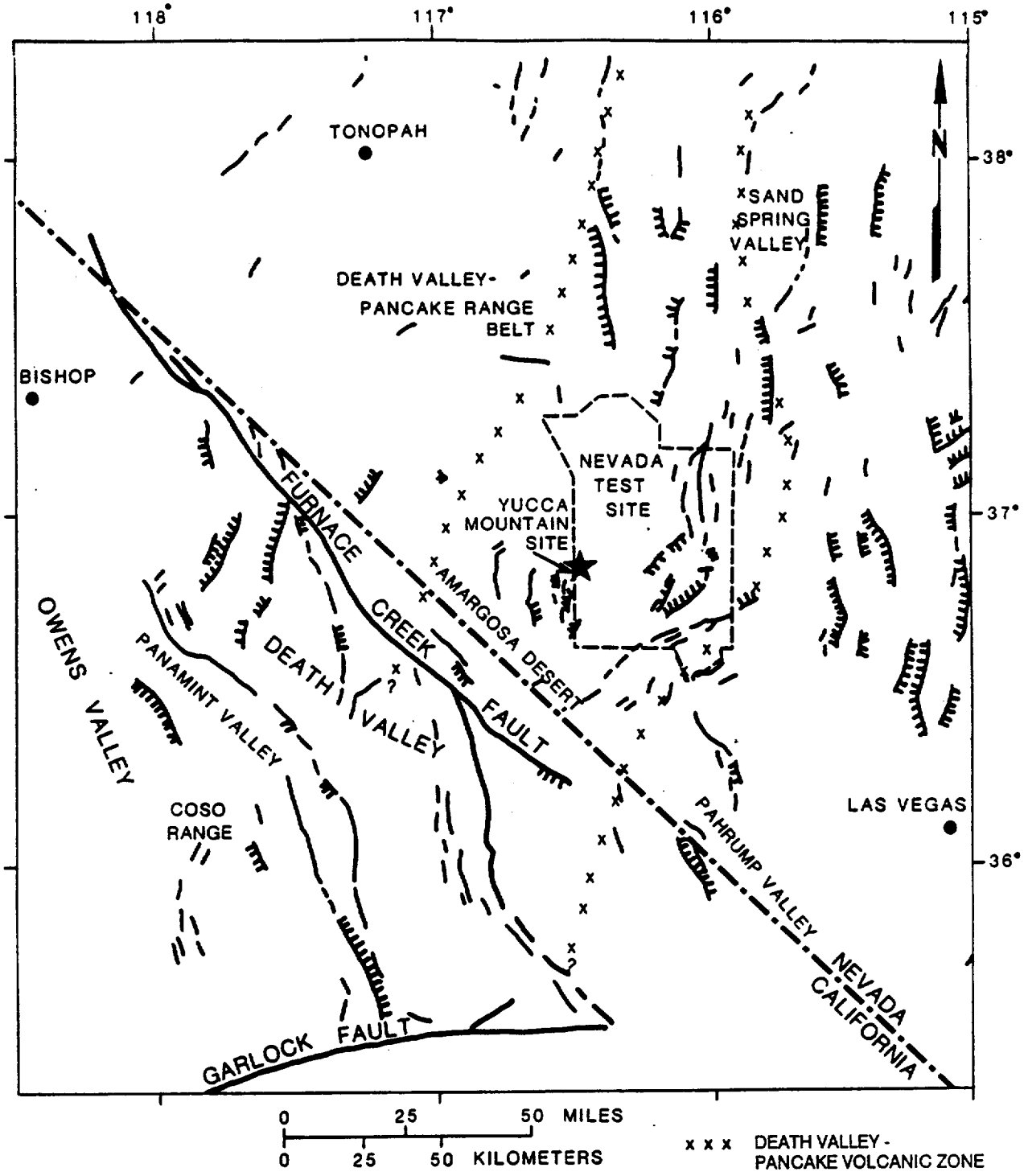

Major late Pliocene and Quaternary faults in the Nevada Test Site region, their relation to the Death Valley-Pancake Volcanic Zone. Modified from Carr, 1984.

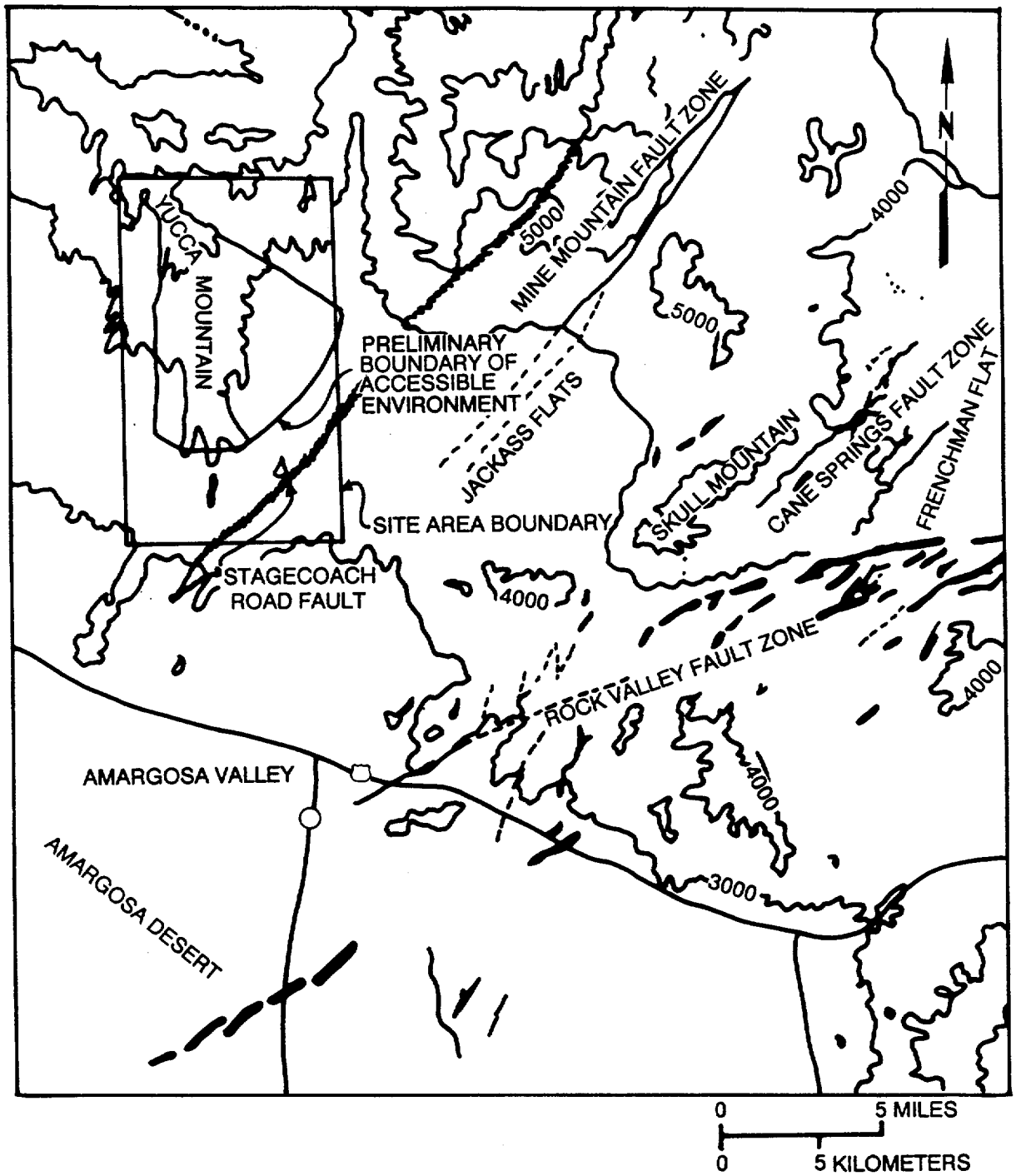

Quaternary faults near proposed repository. Modified from Maldonado, 1985.

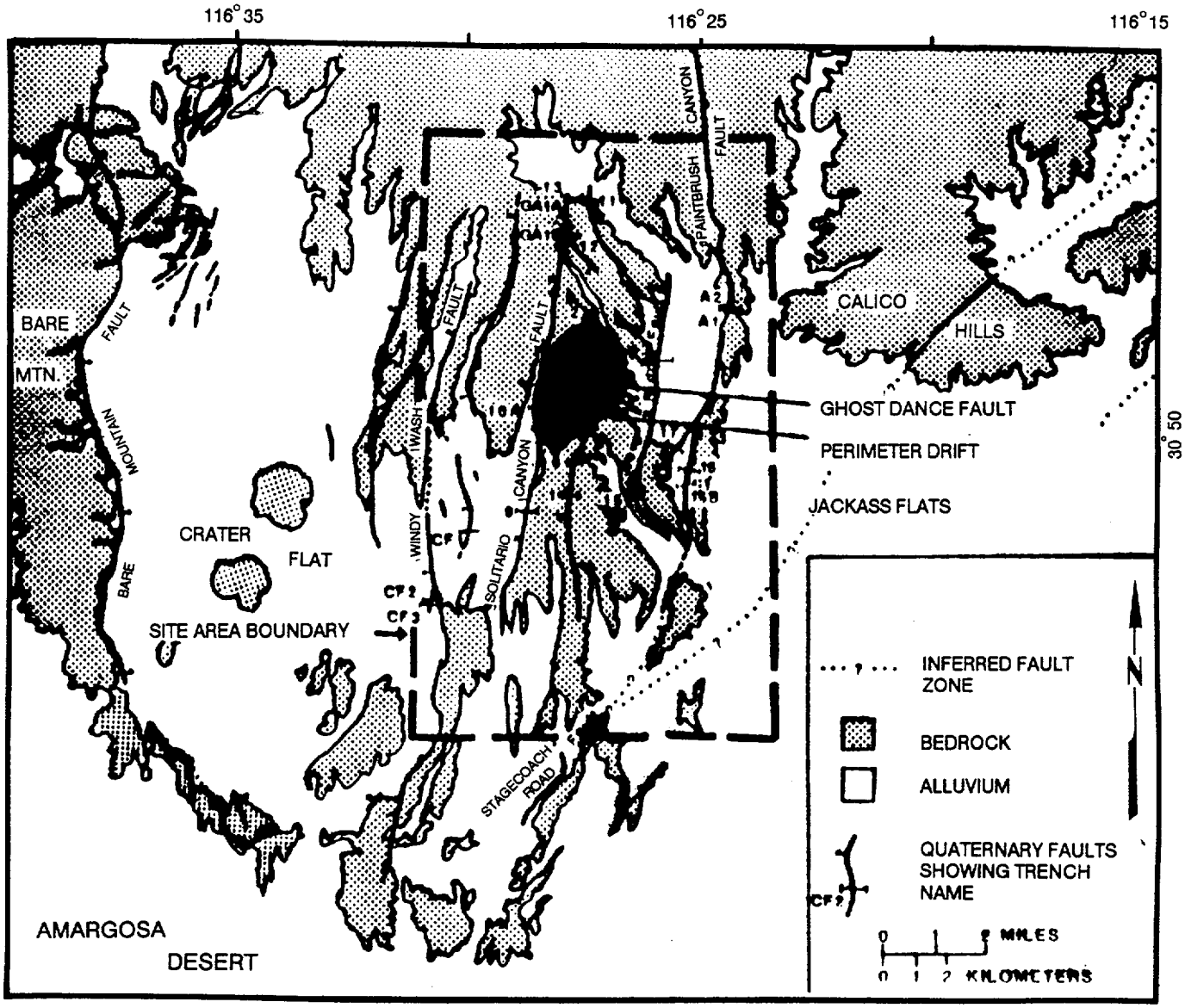

Quaternary faults near proposed repository. Modified from Maldonado, 1985.

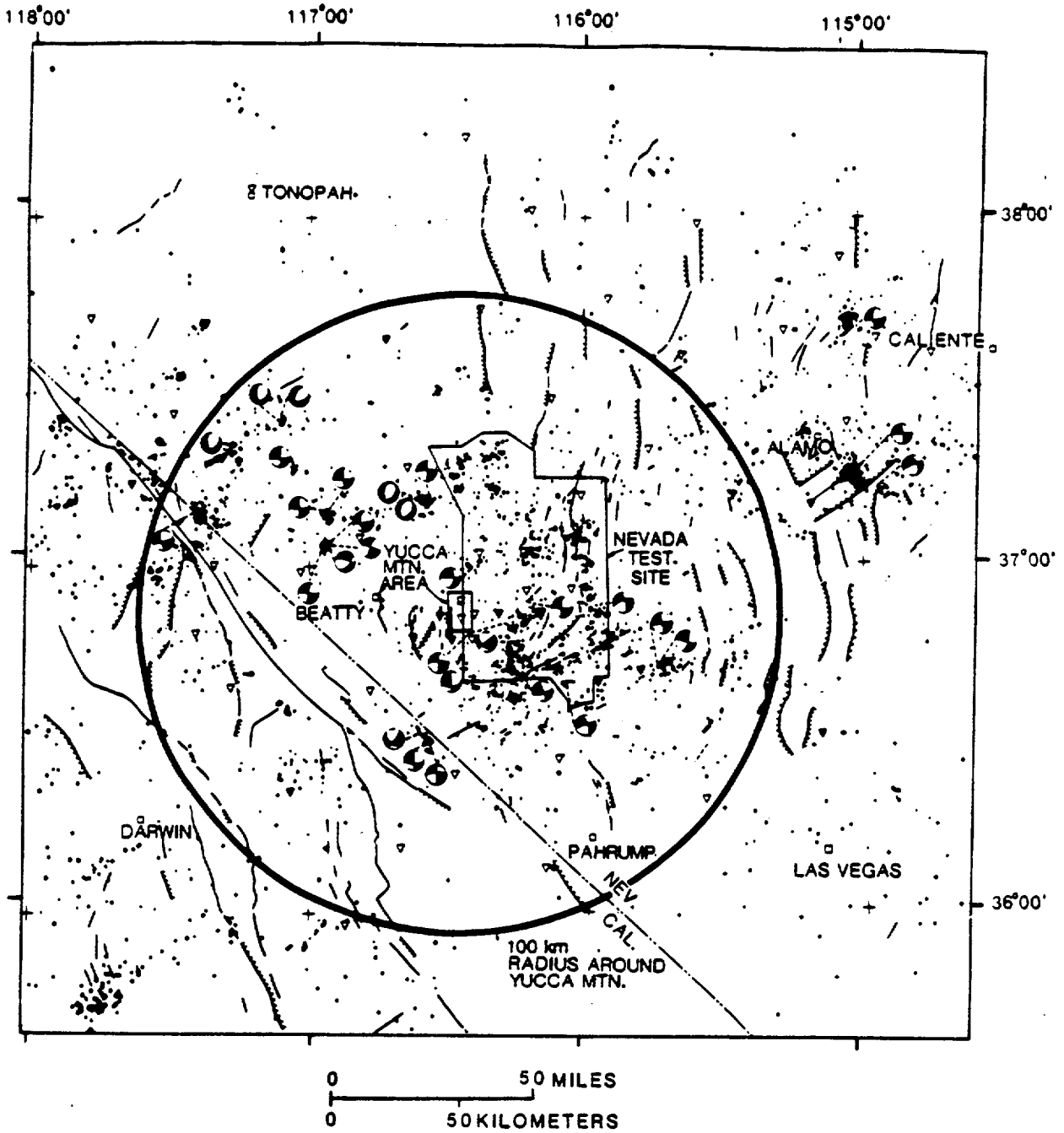

ALL IMPORTANT QUATERNARY FAULTS ARE SHOWN OUT TO A 100 km RADIUS OF YUCCA MOUNTAIN. MAP IS INCOMPLETE IN SOME AREAS BEYOND THAT CIRCLE.

UNUSUALLY LINEAR MTN. FRONT WHERE PERSISTENT FAULT ACTIVITY HAS MAINTAINED A PROMINENT SCARP IN BEDROCK. A STEEP LINEAR MTN. SEGMENT WHERE YOUNG DEPOSITS ARE NOT OBVIOUSLY OFFSET.

FAULT KNOWN OR SUSPECTED TO HAVE HAD A SURFACE MOVEMENT IN LAST 2-3 MILLION YEARS

LINE OF VOLCANIC VENTS OF QUATERNARY AGE ▽ SEISMOGRAPH STATION

SINGLE AND COMPOSITE FOCAL MECHANISMS LOWER HEMISPHERE PROJECTION OF THE FOCAL SPHERE WHERE SHADED AND UNSHADED QUADRANTS REPRESENT COMPRESSIONAL AND DILATIONAL FIRST MOTIONS RESPECTIVELY.

•$M_L < 1$ •$2 \leq M_L < 3$
•$1 \leq M_L < 2$ •$3 \leq M_L$

Seismicity of the southern Great Basin. Period August 1, 1978 through December 31, 1983. From Rogers et al., 1983 and 1987.

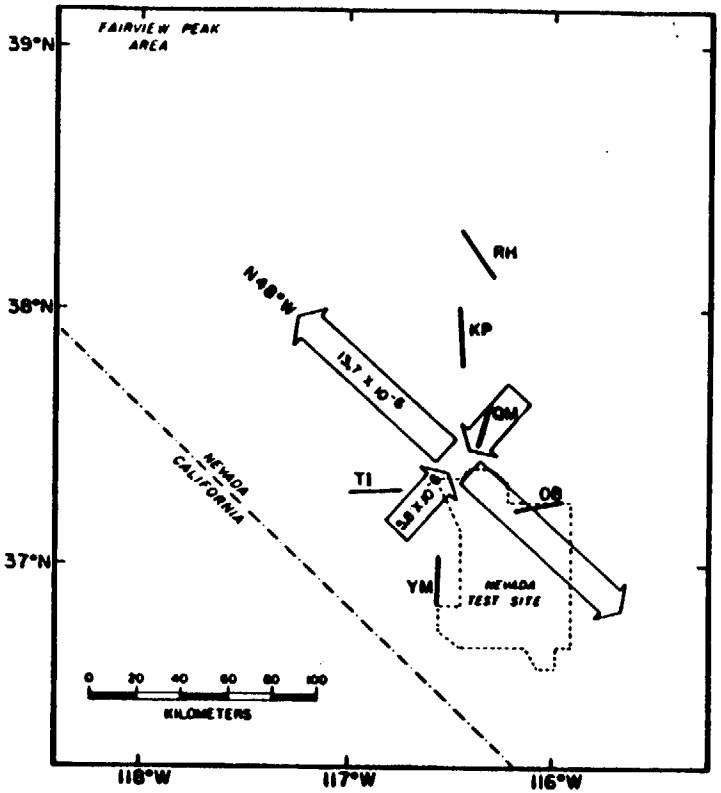

LOCATION OF THE STRAINMETER ARRAY

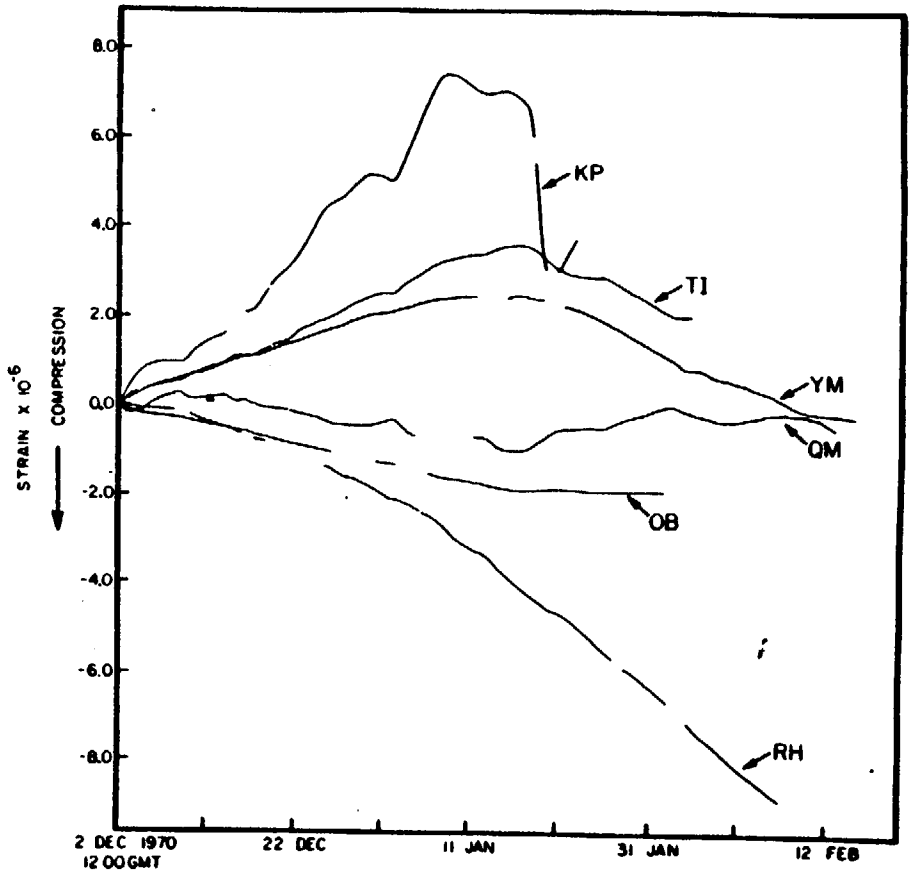

STRAIN RECORD DECEMBER 1970 - FEBRUARY 1971

Strain changes in the vicinity of the Nevada Test Site during a two-month period. From Smith and Kind, 1972.

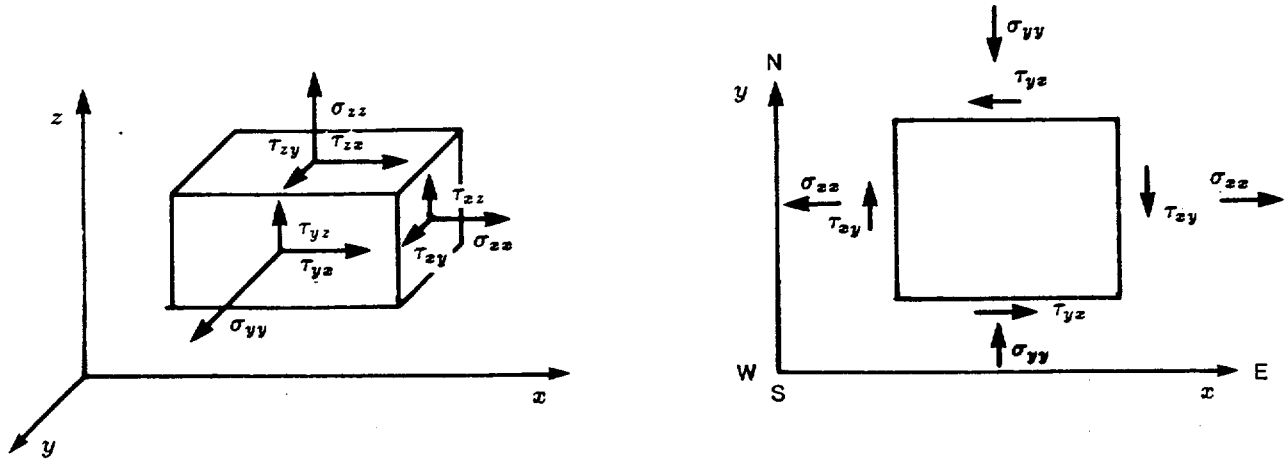

STRAIN COMPONENT	STRAIN RATE OR STRAIN ACCUMULATION	SOURCE
ϵ_{xx}	$\dot{\epsilon}_{xx} = 0.07 \times 10^{-6}$/per year	WERNICKE et. al. 1982.
	$\dot{\epsilon}_{xx} = 0.08 \times 10^{-6}$/per year	SAIC, 1985
	$\dot{\epsilon}_{xx} = 2 \times 10^{-8}$/per year	GREENSFELDER et. al. 1980.
ϵ_{yy}	$\dot{\epsilon}_{yy} = -0.10 \times 10^{-6}$/per year	SAIC, 1985
γ_{xy}	$\gamma_{xy} = \int_0^{12\times10^6} \int_0^{25} \gamma_{xy(y)} dy \cdot dt$ $= \tan 30°$ in 25 km in $\approx 12 \times 10^6$ years	SCOTT AND ROSENBAUM, 1986.
γ_{xy}	$\gamma_{xy} = 3 - 7 \times 10^{-3} in$ 3×10^6 years	CARR, 1984.

Summary of strain rates and of accumulated shear strain for the region of Yucca Mountain groundwater system.

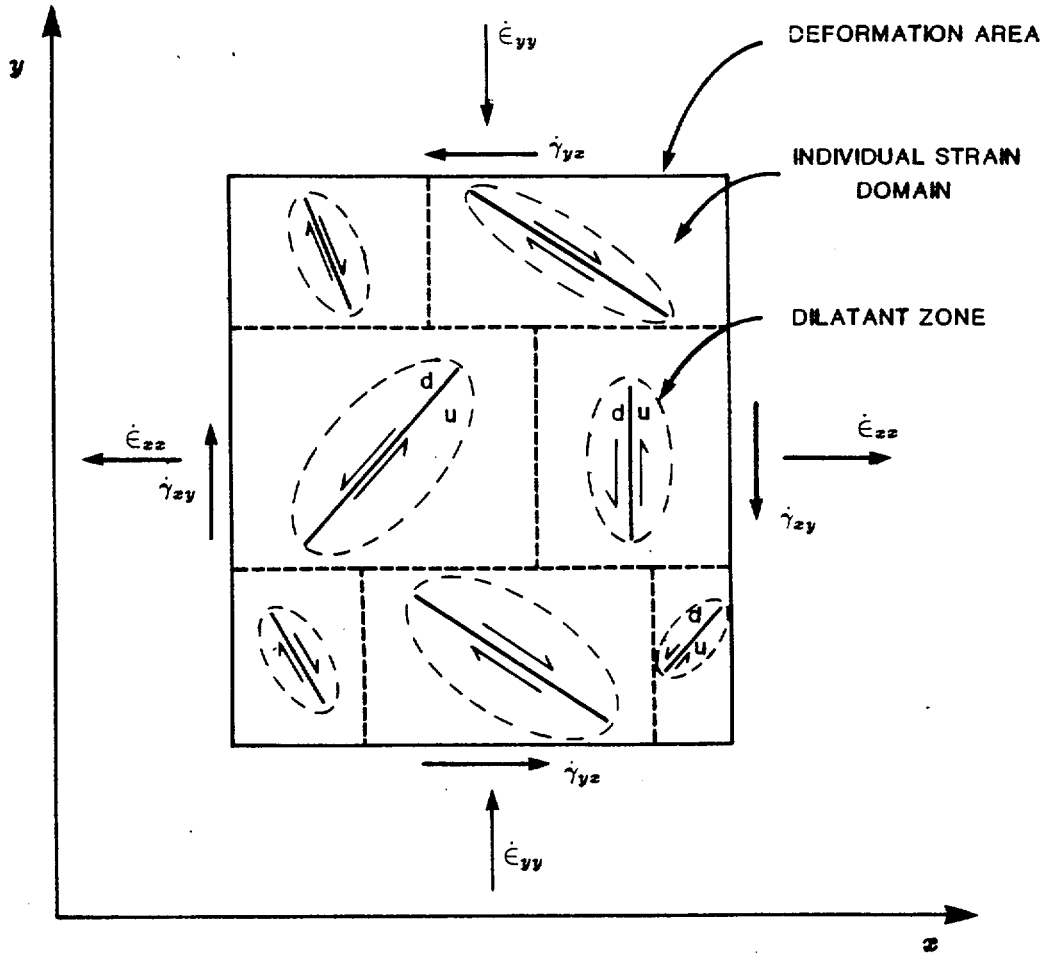

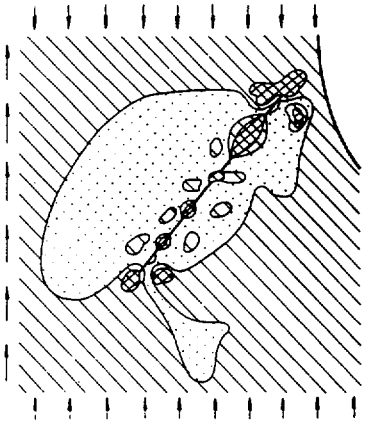

OBSERVED PHOTOELASTIC FRINGES IN A FAULT MODEL IN GELATIN. FROM LOMNITZ, 1974

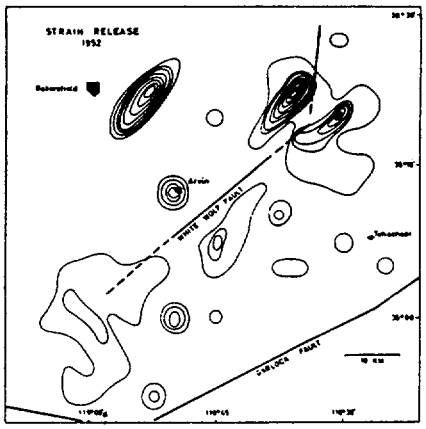

STRAINS CALCULATED FROM THE ENERGY RELEASE OF THE KERN COUNTY AFTERSHOCK SEQUENCE FROM LOMNITZ, 1974

Division of deformation area into strain domains.

CHARACTERISTIC EARTHQUAKE — CHARACTERISTIC EARTHQUAKE

REPEAT TIME t_c

TIME

COMPLETE TECTONIC CYCLE	
PHASE I	PHASE II
SLOW BUILD-UP OF TECTONIC STRESS. NORMAL AND SHEAR STRESSES EXHIBIT TIME-DEPENDENCY.	RATE OF LOCAL TECTONIC STRAINING INCREASES. INHOMOGENEITIES IN THE STRESS FIELD (NORMAL AND SHEAR STRESS GRADIENTS) BECOME MORE PRONOUNCED WITH TIME. AT THE END, LARGE AND FAST CHANGES IN THE CUMULATIVE STRAIN ENERGY OCCUR IN ASSOCIATION WITH A SEQUENCE OF SEISMIC EVENTS.
MORE OR LESS HOMOGENOUS STRAIN	NON-HOMOGENEOUS STRAIN
$\frac{\partial(\sigma_{xx}, \tau_{yx})}{\partial t} \neq 0$ $\frac{\partial(\sigma_{yy}, \tau_{xy})}{\partial t} \neq 0$	TIME-DEPENDENCE OF STRESS $\frac{\partial(\sigma_{xx}, \tau_{yx})}{\partial t} \neq 0 \neq \text{const.}$ $\frac{\partial(\sigma_{yy}, \tau_{xy})}{\partial t} \neq 0 \neq \text{const.}$ STRESS GRADIENTS $\frac{\partial(\sigma_{xx}, \tau_{yx})}{\partial x} \neq \text{const.}$ $\frac{\partial(\sigma_{yy}, \tau_{xy})}{\partial y} \neq \text{const.}$ TIME-DEPENDENCE OF STRESS GRADIENTS $\frac{\partial^2(\sigma_{xx}, \tau_{yx})}{\partial t \cdot \partial x} \neq 0$ $\frac{\partial^2(\sigma_{yy}, \tau_{xy})}{\partial t \cdot \partial y} \neq 0$

Idealization of tectonic cycle for a strain domain.

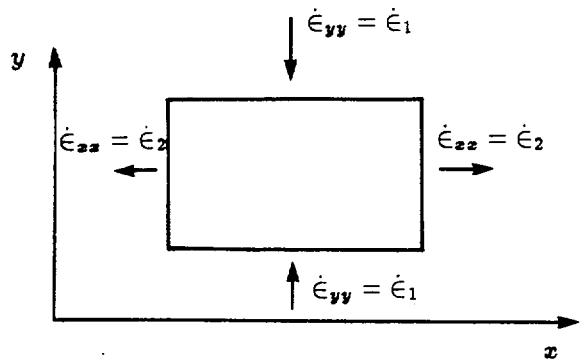

HOMOGENOUS STRAIN

$\frac{\partial \sigma_{xx}}{\partial t} \neq 0$; but $\frac{\partial^2 \sigma_{xx}}{\partial x \cdot \partial t} \cong 0$; and

$\frac{\partial \sigma_{yy}}{\partial t} \neq 0$; but $\frac{\partial^2 \sigma_{yy}}{\partial y \cdot \partial t} \cong 0$.

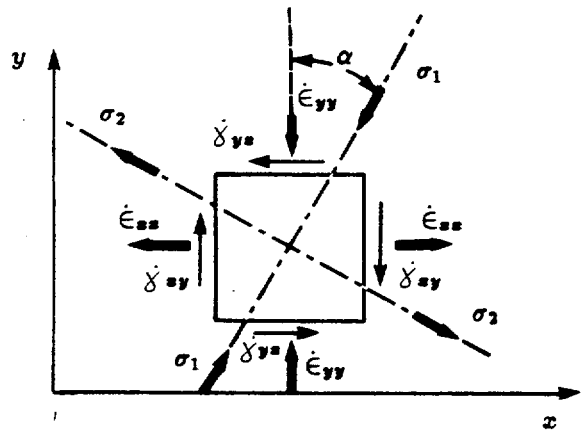

HOMOGENOUS STRAIN

INCLUDES SHEAR COUPLE

$\frac{\partial \sigma_{xx}}{\partial t} \neq 0$; but $\frac{\partial^2 \sigma_{xx}}{\partial x \cdot \partial t} \cong 0$; and

$\frac{\partial \sigma_{yy}}{\partial t} \neq 0$; but $\frac{\partial^2 \sigma_{yy}}{\partial y \cdot \partial t} \cong 0$;

$\frac{\partial \alpha}{\partial t} \neq 0$.

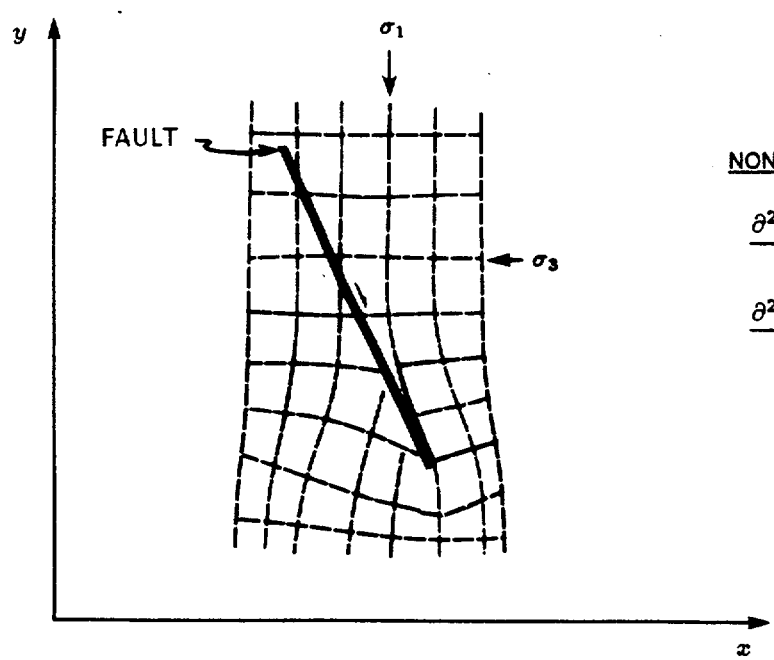

NON-HOMOGENOUS STRAIN

$\frac{\partial^2 (\sigma_{xx}, \tau_{yx})}{\partial x \partial t} \neq 0$; and

$\frac{\partial^2 (\sigma_{yy}, \tau_{xy})}{\partial y \partial t} \neq 0$.

Idealization of changes in stress field during a tectonic cycle.

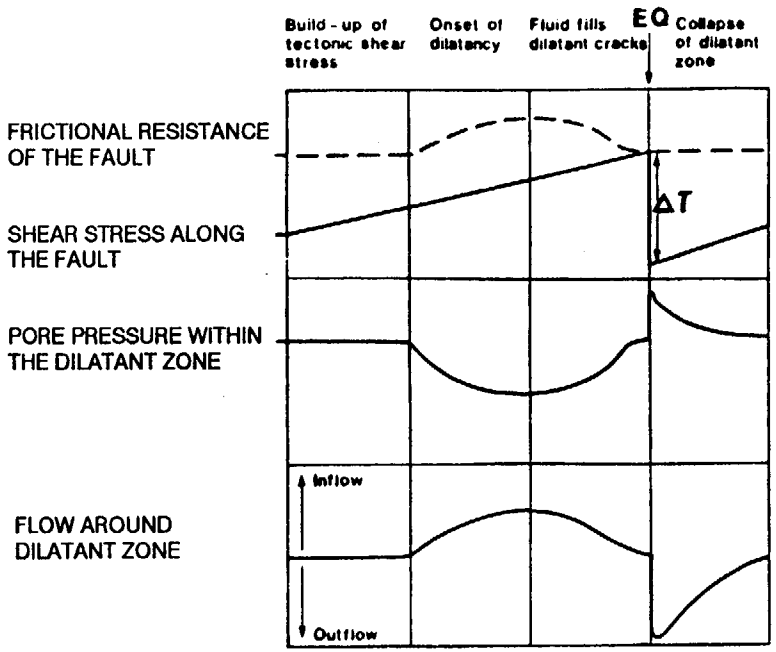

a) IDEALISATION OF THE EARTHQUAKE NUCLEATION PROCESS

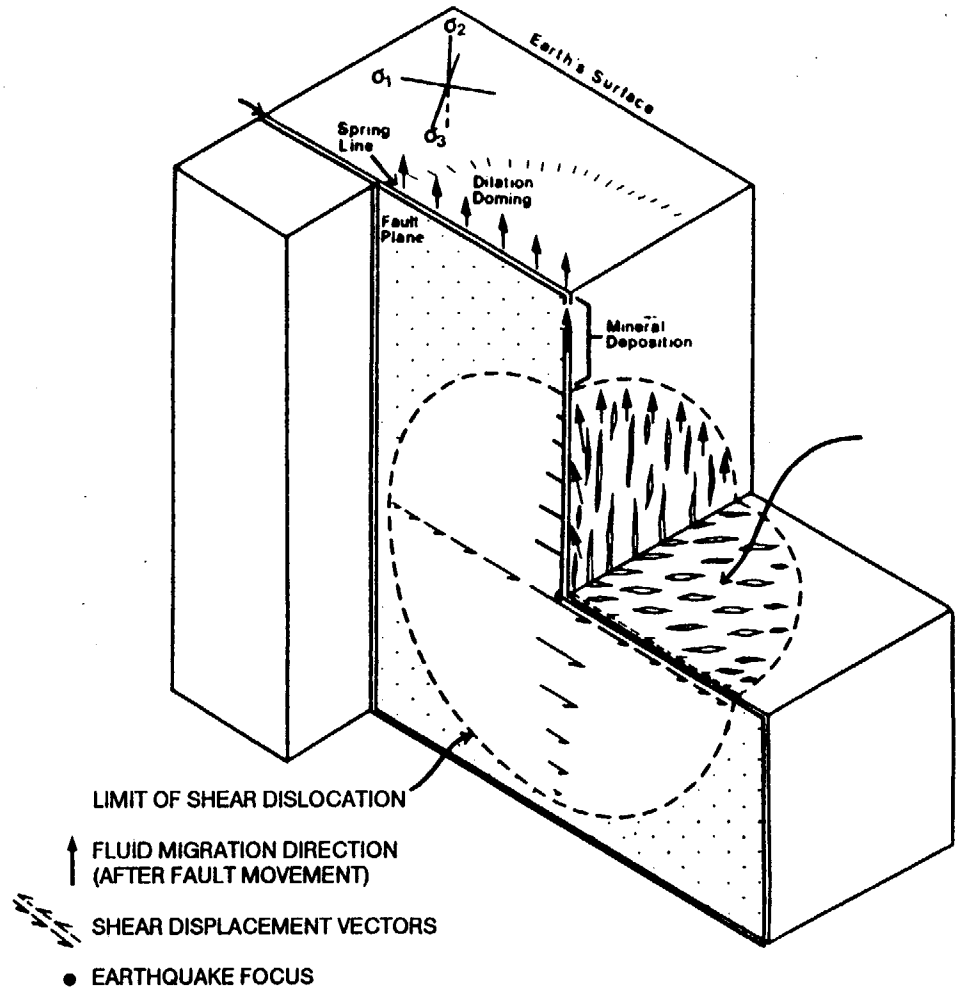

b) SCHEMATIC REPRESENTATION OF THE PROCESS OF "SEISMIC PUMPING" FOR STRIKE-SLIP FAULTING

The dilatancy/fluid diffusion model of an earthquake nucleation process. From Sibson et al., 1975.

DIAGRAM 1

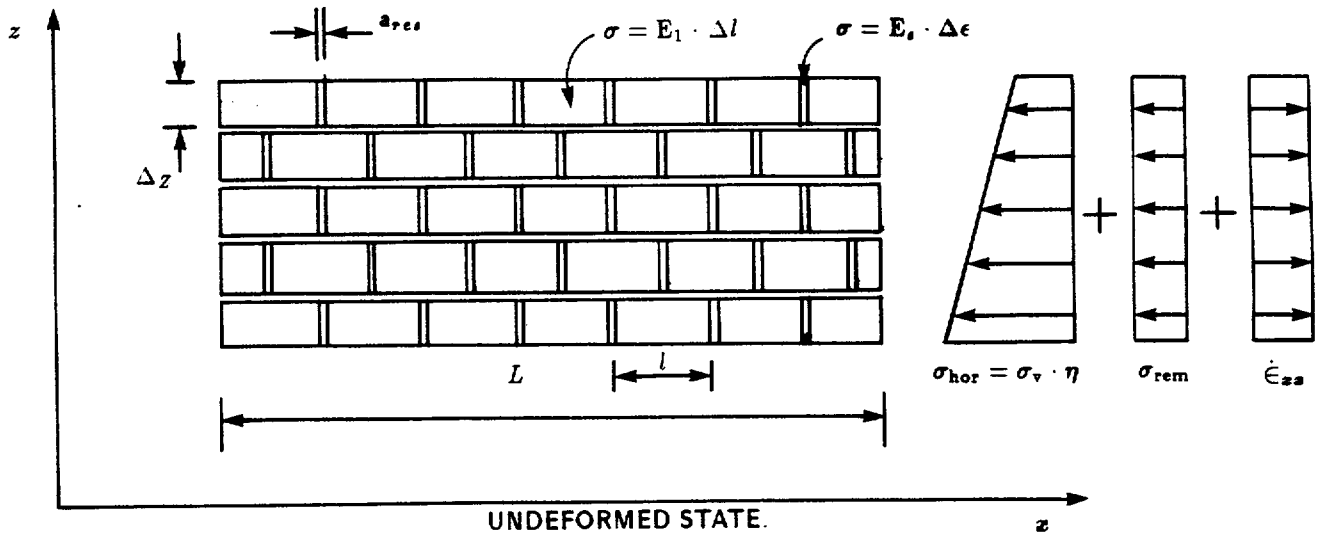

DIAGRAM 2

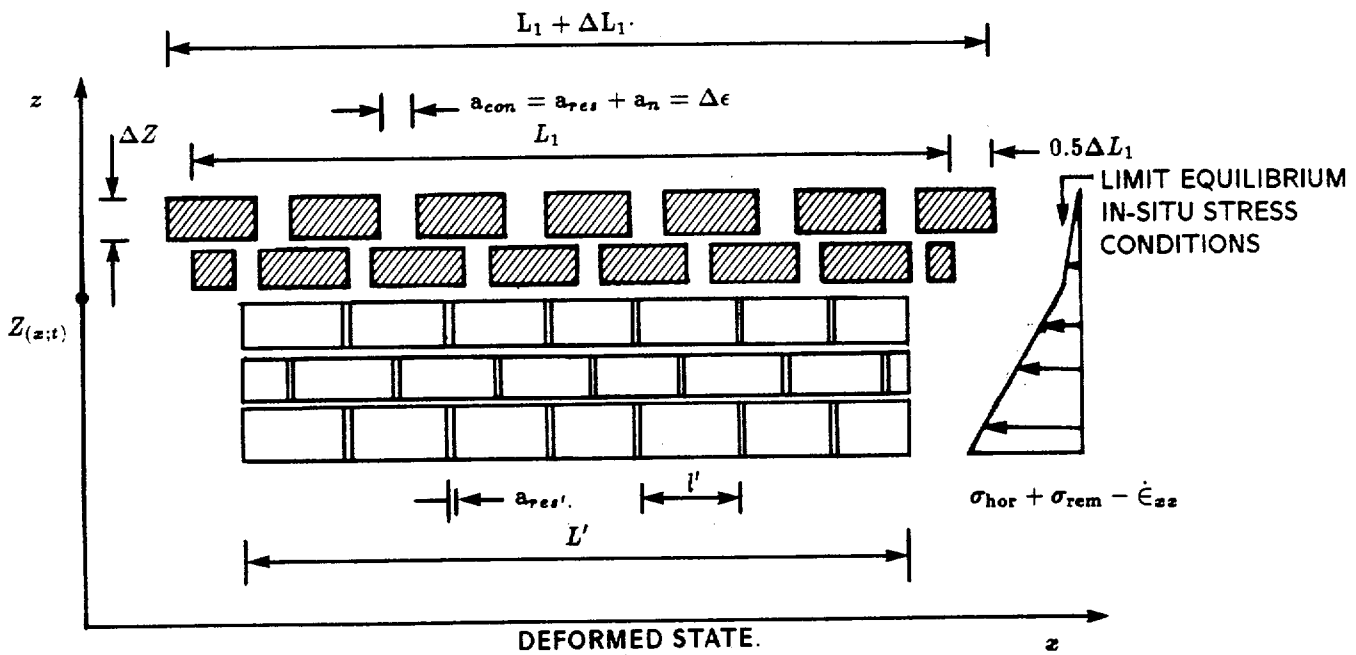

Idealized response of a fractured medium during uniform extension.

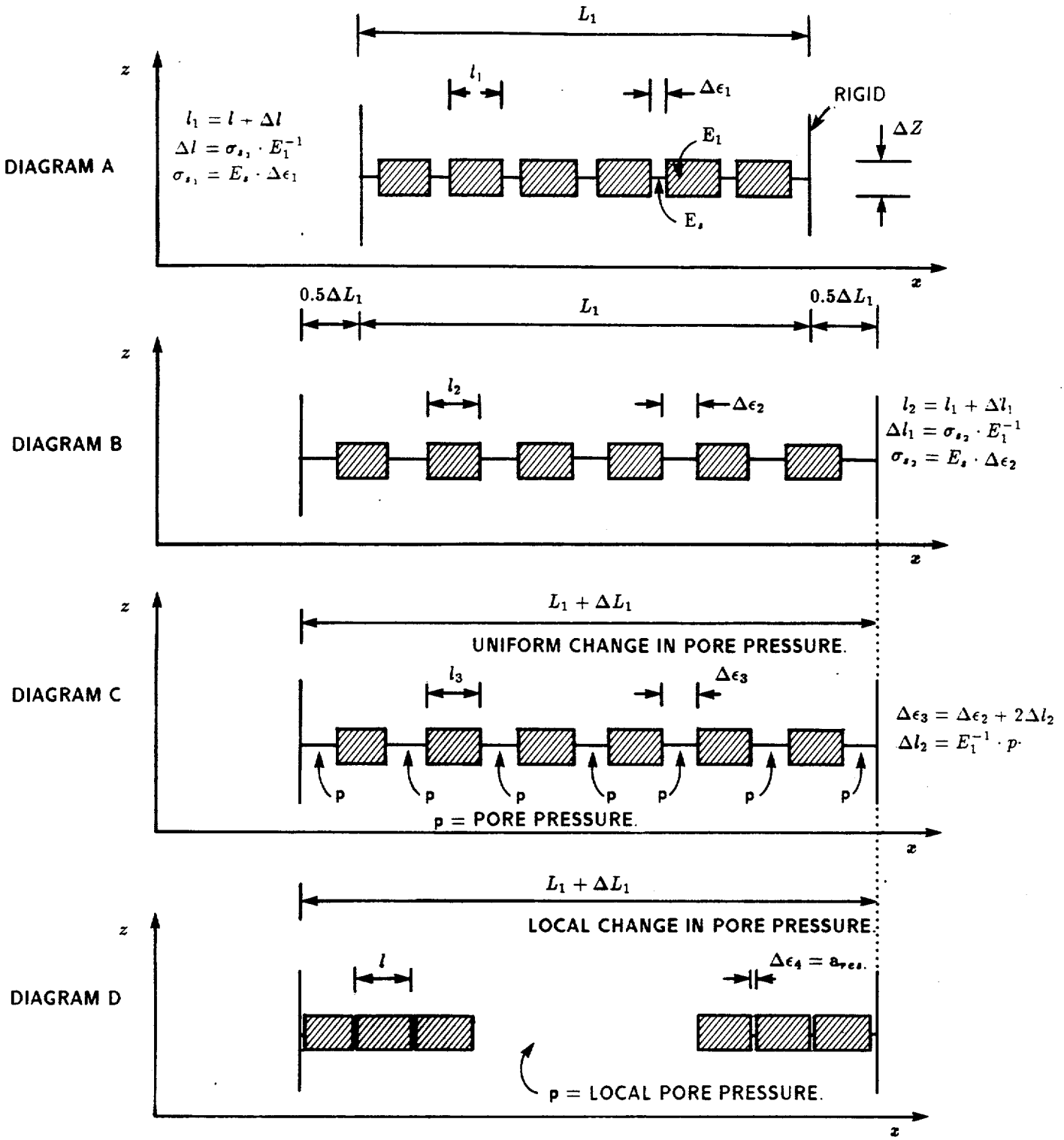

Idealized response of a dilated fractured medium to sudden changes in pore pressure.

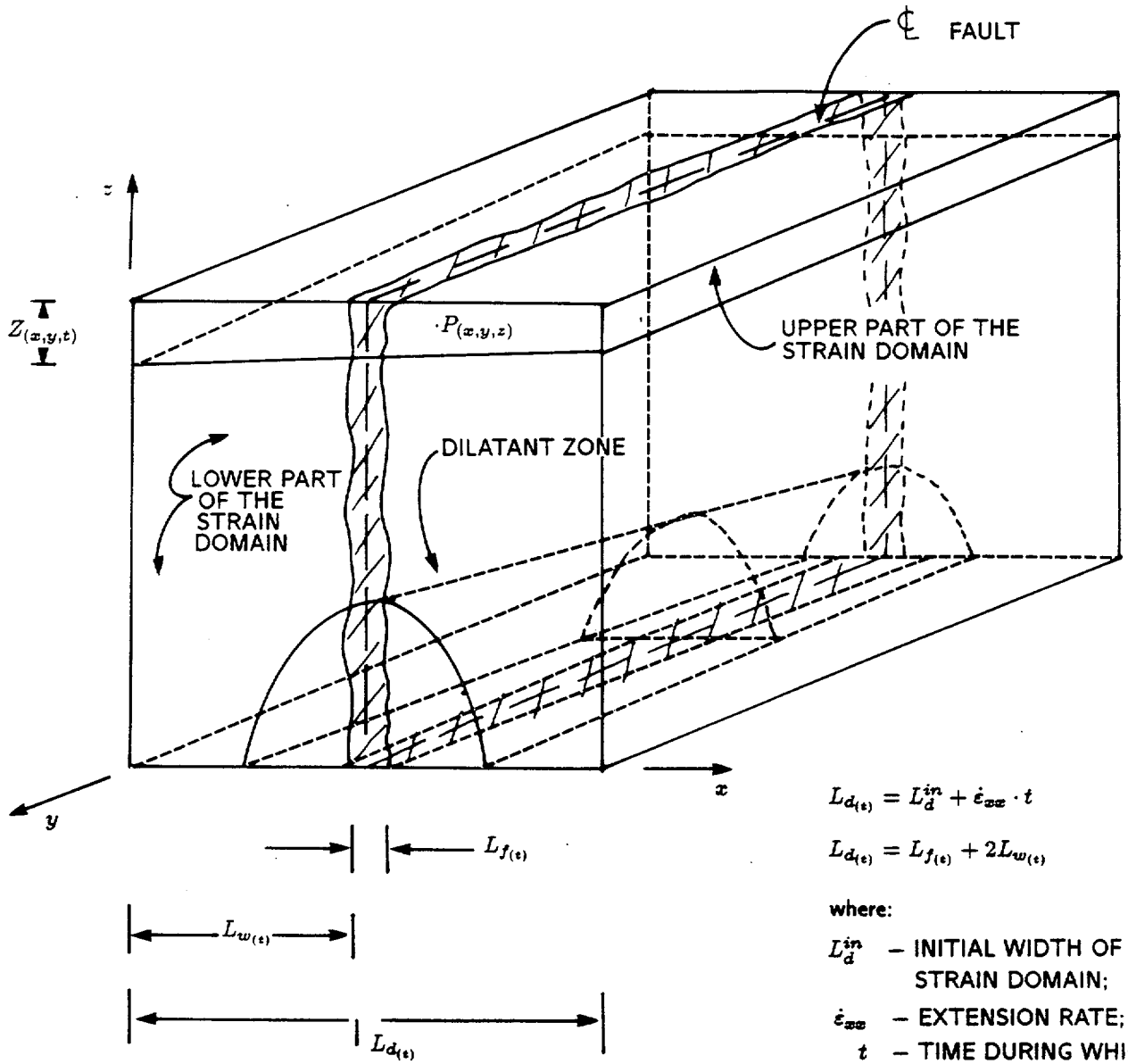

$$L_{d_{(t)}} = L_d^{in} + \dot{\varepsilon}_{xx} \cdot t$$

$$L_{d_{(t)}} = L_{f_{(t)}} + 2L_{w_{(t)}}$$

where:

L_d^{in} – INITIAL WIDTH OF THE STRAIN DOMAIN;

$\dot{\varepsilon}_{xx}$ – EXTENSION RATE; AND

t – TIME DURING WHICH EXTENSION WAS OCCURRING

Schematic illustration of: a) division of the strain domain into the upper and lower parts with different in situ stress conditions; and b) division of the lower part of the strain domain into the dilatant zone and the "outside" zone.

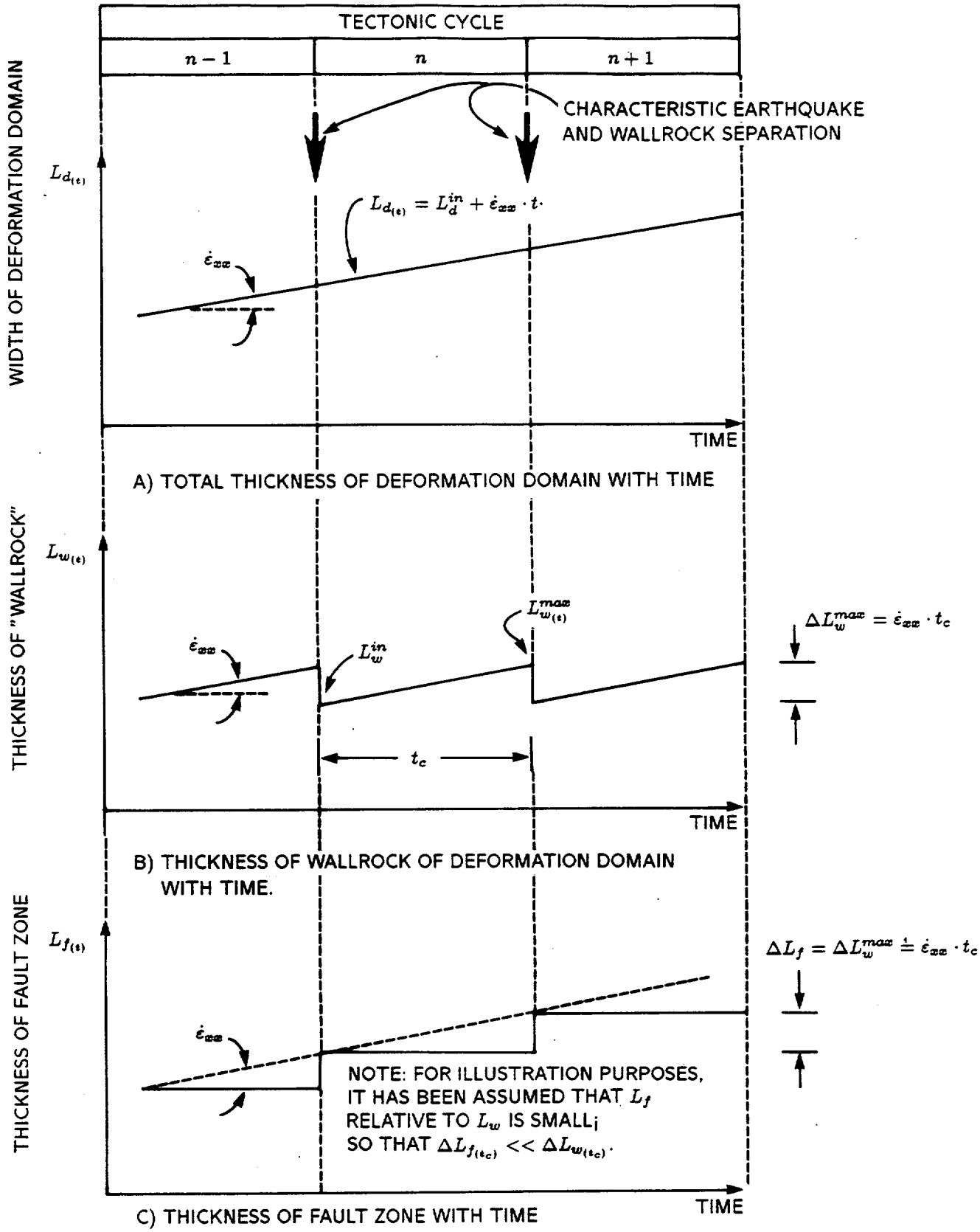

Schematic representation of strain accumulation within a single strain domain during three cycles of deformation.

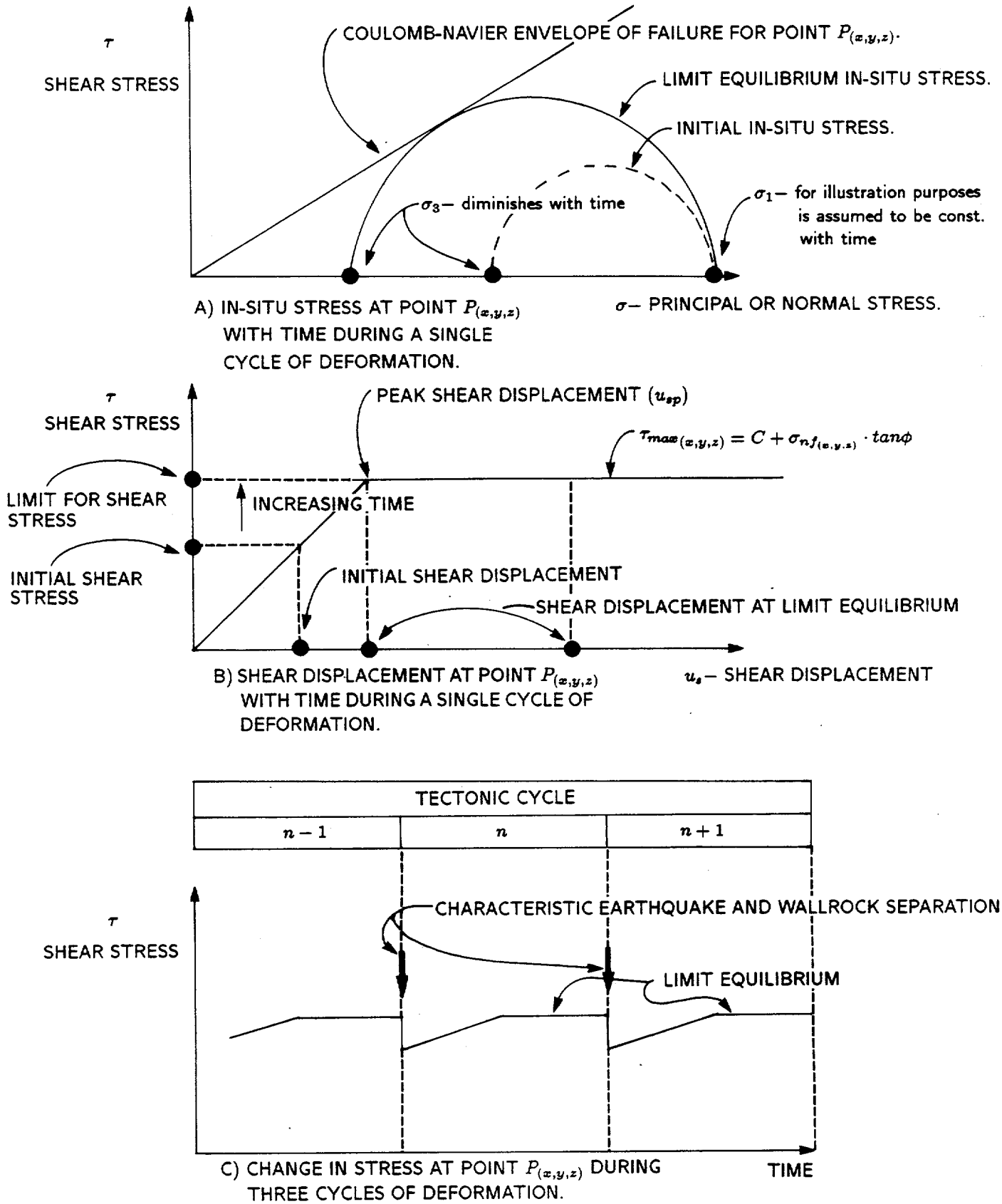

Schematic representation of changes in the in situ stress conditions occurring near the ground surface in a cyclically deforming fractured medium.

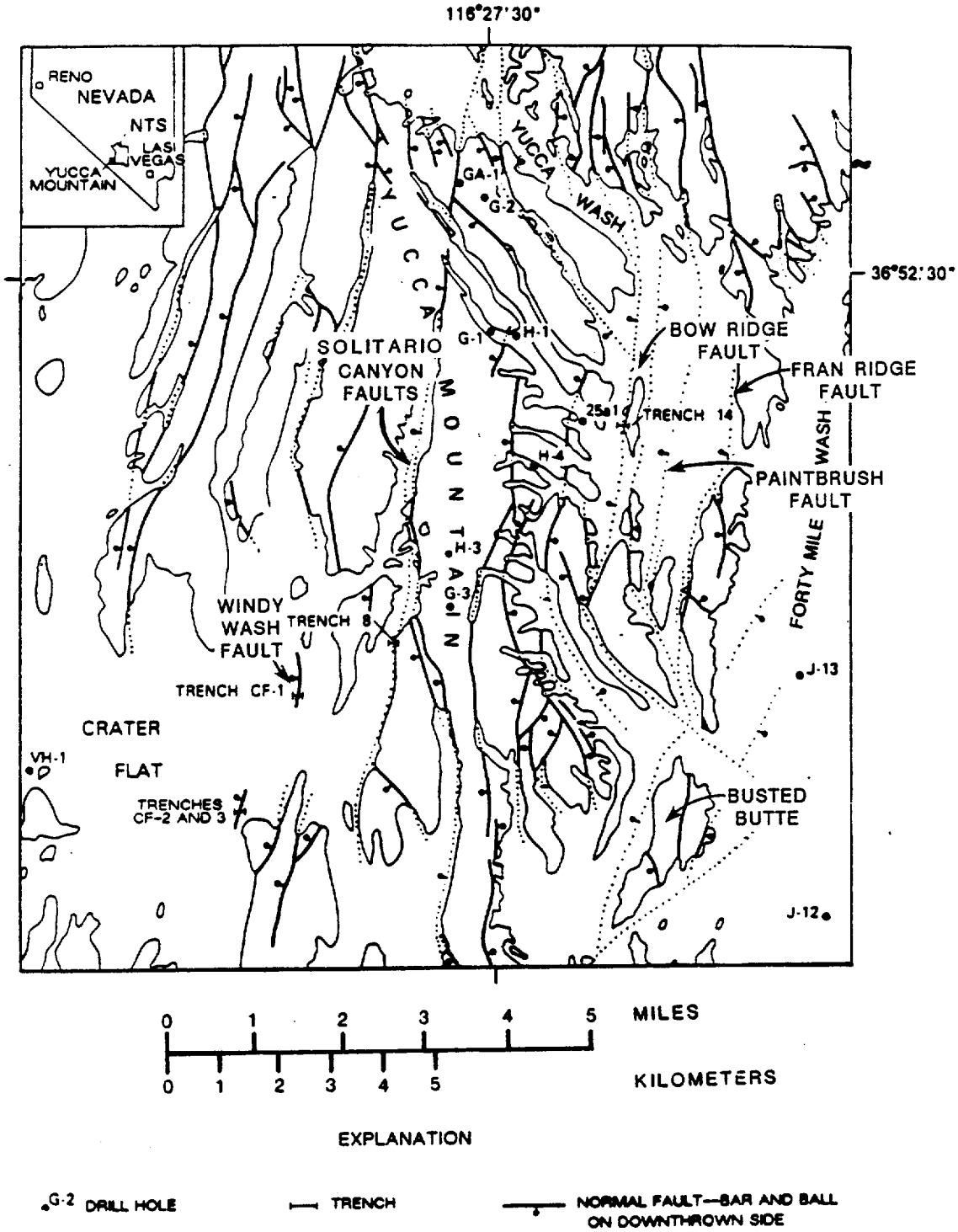

Location of faults containing calcite-silica veins of Quaternary age in the Yucca Mountain area.

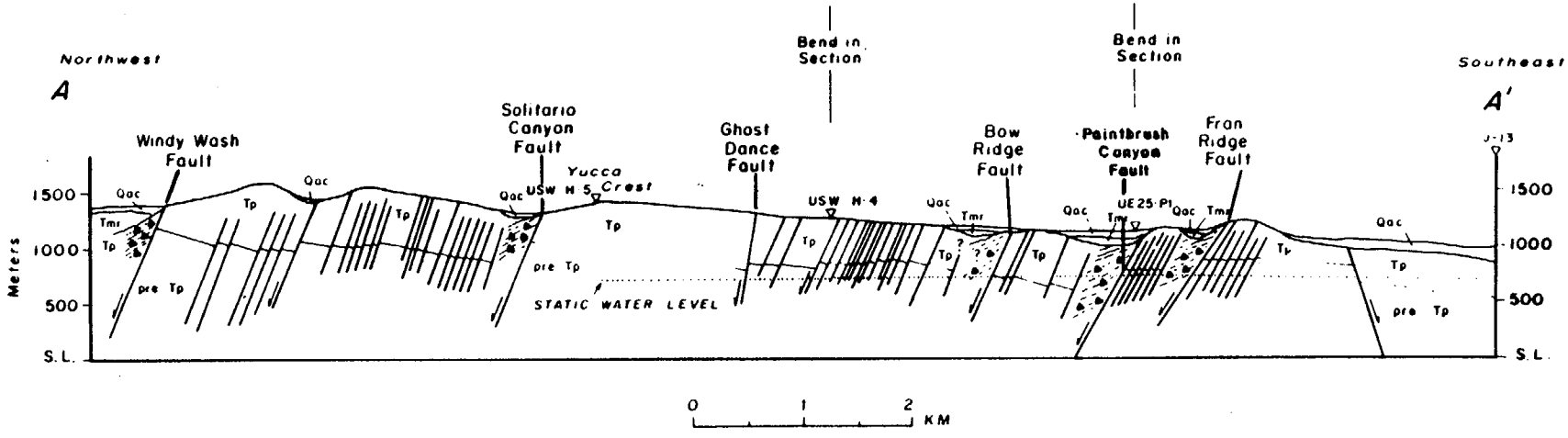

Geologic section across Yucca Mountain showing location and thicknesses of mosaic breccias. From Scott and Bonk, 1985.

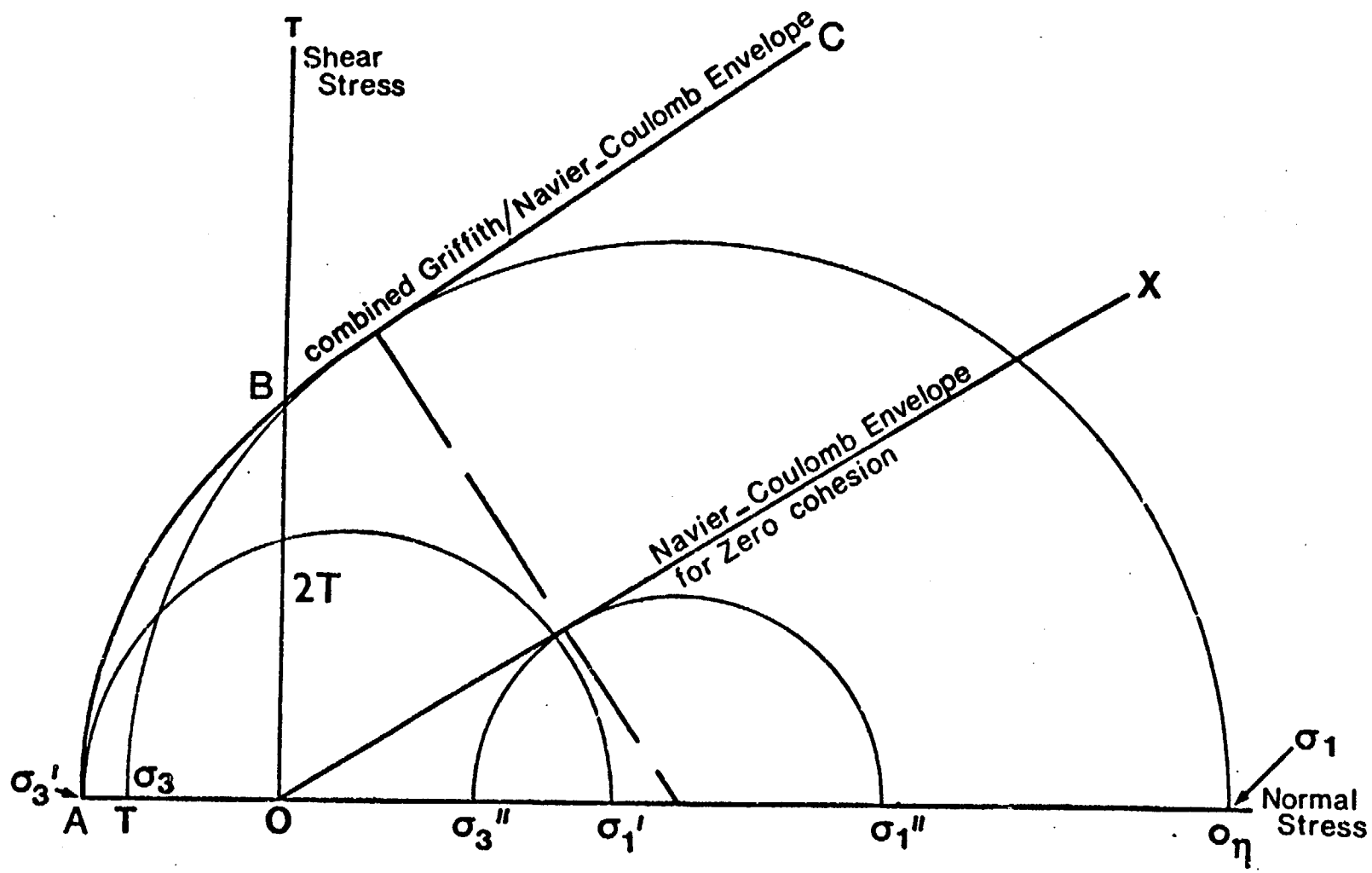

Mohr's representation of stresses in two dimensions and combined Griffith/Navier - Coulomb failure envelope.

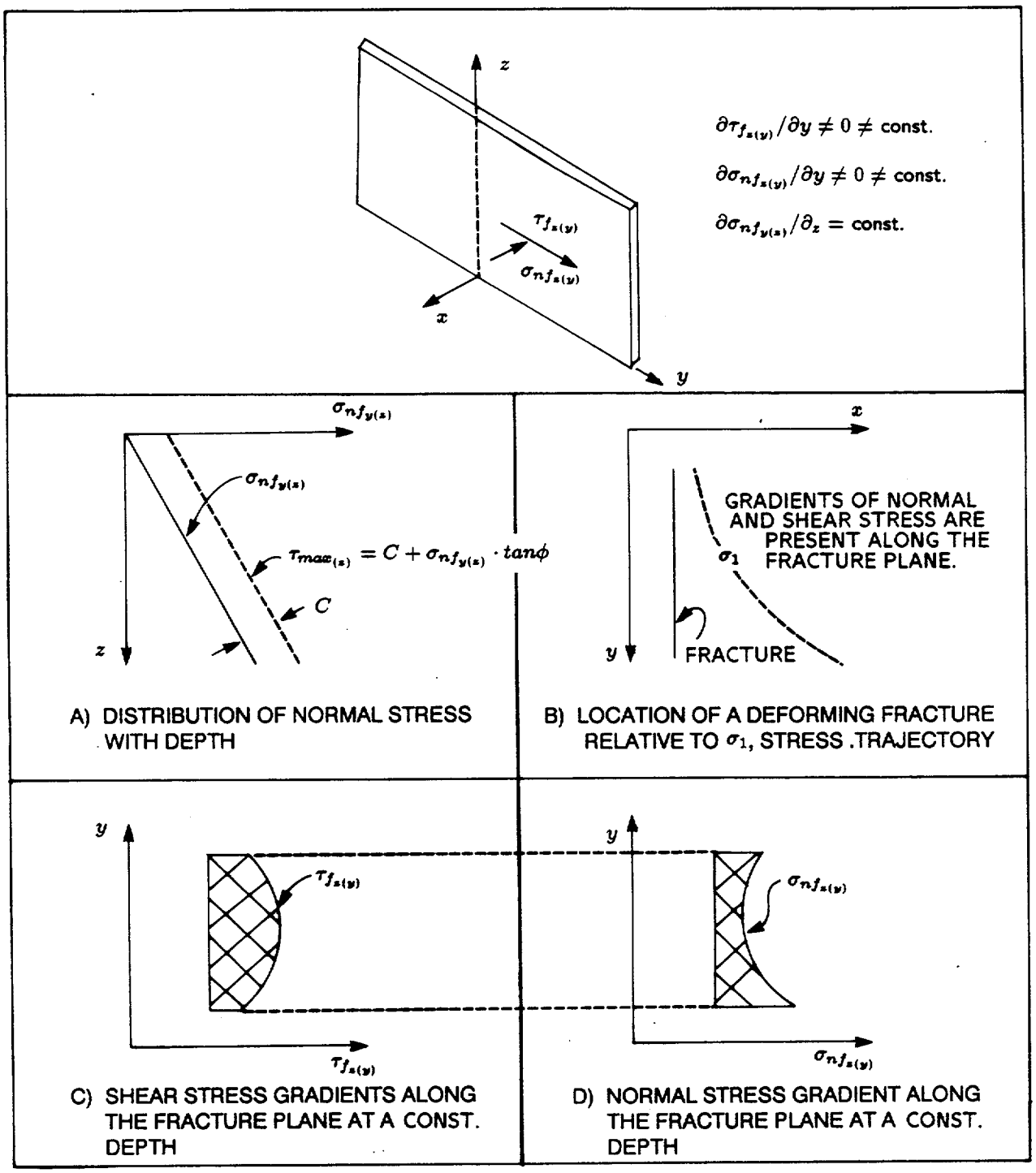

Assumed initial in situ stresses around a deforming fracture.

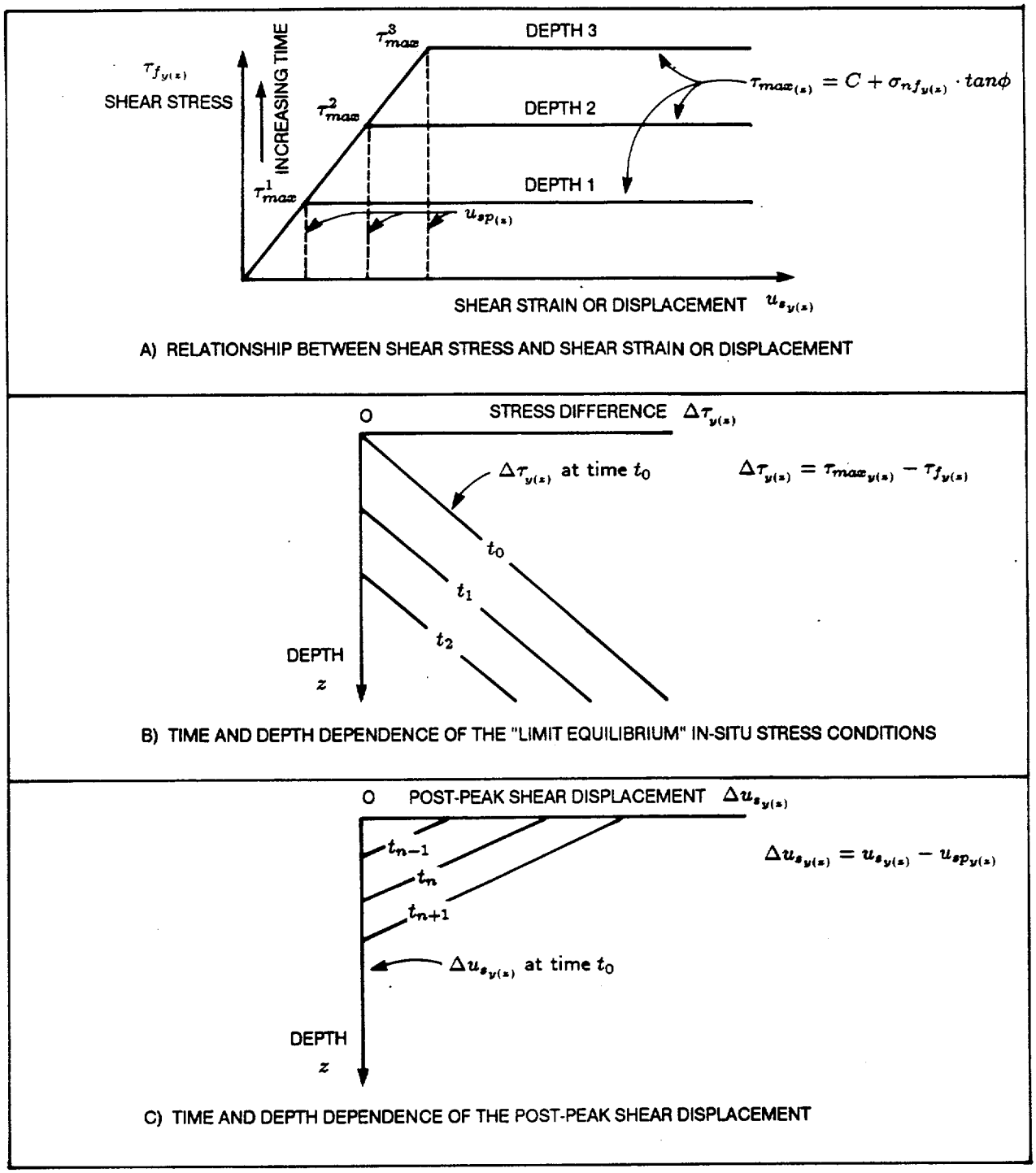

Idealization of changes in stresses and displacements occurring along a deforming fracture as a function of depth and time.

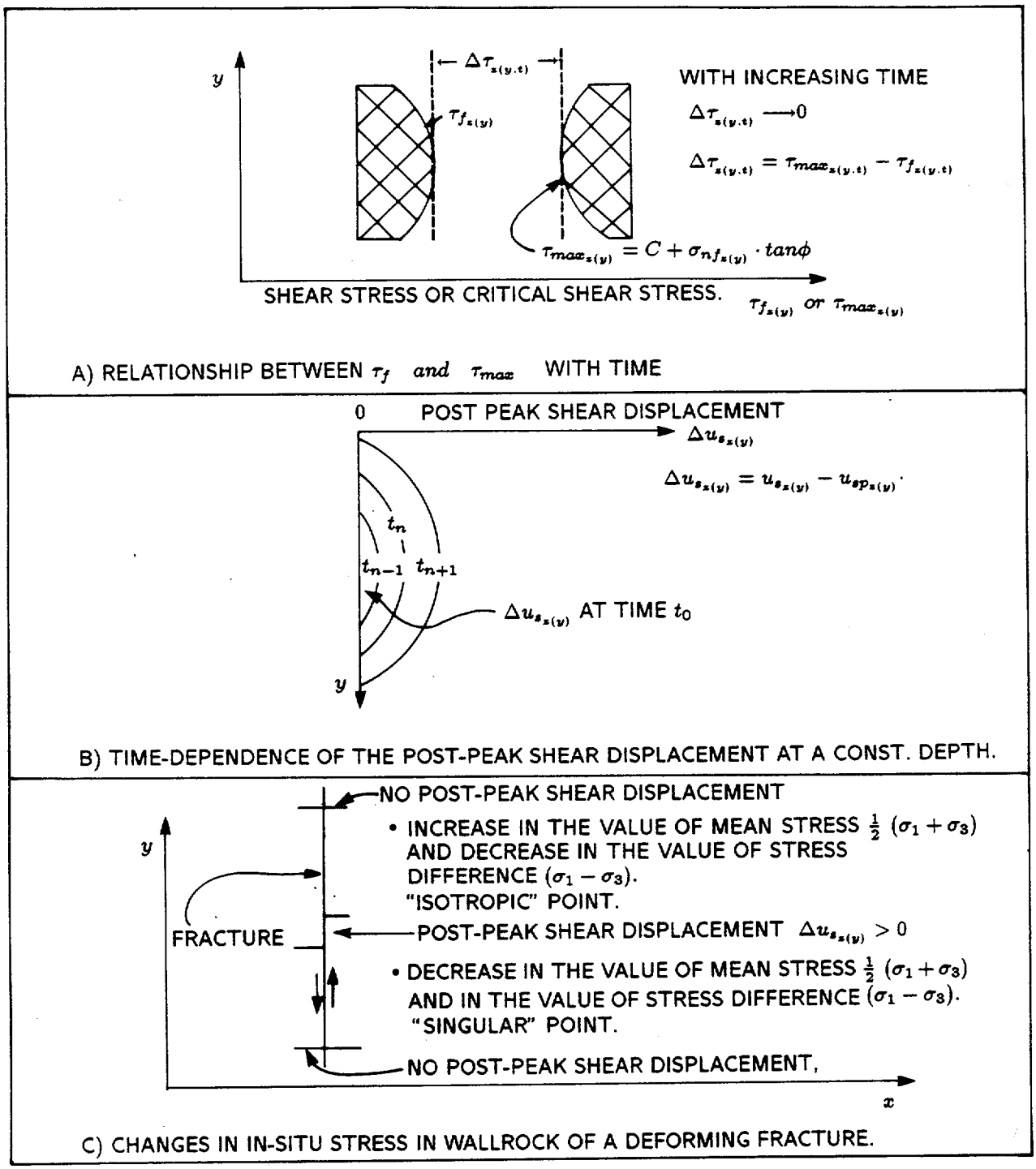

Idealization of changes in stresses and displacements occurring along a strike of a deforming fracture.

plate 3.3.3.2-4.

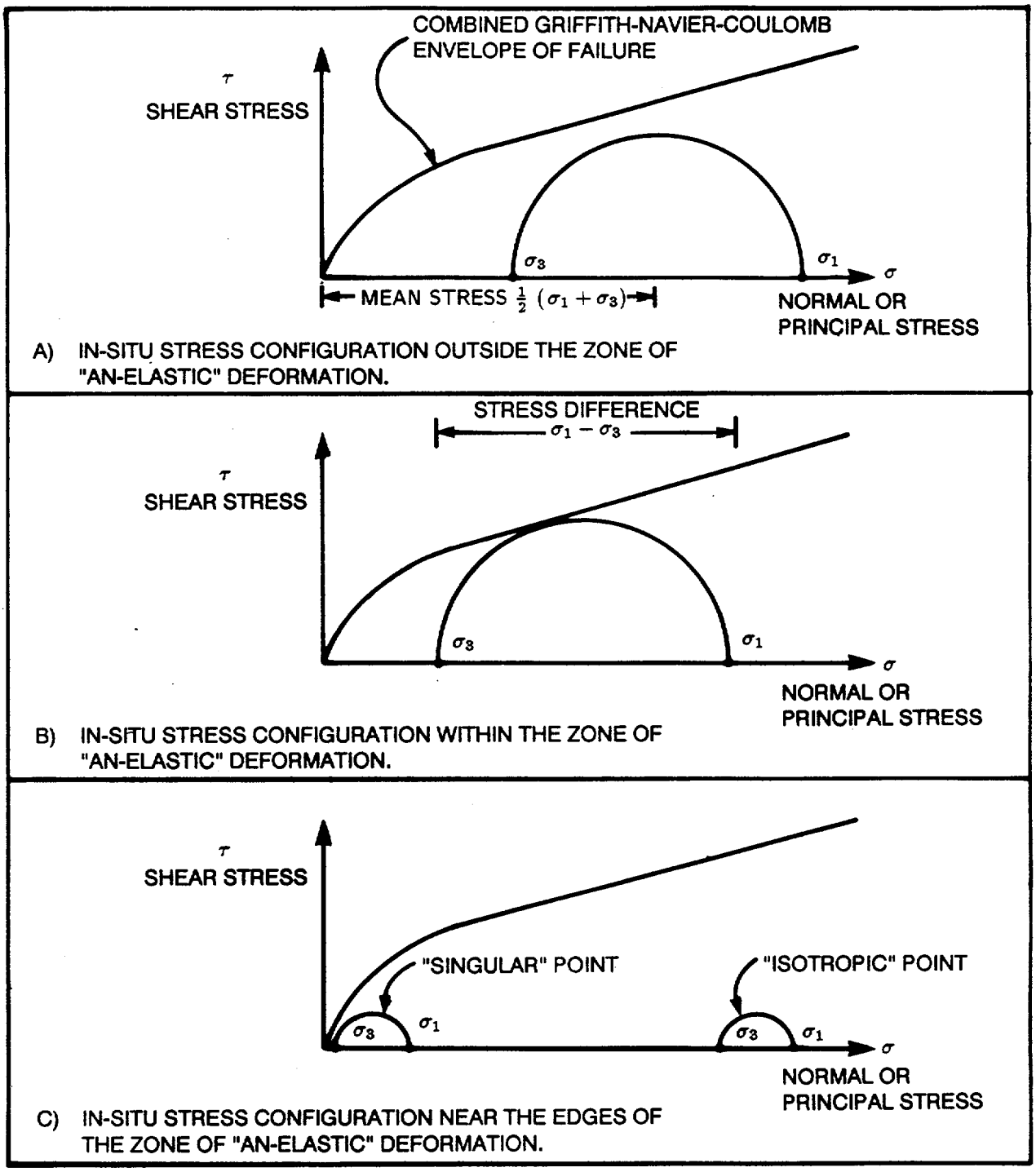

In situ stress states around a deforming fracture.

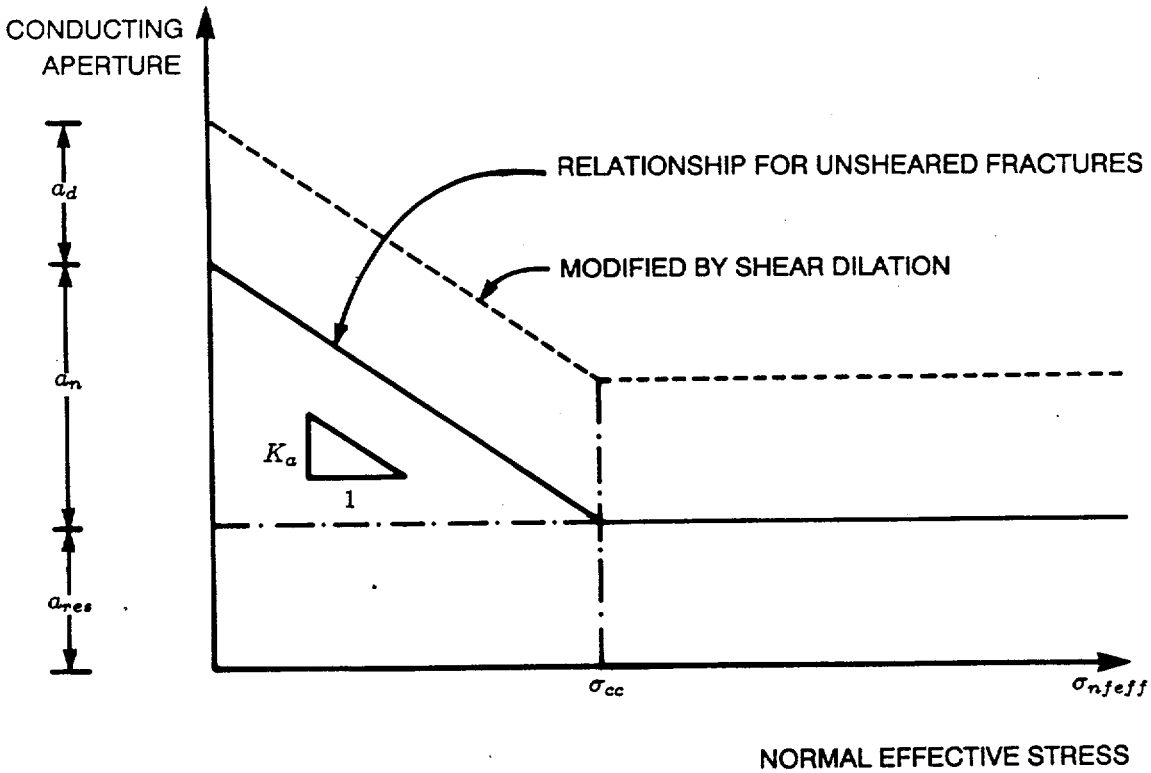

$a_{con} = a_{res} + a_n + a_d$

$a_d = f\left[K_s; (u_s - u_{sp})\right]$

$a_n = r \cdot f\left(K_a; \sigma_{nfeff}\right)$

$r = 1$ if $0 < \sigma_{nfeff} < \sigma_{cc}$

otherwise

$r = 0$

EXPLANATION:

a_{con} - FRACTURE CONDUCTING APERTURE;
a_{res} - RESIDUAL APERTURE;
a_n - NORMAL DILATION COMPONENT OF CONDUCTING APERTURE
a_d - SHEAR DILATION COMPONENT OF CONDUCTING APERTURE;
$u_s - u_{sp}$ - POST-PEAK SHEAR DISPLACEMENT; AND
K_s, K_a - COMPLIANCES

Conceptual model of conducting aperture of fractures. Modified from Harper and Last, 1987.

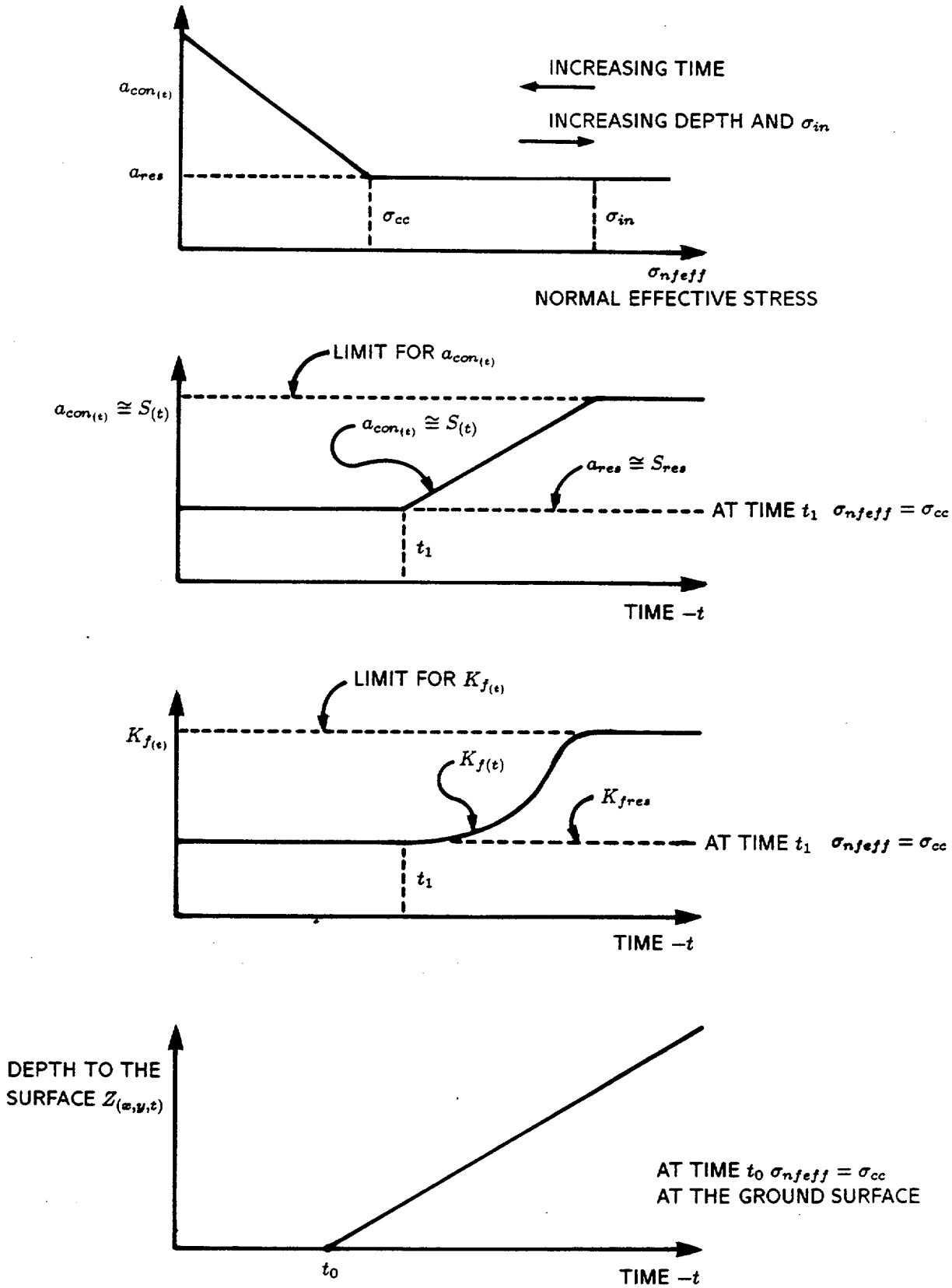

Relationships between time and hydraulic properties for decreasing σ_{nfeff}.

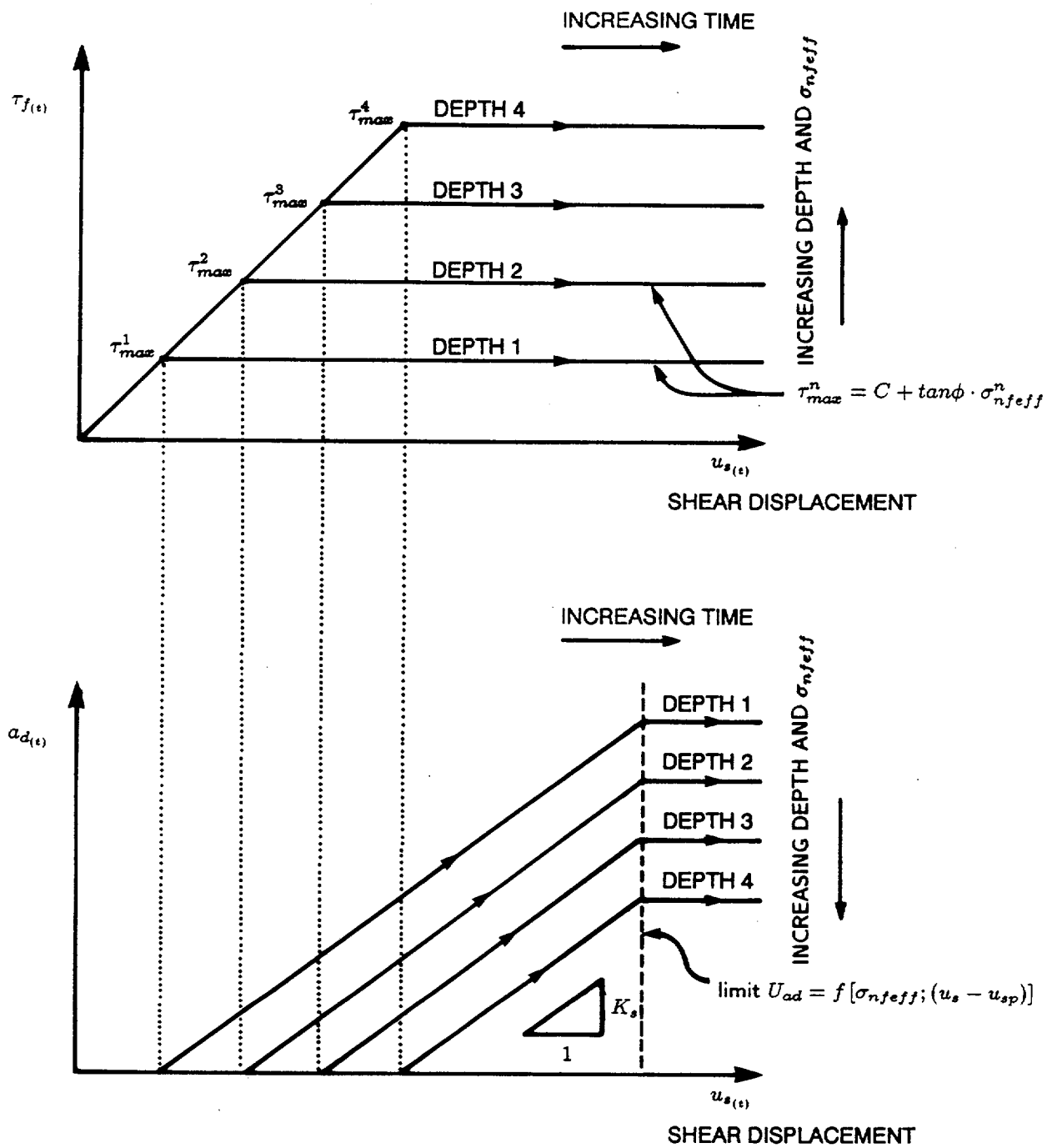

Idealized joint response during shear displacement. Modified from Harper and Last, 1987.

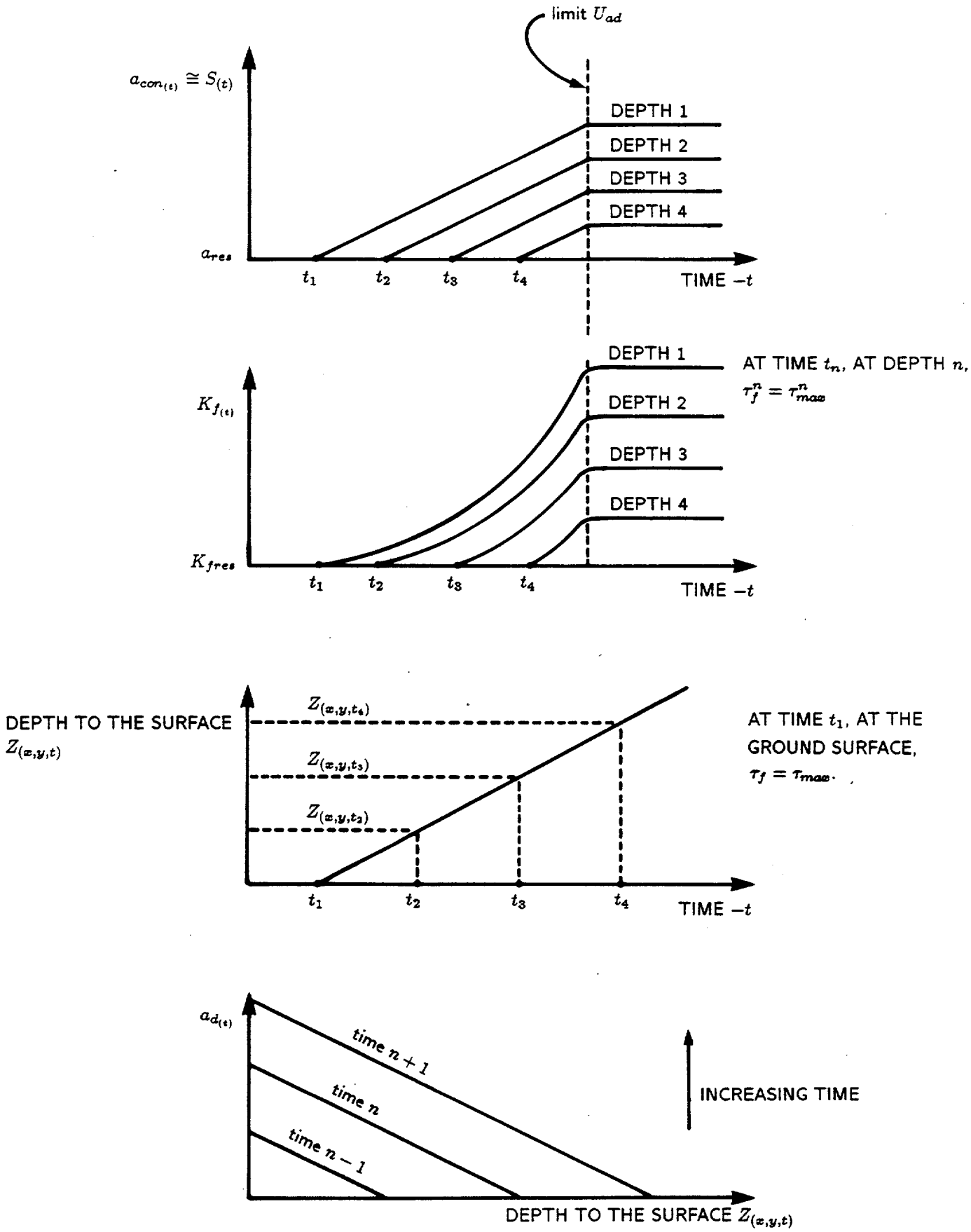

Relationships between time and hydraulic properties for increasing τ_f.

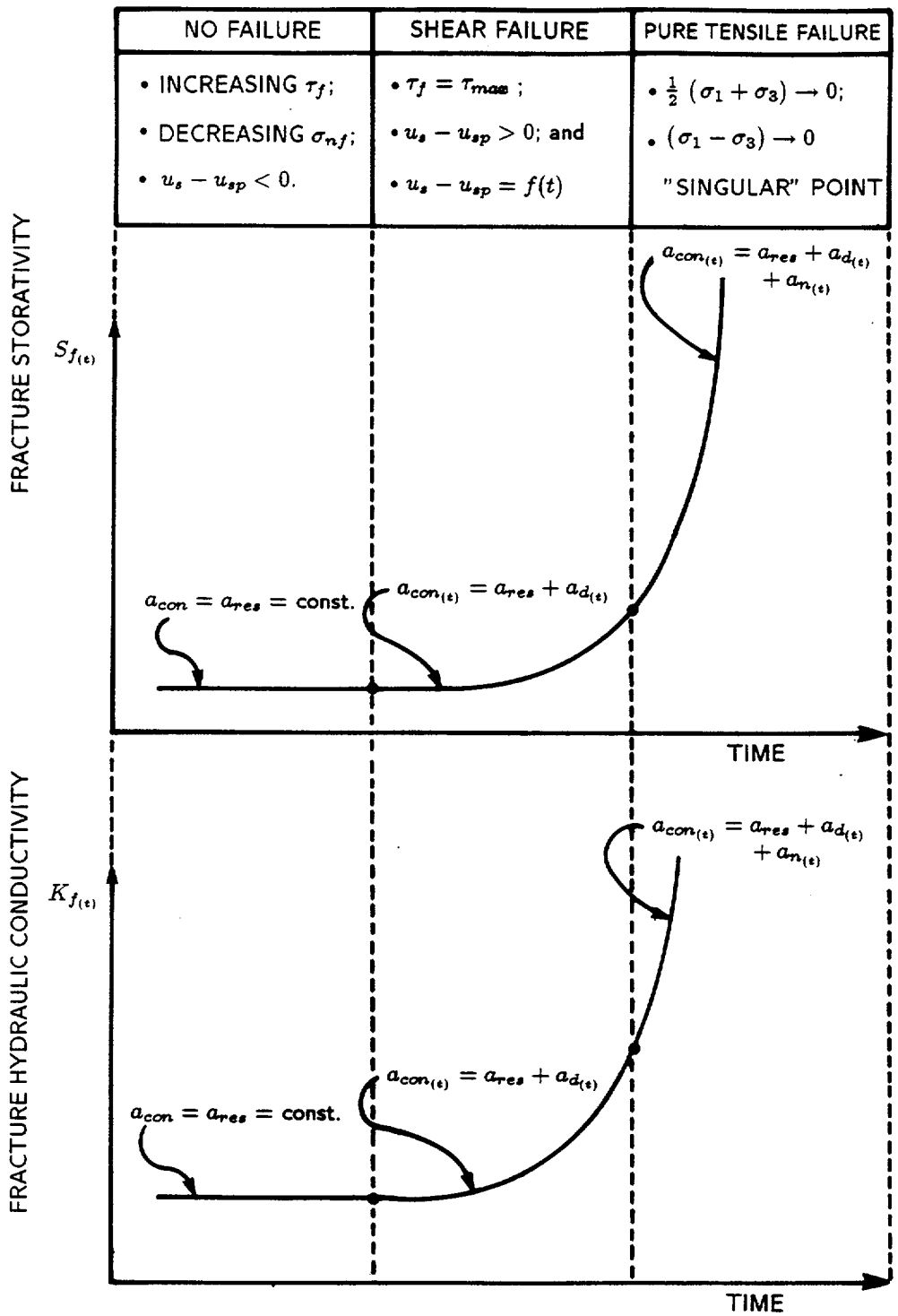

Time-dependence of S_f and K_f around a segment of a deforming fracture at a const. depth.

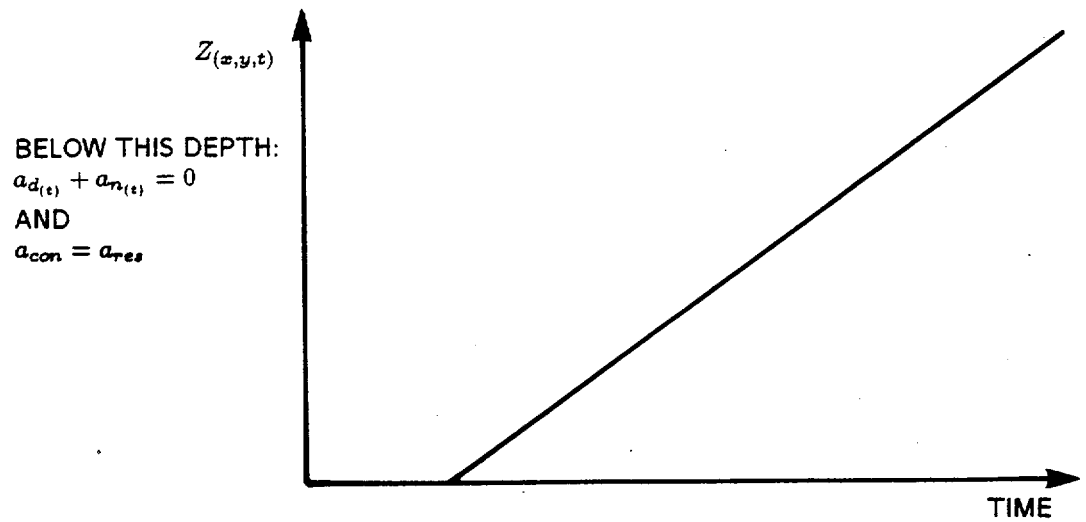

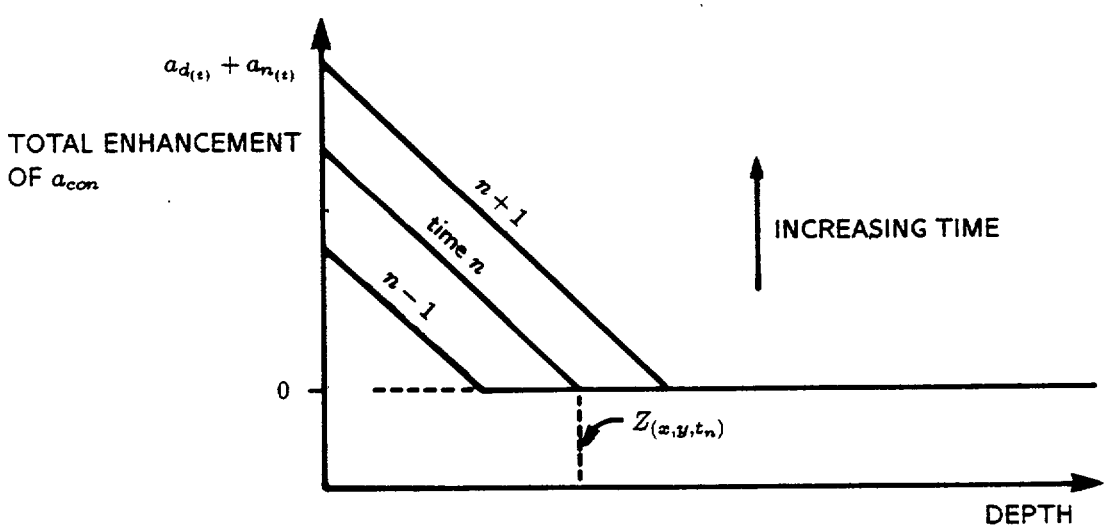

Time-dependence of vertical extent of a segment of a deforming fracture and time-dependence of the total enhancement of the conducting aperture.

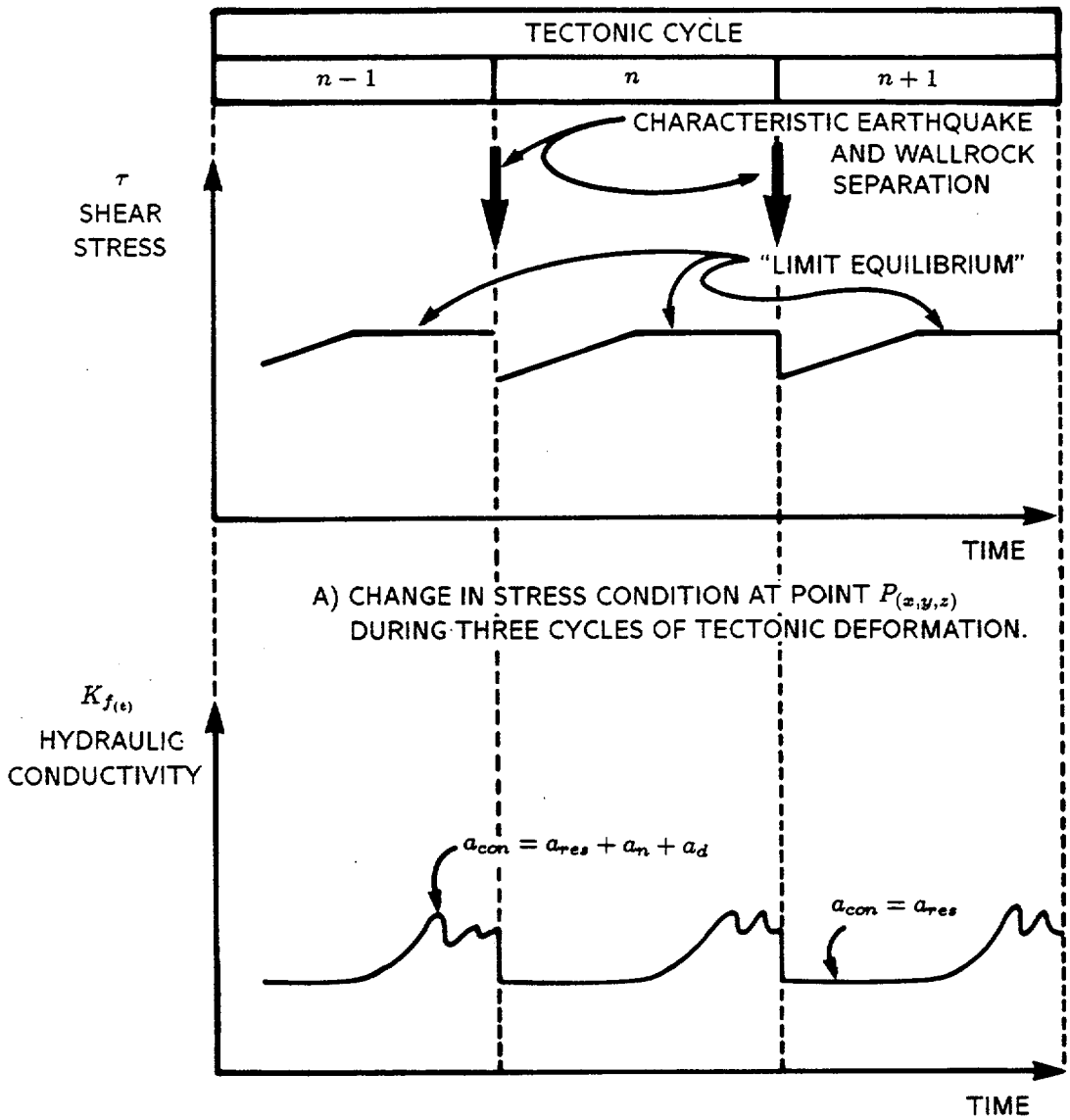

Schematic representation of changes in: a) the in situ stress conditions; and b) the hydraulic conductivity structure, occurring near the ground surface in a cyclically deforming fractured medium.

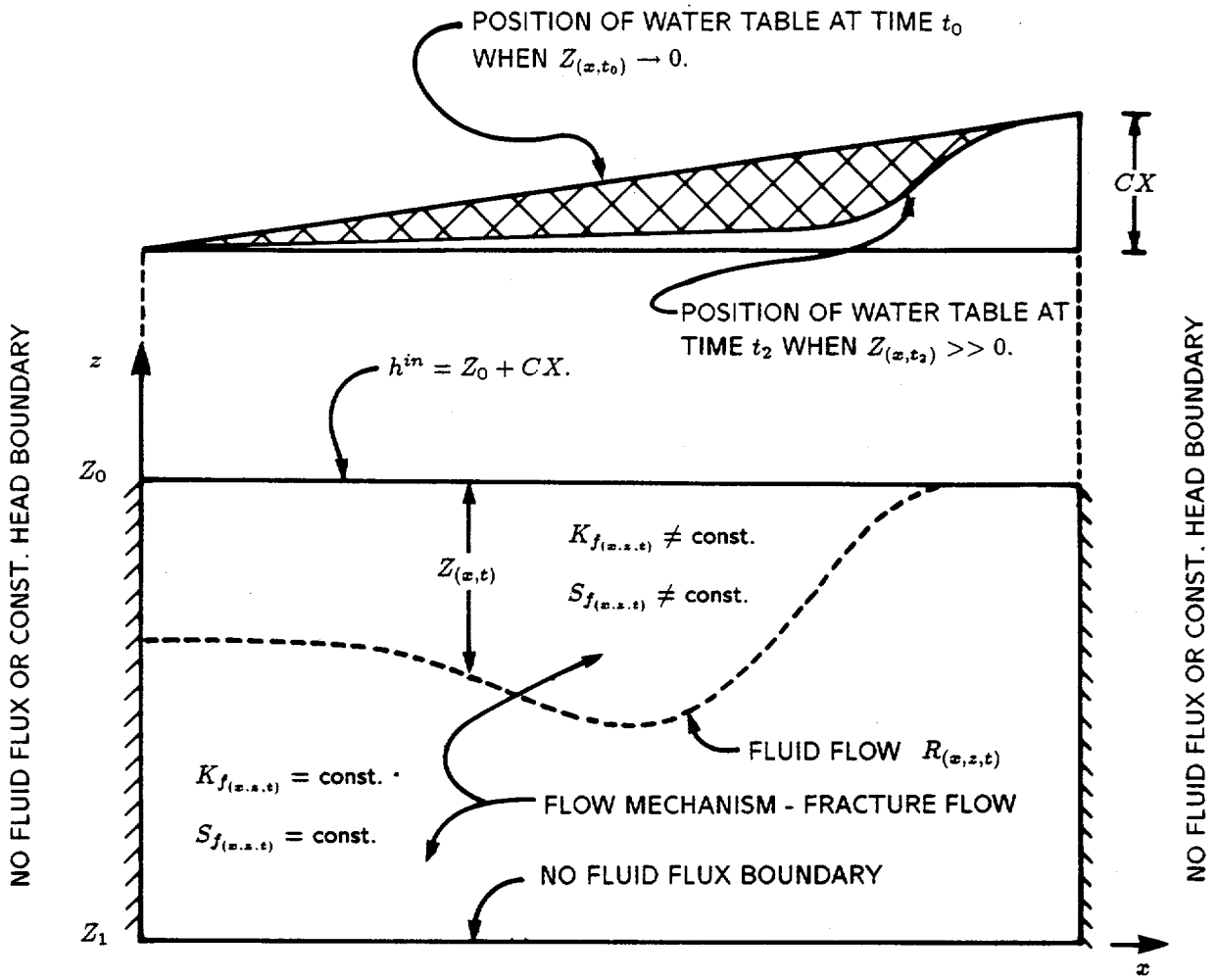

$[\sigma;\tau] = f(t)$.

$Z_{(x,t)} = f([\sigma;\tau])$

$K_{f_{(x,z,t)}} = f([\sigma;\tau])$

$S_{f_{(x,z,t)}} = f([\sigma;\tau])$

$K_{f_{(x,z)}} \neq$ const.

$S_{f_{(x,z)}} \neq$ const.

Conceptual model of groundwater flow in a deforming fractured medium.

t_0 - START OF TECTONIC DEFORMATION

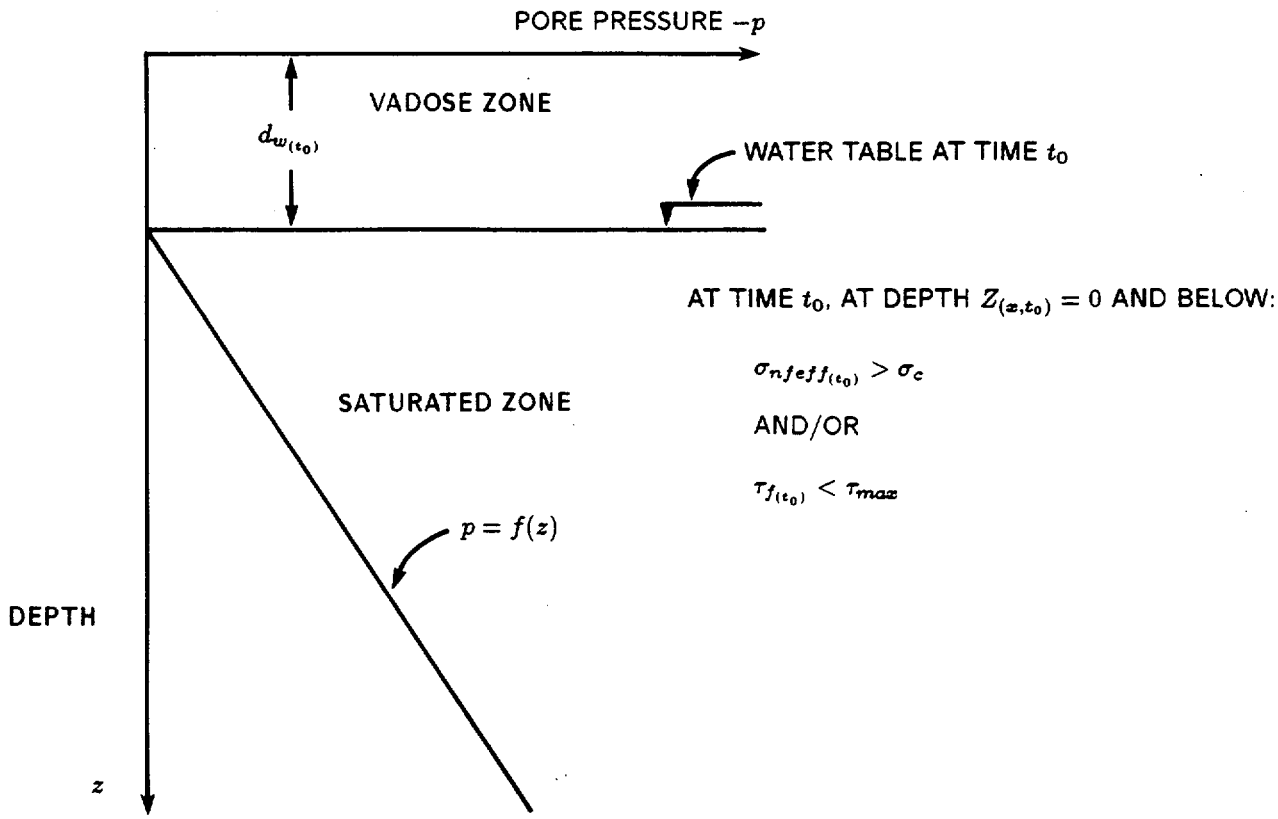

$$a_{con_{(t_0)}} = a_{res.} = \text{CONST.}$$

$$S^{UZ}_{(t_0)} = S^{SZ}_{(t_0)}$$

$$K^{UZ}_{(t_0)} = K^{SZ}_{(t_0)}$$

$$K_x = K_y$$

Deforming fractured medium - idealized history of changes in hydraulic potential.

plate 3.3.4-2.

t_1 - EARLY STAGES OF TECTONIC DEFORMATION

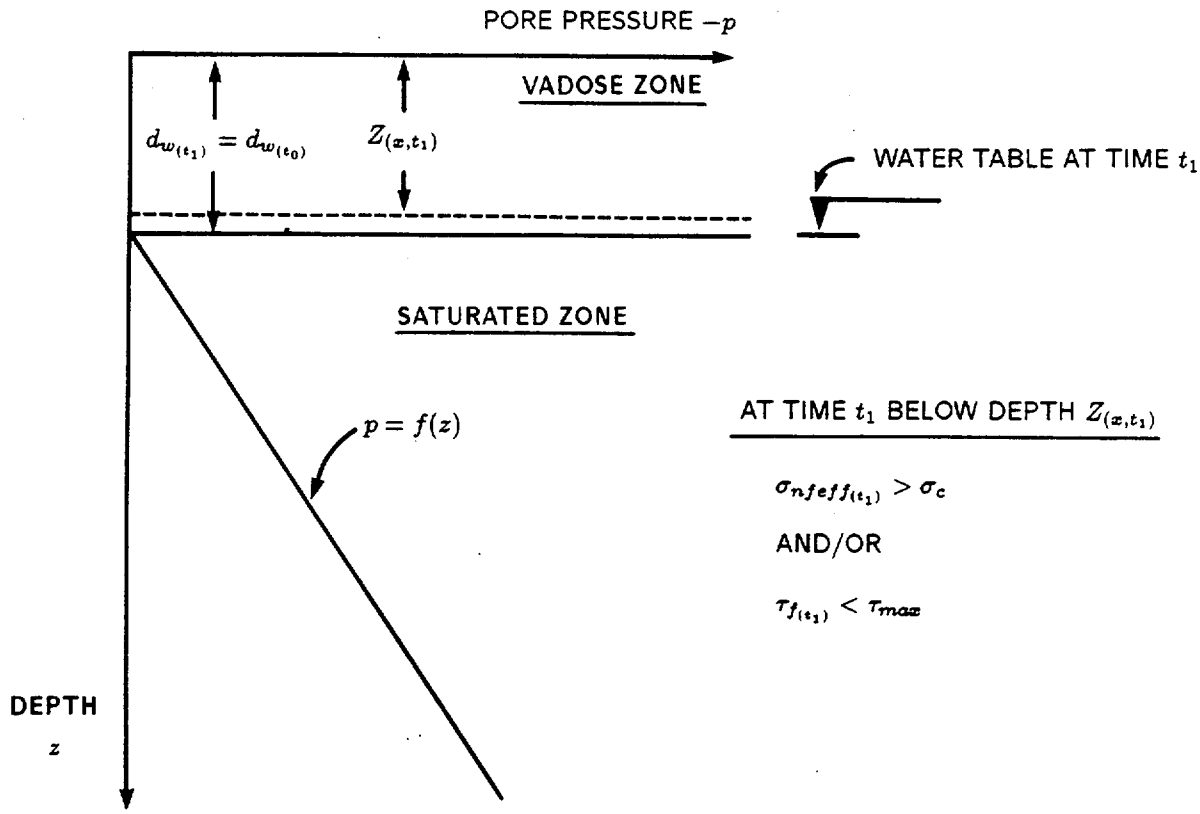

AT TIME t_1 BELOW DEPTH $Z_{(x,t_1)}$

$\sigma_{nfeff_{(t_1)}} > \sigma_c$

AND/OR

$\tau_{f_{(t_1)}} < \tau_{max}$

ABOVE DEPTH $Z_{(x,t_1)}$	BELOW DEPTH $Z_{(x,t_1)}$
$a_{con_{(t_1)}} = a_{res} + a_{n_{(t_1)}} + a_{d_{(t_1)}}$	$a_{con} = a_{res} =$ CONST.
$S^{UZ}_{(t_1)} = S^{UZ}_{(t_0)} + \Delta S^{UZ}_{(t_1)}$	$S^{SZ}_{(t_1)} = S^{SZ}_{(t_0)}$
$K^{UZ}_{(t_1)} = K^{UZ}_{(t_0)} + \Delta K^{UZ}_{(t_1)}$	$K^{SZ}_{(t_1)} = K^{SZ}_{(t_0)}$
$K_x \neq K_y$	$K_x = K_y$

Deforming fractured medium - idealized history of changes in hydraulic potential.

t_2 - ADVANCED STAGES OF TECTONIC DEFORMATION

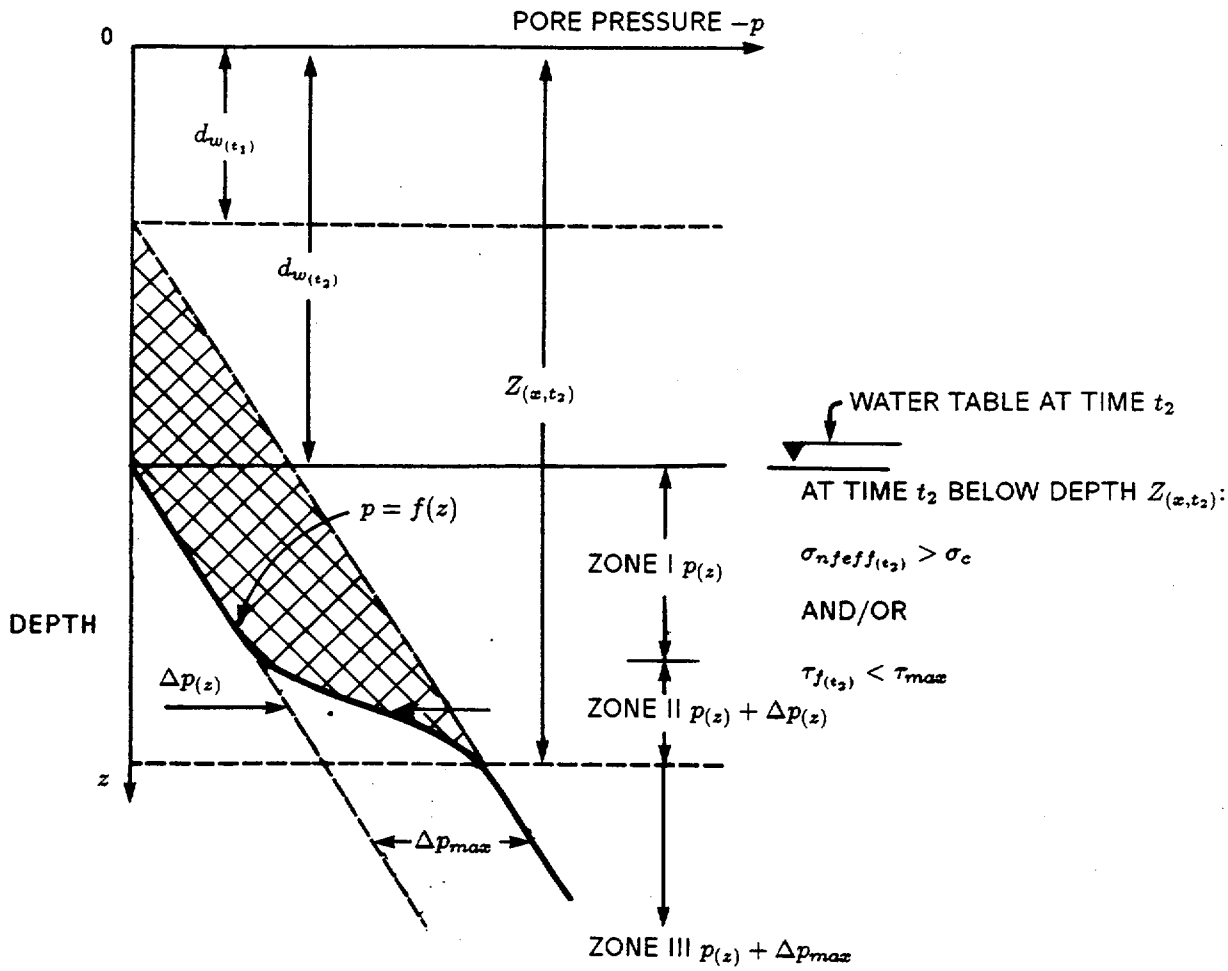

ABOVE DEPTH $Z_{(x,t_2)}$	BELOW DEPTH $Z_{(x,t_2)}$
$S^{UZ}_{(t_2)} = S^{UZ}_{(t_0)} + \Delta S^{UZ}_{(t_1)} + \Delta S^{UZ}_{(t_2)}$ $S^{SZ}_{(t_2)} = S^{SZ}_{(t_0)} + \Delta S^{SZ}_{(t_1)} + \Delta S^{SZ}_{(t_2)}$ $K^{UZ}_{f(t_2)} = K^{UZ}_{f(t_0)} + \Delta K^{UZ}_{f(t_1)} + \Delta K^{UZ}_{f(t_2)}$ $K^{SZ}_{f(t_2)} = K^{SZ}_{f(t_0)} + \Delta K^{SZ}_{f(t_1)} + \Delta K^{SZ}_{f(t_2)}$ $K_x \neq K_y$ FRACTURE FLOW	$S^{SZ}_{(t_2)} = S^{SZ}_{(t_0)}$ $K^{SZ}_{(t_2)} = K^{SZ}_{(t_0)}$ $K_x = K_y$

Deforming fractured medium-idealized history of changes in hydraulic potential.

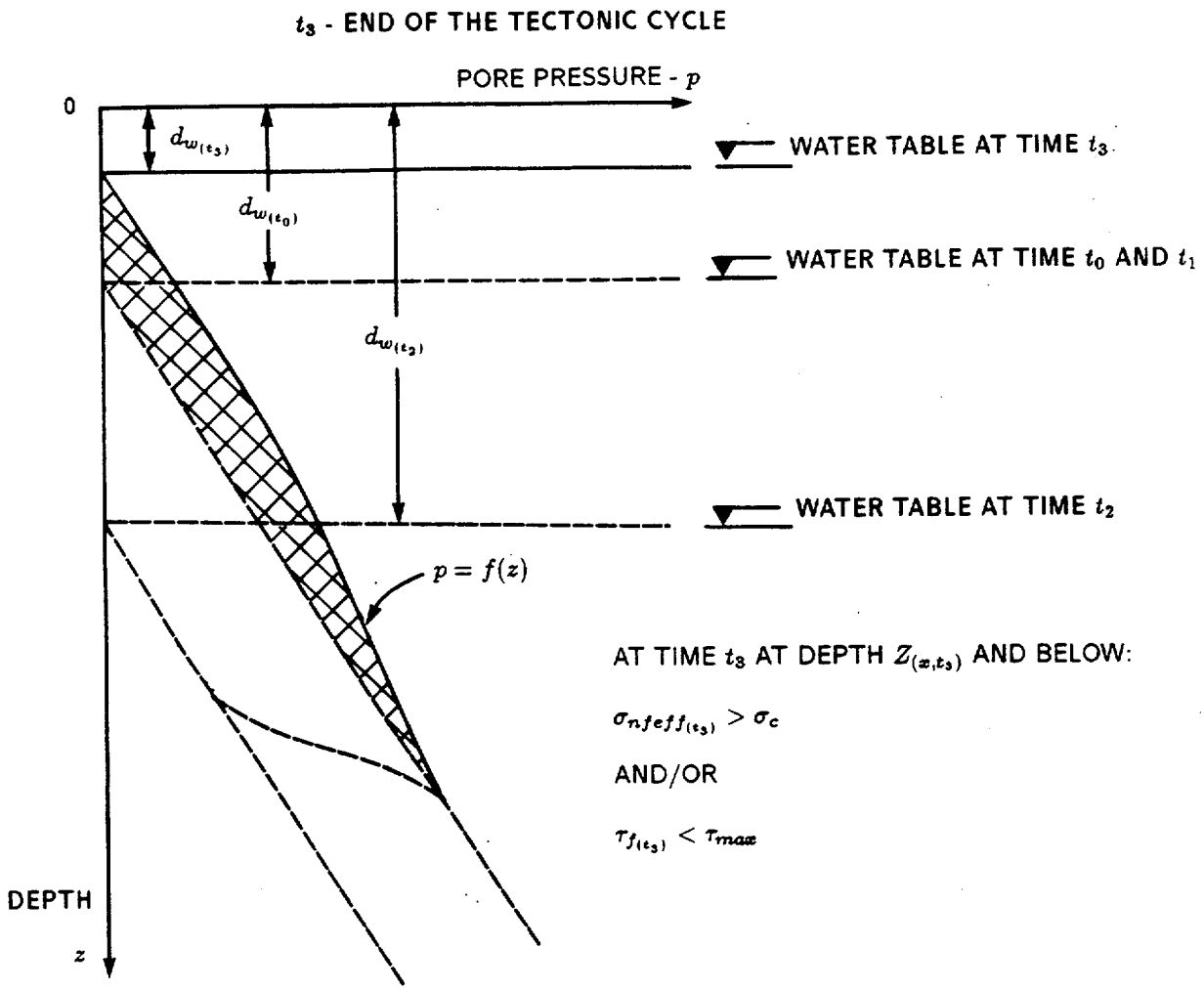

AT DEPTH $Z_{(x,t_3)}$ AND BELOW
$a_{con_{(t_3)}} = a_{res}$
$S^{UZ}_{(t_3)} = S^{UZ}_{(t_0)} < S^{UZ}_{(t_2)}$
$S^{SZ}_{(t_3)} = S^{SZ}_{(t_0)} < S^{SZ}_{(t_2)}$
$K^{UZ}_{f_{(t_3)}} = K^{UZ}_{f_{(t_0)}} < K^{UZ}_{f_{(t_2)}}$
$K^{SZ}_{f_{(t_3)}} = K^{SZ}_{f_{(t_0)}} + < K^{SZ}_{f_{(t_2)}}$
POROUS OR EQUIVALENT FLOW

Deforming fractured medium-idealized history of changes in hydraulic potential.

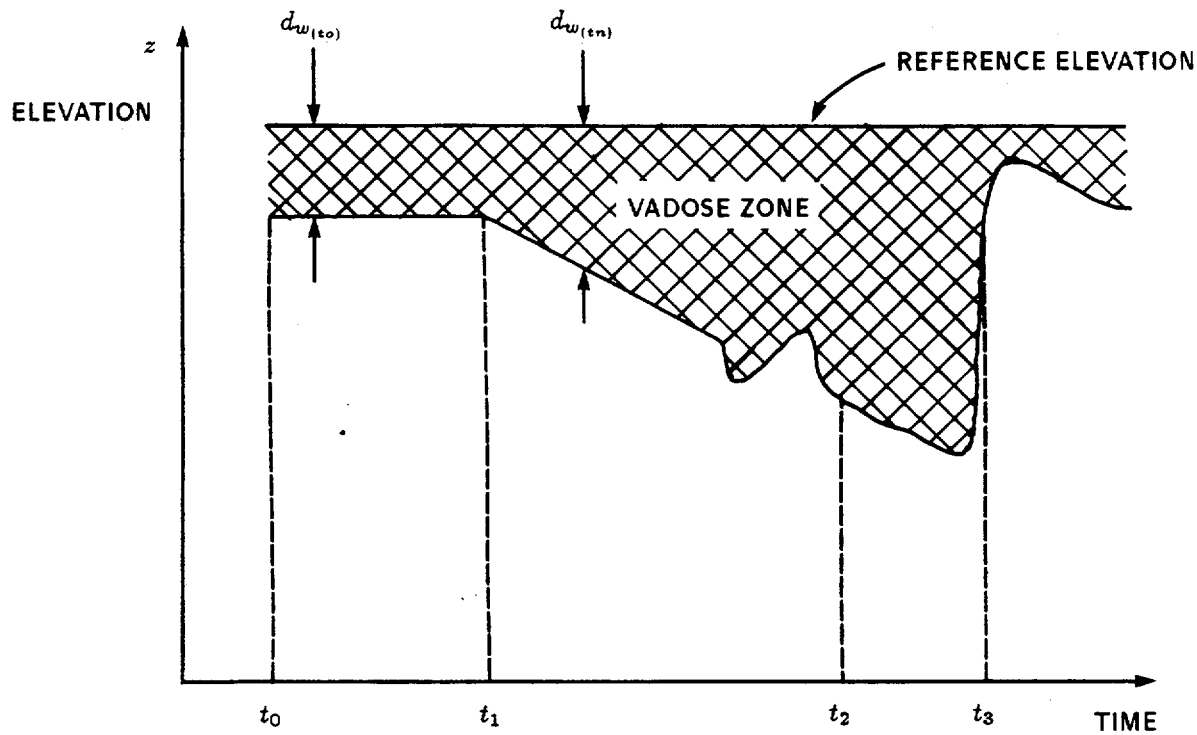

Note: The drawing is diagramatic - no relationship between initial thickness of the vadose zone and magnitude of tectonic lowering of the water table is implied.

Idealized history of the position of the water table for a single point $P_{(x,y)}$.

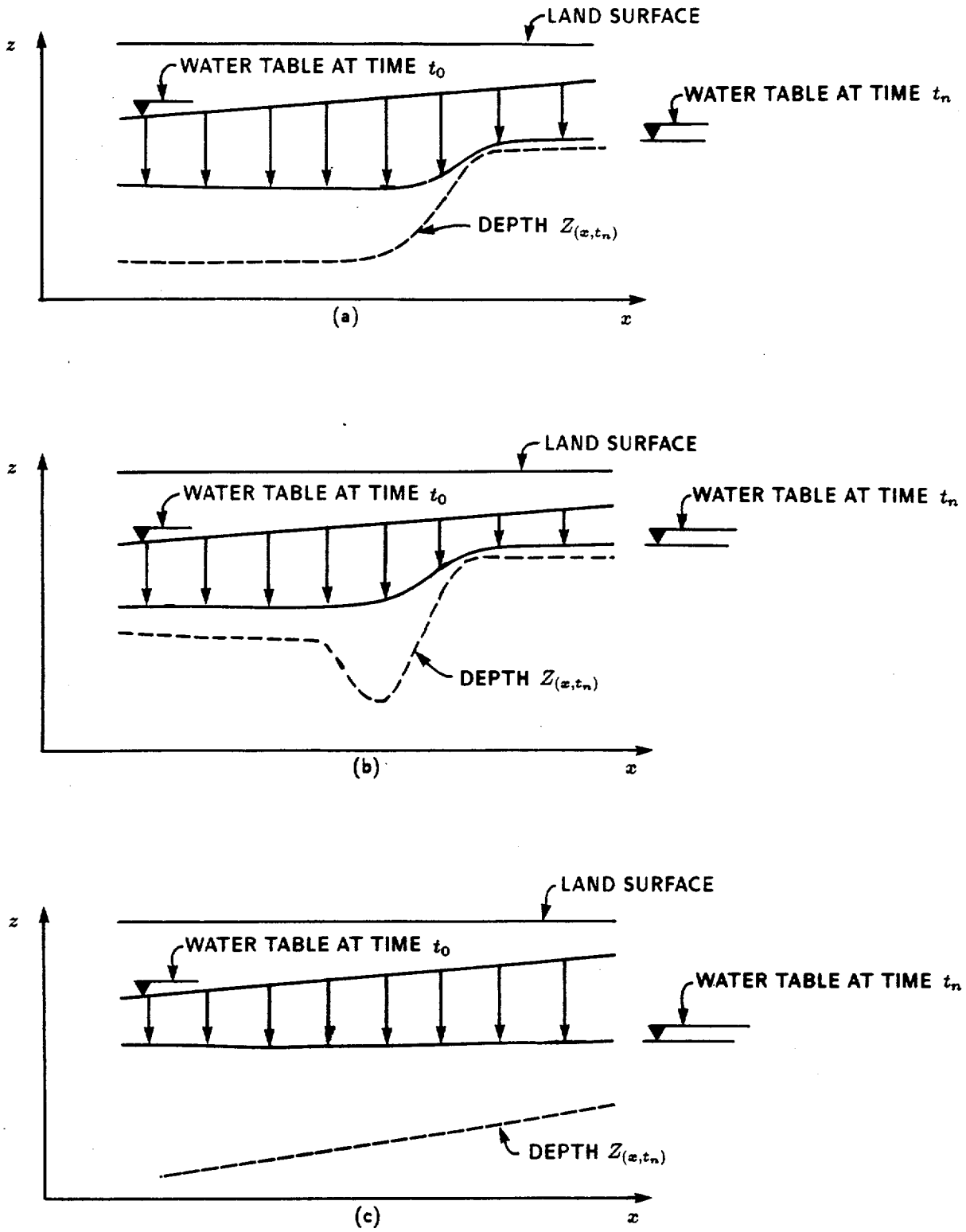

Non-homogeneous strain-its relationship to configuration of the water table.

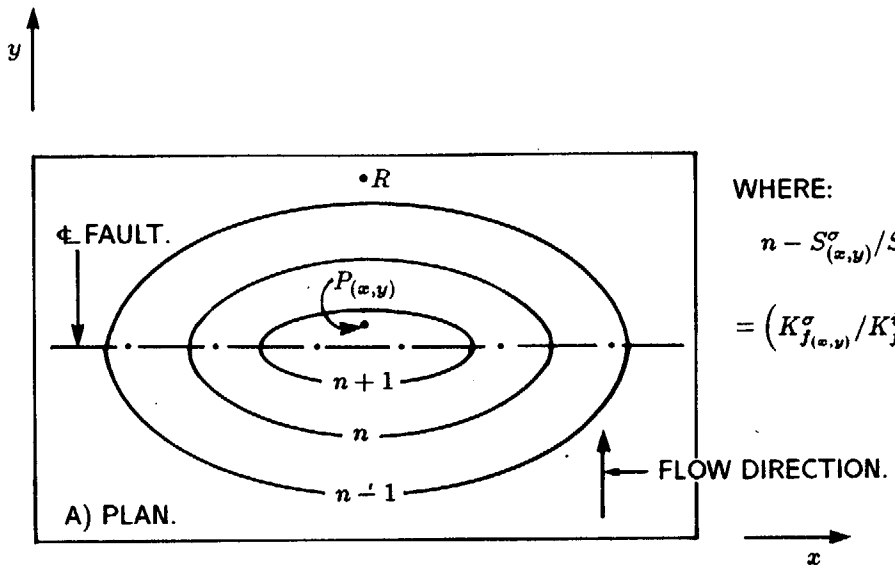

WHERE:

$$n - S^{\sigma}_{(x,y)}/S^{in}_{(x,y)} = \left(K^{\sigma}_{f(x,y)}/K^{in}_{f(x,y)}\right)^{\frac{1}{2}}$$

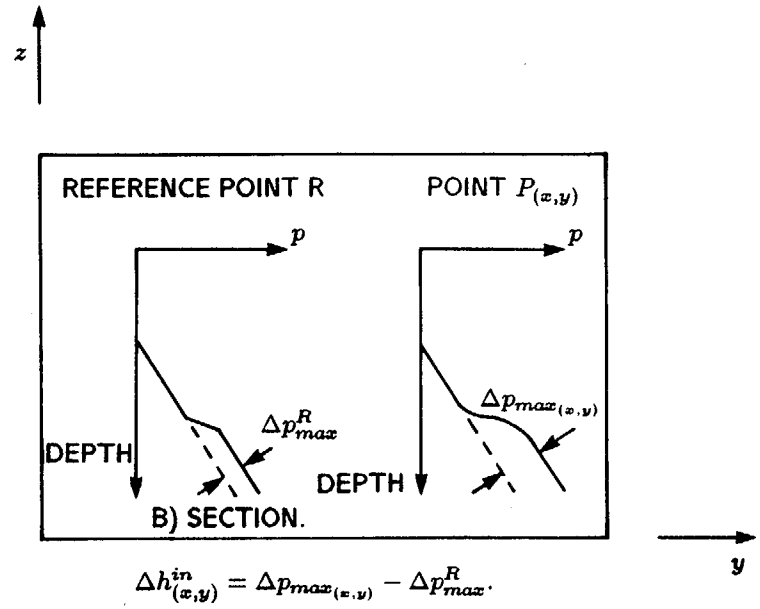

$$\Delta h^{in}_{(x,y)} = \Delta p_{max(x,y)} - \Delta p^{R}_{max}.$$

$$\max \Delta h^{\sigma}_{(x,y)} = \max \Delta h^{ov}_{(x,y)} + \max \Delta h^{sr}_{(x,y)}$$

$$\max \Delta h^{sr}_{(x,y)} = \Delta h^{in}_{(x,y)} \cdot S^{\sigma}/S^{in};$$

S^{σ}/S^{in} – RATIO OF AVERAGE AMOUNT OF FLUID IN STORAGE IN "STRAINED" STATE TO AVERAGE AMOUNT OF FLUID IN STORAGE IN "UNSTRAINED" STATE;

$$S^{\sigma}/S^{in} = \sqrt{K^{\sigma}_{f}/K^{in}_{f}};$$

K^{σ}_{f} – AVERAGE VALUE OF HYDRAULIC CONDUCTIVITY IN "STRAINED" STATE;

K^{in}_{f} – AVERAGE VALUE OF HYDRAULIC CONDUCTIVITY IN "UNSTRAINED" STATE.

WHERE:

$\max \Delta h^{\sigma}_{(x,y)}$ – MAX. POTENTIAL RISE OF WATER TABLE AT $P_{(x,y)}$;

$\max \Delta h^{ov}_{(x,y)}$ – "OVERPRESSURE" COMPONENT OF THE TOTAL RISE;

$\max \Delta h^{ov}_{(x,y)} = \Delta p_{max(x,y)}$.

$\max \Delta h^{sr}_{(x,y)}$ – STORAGE RELEASE COMPONENT OF THE TOTAL RISE;

Maximum rise of the water table at point $P_{(x,y)}$ caused by change in the in situ stress conditions.

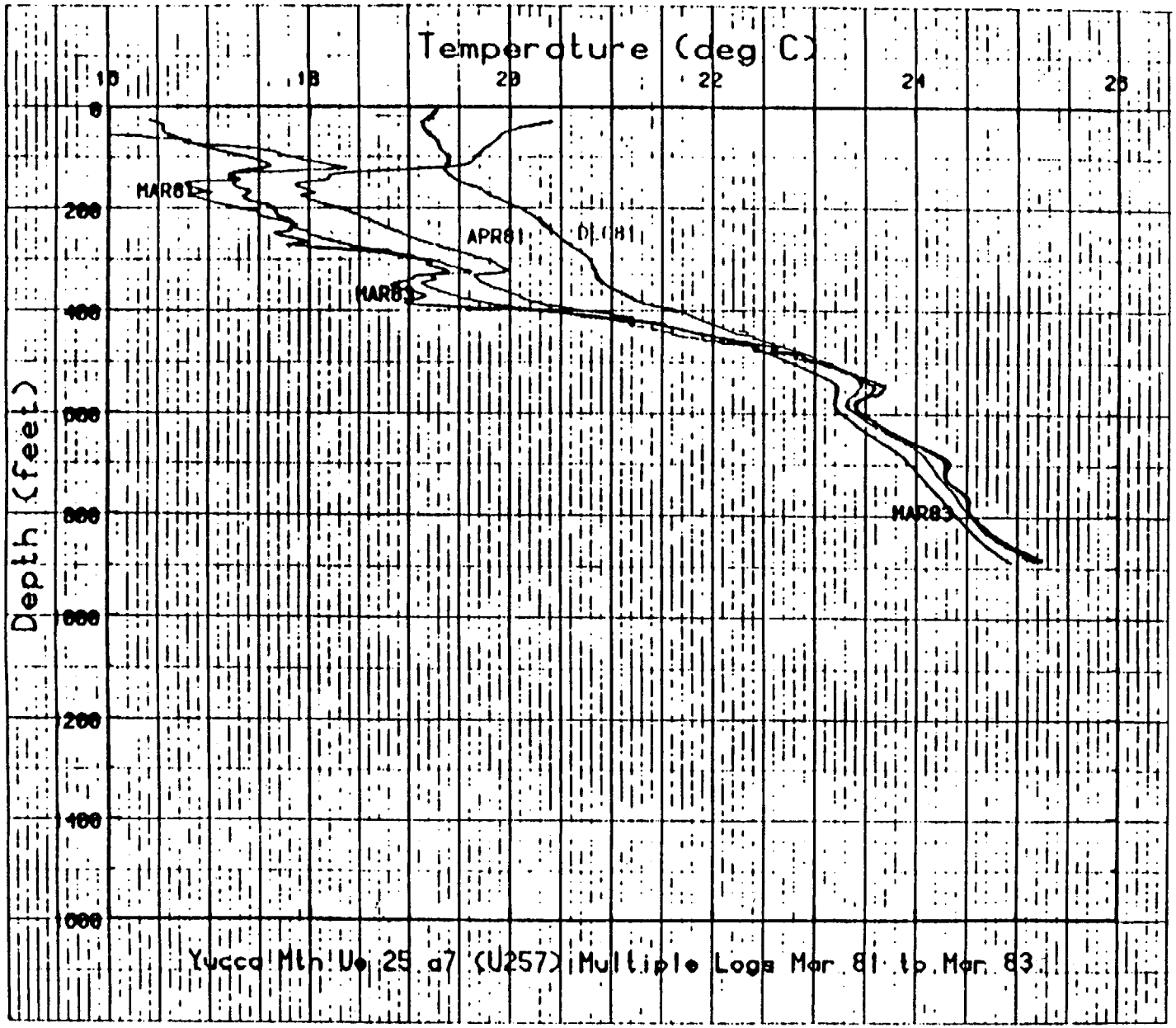

Repeated temperature profiles from Well UE-25a7. From Sass et al., 1983.

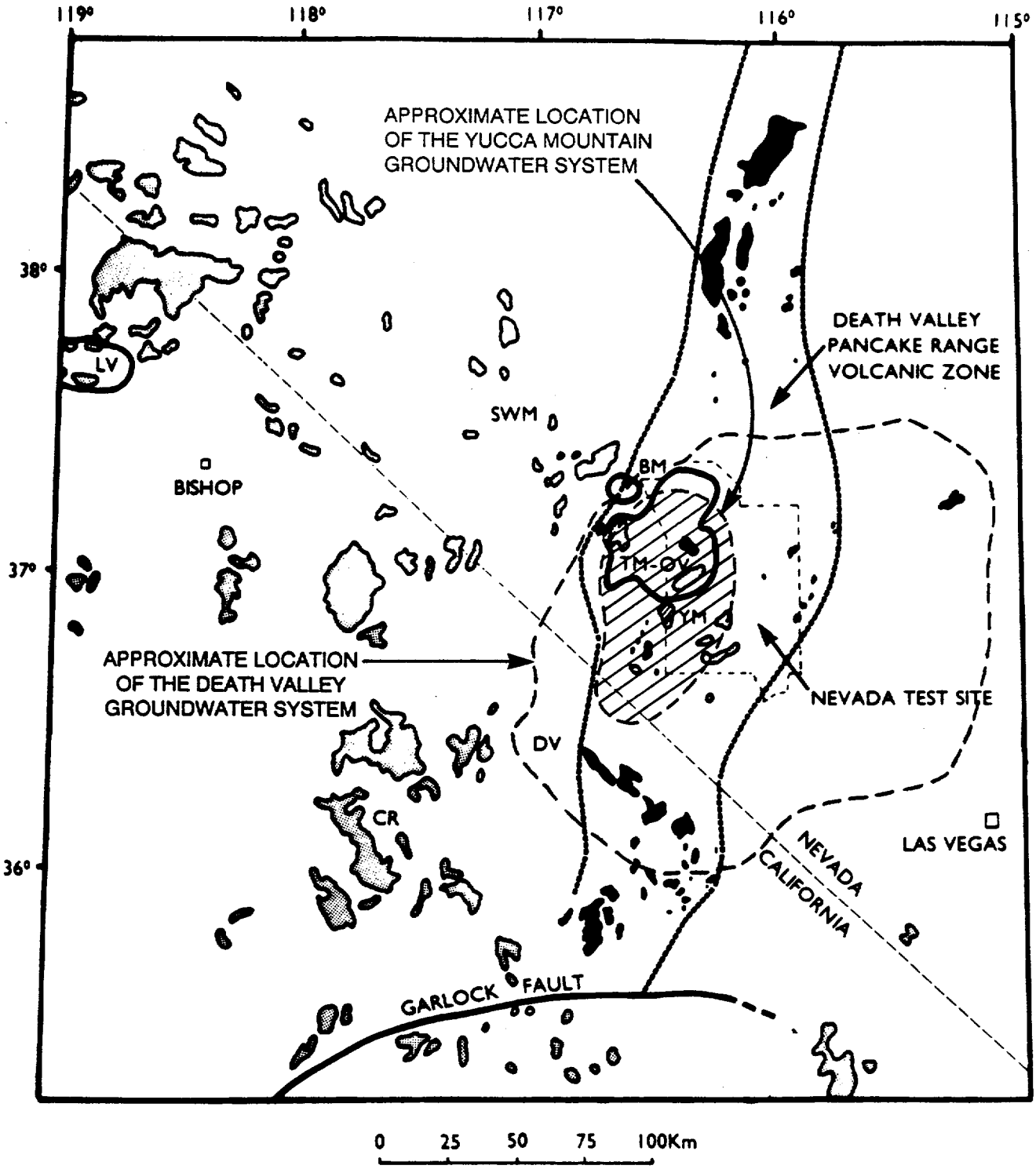

Explanation: SWM: Stonewall; BM: Black Mountain; TM-OV: Timber Mountain-Oasis Valley caldera complex; YM: Yucca Mountain exploration block; LV: Long Valley; DV: Death Valley; and CR: Coso Range. Black-shaded areas are volcanic rocks of the DV-PR volcanic zone; light-shaded areas are part of the western Cordillera rift zone.

Generalized geologic map of the Death Valley Pancake Range Volcanic Zone and of the Death Valley groundwater system. From Crowe et al., 1986.

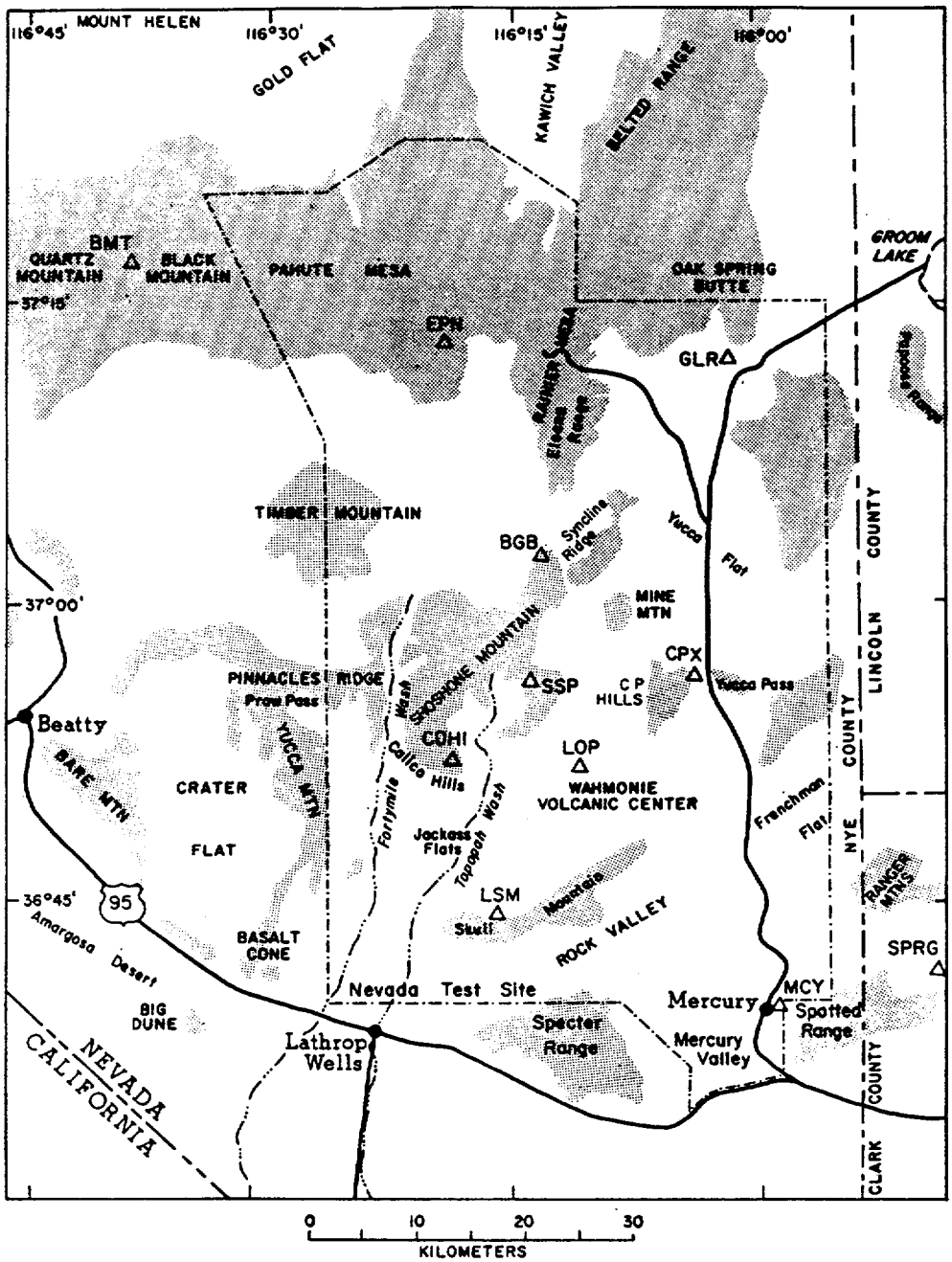

Location of seismic monitoring stations used for detailed analyses of the P-wave residuals. From Monfort and Evans, 1982.

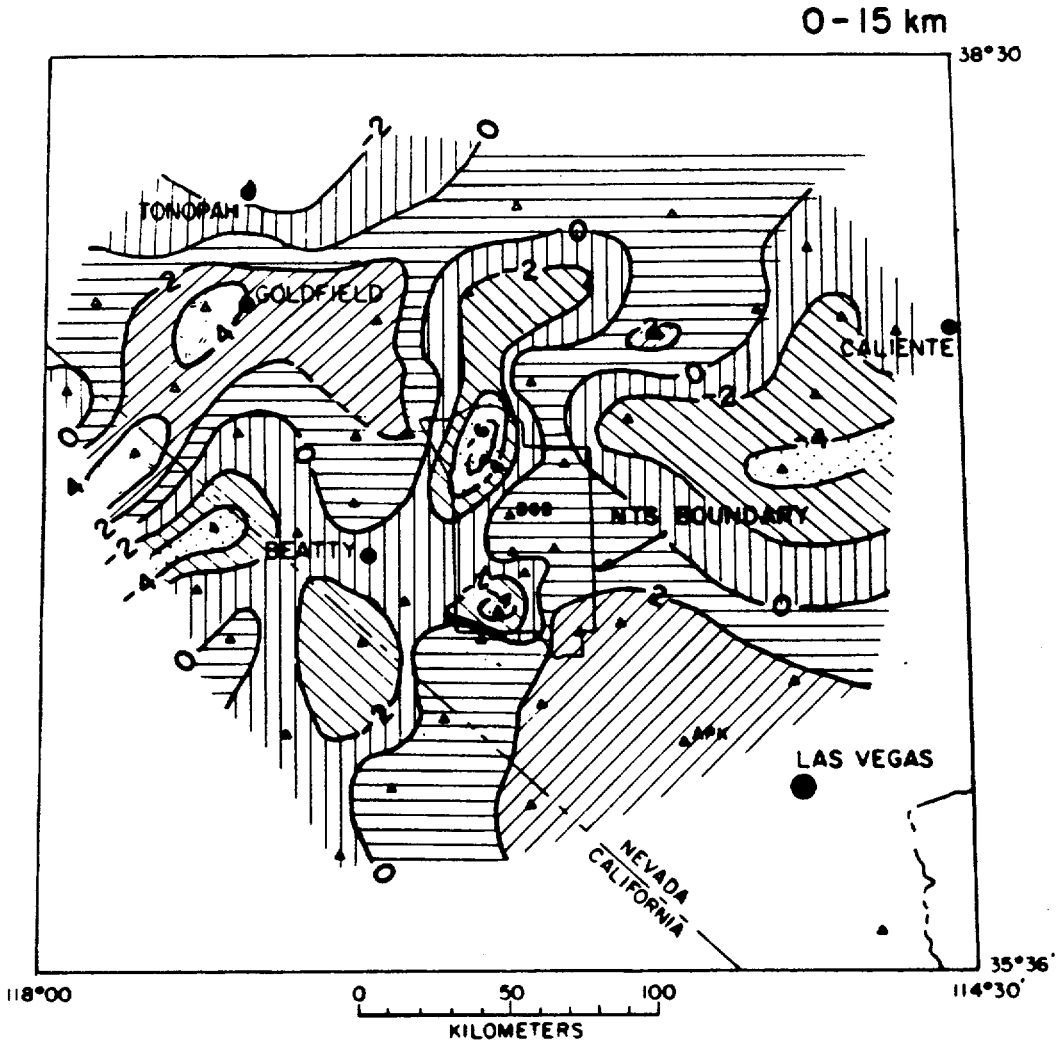

EXPLANATION:

- ZERO VELOCITY PERTURBATION IS THE MEAN LAYER VELOCITY
- VELOCITY PERTURBATIONS ARE IN PERCENTS
- POSITIVE VELOCITY PERTURBATIONS ARE RELATIVE HIGH VELOCITIES

Seismic velocity structure of the upper crust from teleseismic P-wave residuals for the region of Death Valley groundwater system. From Monfort and Evans, 1982.

Model nov9b Layer 2 15 – 31 km

	-.01 .37 .62	-2.95 .38 .62		-.45 .33 .66				
5.19 .34 .57	4.30 .49 .71	1.19 .15 .58	2.38 .65 .68	-.60 .61 .73	.05 .59 .73	-2.40 .66 .76	-3.55 .64 .68	.78 .29 .74
-.50 .54 .70	3.08 .63 .67	.40 .03 .30	-.76 .64 .70	.88 .58 .70	-1.76 .72 .67	.43 .70 .72	-1.17 .70 .63	-.91 .50 .72
-2.54 .54 .72	.80 .73 .61	-1.19 .73 .67	.63 .64 .72	-.21 .79 .57	.03 .70 .69	-1.85 .53 .73	-2.75 .55 .69	
	.23 .64 .67	-.21 .60 .72	-1.40 .72 .69	1.64 .83 .49	1.23 1.72 1.68			
	.57 .48 .71	.49 .70 .71	.17 .79 .60	-.15 .80 .59	-.80 .72 .65	2.07 .12 .57	.79 .29 .48	
		-.02 .44 .66	2.06 .64 .69	.51 .67 .71	-.16 .50 .79	-.03 .39 .68		
		-1.82 .39 .55	2.24 .25 .60	-.22 .35 .70				

NTS BOUNDARY

35 KM

EXPLANATION:

- CONTOURS SHOWN ARE ZERO VELOCITY PERTURBATIONS
- IN EACH BLOCK, THE UPPER NUMBER IS VELOCITY PERTURBATION (%), THE MIDDLE NUMBER IS THE DIAGONAL ELEMENT OF THE RESOLUTION MATRIX, AND THE BOTTOM NUMBER IS THE STANDARD ERROR FOR THE BLOCK

Seismic velocity structure of the lower crust from teleseismic P-wave residuals for the region of Death Valley groundwater system. From Monfort and Evans, 1982.

Model nov9b Layer 3 31 - 81 km

	.81 .56 .82	3.37 .74 .65			.12 .70 .75				
-.50 .75 .66	1.71 .83 .60	2.21 .83 .54	-2.05 .78 .64	1.16 .85 .53	-1.44 .87 .48	-3.04 .85 .55	-2.01 .89 .45	.60 .78 .66	
-1.58 .89 .40	-.12 .92 .36	.09 .84 .56	.72 .89 .46	-.84 .92 .38	-.43 .93 .34	-.27 .91 .41	-.99 .91 .38	-2.22 .91 .38	-1.62 .68 .75
-.43 .90 .40	-.67 .93 .34	-.20 .91 .42	.67 .92 .41	.98 .94 .33	.77 .94 .32	.47 .91 .42	-1.17 .92 .37	-1.72 .87 .48	-2.18 .84 .52
1.16 .65 .77	-.52 .92 .39	.63 .94 .34	1.66 .93 .36	.85 .95 .27	2.07 .95 .30	-.61 .85 .56	.74 .88 .49	1.57 .74 .63	
	-.06 .89 .45	1.22 .92 .39	-.28 .94 .34	-1.08 .95 .28	-.50 .95 .28	-2.19 .90 .45	1.32 .82 .54		
	1.92 .65 .78	1.63 .90 .42	.51 .92 .38	-1.06 .94 .33	-.92 .92 .39	.16 .90 .40	-1.24 .85 .48	-1.11 .67 .59	
		2.87 .85 .53	2.78 .91 .40	2.37 .89 .44	.77 .84 .54	-.11 .76 .67	.46 .79 .59		
		3.24 .51 .70	4.07 .74 .67	1.51 .69 .69	2.03 .18 .67				

35 KM

EXPLANATION:

- CONTOURS SHOWN ARE ZERO VELOCITY PERTURBATIONS;
- IN EACH BLOCK, THE UPPER NUMBER IS VELOCITY PERTURBATION (%), THE MIDDLE NUMBER IS THE DIAGONAL ELEMENT OF THE RESOLUTION MATRIX, AND THE BOTTOM NUMBER IS THE STANDARD ERROR FOR THE BLOCK.

Seismic velocity structure of the upper mantle from teleseismic P-wave residuals for the region of Death Valley groundwater system. From Monfort and Evans, 1982.

Model nov9b Layer 4 81 - 131 km

	1.07 .72 .73		.40 .76 .71	.68 .70 .72	-1.88 .79 .62	-2.36 .80 .62	1.43 .77 .71		
-.74 .85 .62	.30 .83 .58	-1.30 .85 .54	-1.46 .86 .54	1.50 .87 .49	2.78 .87 .50	-.03 .89 .46	-.69 .87 .49	1.18 .75 .67	
-1.16 .92 .46	-.44 .89 .49	-.16 .91 .44	1.29 .92 .40	3.90 .92 .41	1.37 .91 .43	-.77 .92 .40	-1.00 .89 .48	-1.41 .85 .56	-1.01 .74 .74
1.59 .93 .42	-1.08 .89 .47	-.98 .93 .37	1.21 .94 .35	4.03 .93 .36	3.60 .93 .35	.60 .92 .39	-.54 .91 .41	-1.30 .84 .56	1.59 .89 .52
1.44 .88 .51	-.15 .90 .46	.96 .94 .36	1.38 .94 .34	3.37 .94 .32	2.96 .93 .36	-.18 .92 .39	-.84 .88 .51	-.36 .81 .63	1.64 .85 .57
1.08 .74 .74	.93 .88 .51	.28 .91 .43	1.62 .94 .35	.81 .94 .32	-.56 .93 .36	-2.17 .92 .40	-1.88 .84 .58	-1.72 .80 .61	.24 .67 .74
	.82 .84 .56	1.37 .90 .46	.97 .93 .35	-.72 .93 .36	-1.64 .93 .37	-2.27 .90 .43	-3.97 .78 .62	.74 .53 .83	
	1.10 .77 .71	.45 .83 .59	1.99 .87 .54	-.85 .89 .47	-.18 .89 .47	-1.23 .82 .60	-1.40 .81 .61	-.05 .62 .77	-1.00 .69 .69
		1.37 .68 .66	1.49 .69 .74	.01 .75 .64	1.14 .75 .67	.25 .64 .70			

35 KM

EXPLANATION:

- CONTOURS SHOWN ARE ZERO VELOCITY PERTURBATIONS
- IN EACH BLOCK, THE UPPER NUMBER IS VELOCITY PERTURBATION (%), THE MIDDLE NUMBER IS THE DIAGONAL ELEMENT OF THE RESOLUTION MATRIX, AND THE BOTTOM NUMBER IS THE STANDARD ERROR FOR THE BLOCK

Seismic velocity structure of the mantle (depth 81-131 km) from teleseismic P-wave residuals for the region of Death Valley groundwater system. From Monfort and Evans, 1982.

Model nov9b Layer 5 131 - 231 km

-.82 .88 .51	.46 .85 .63	2.05 .89 .51	2.59 .86 .60	3.74 .91 .45	3.36 .89 .50	2.70 .88 .54			
-.02 .95 .39	-.72 .94 .40	1.48 .94 .42	.67 .95 .36	.75 .95 .35	1.69 .96 .33	1.24 .96 .32	4.19 .93 .42	-.87 .89 .53	-1.33 .87 .57
-.37 .97 .30	-.41 .96 .32	.00 .97 .29	-.22 .97 .28	1.61 .97 .28	1.93 .96 .29	1.90 .97 .28	1.11 .95 .33	.67 .86 .59	.16 .91 .48
.74 .97 .28	.35 .97 .27	.05 .98 .23	-.04 .98 .23	2.26 .97 .25	2.54 .97 .25	.86 .97 .24	.81 .96 .31	-.53 .94 .39	.28 .85 .61
2.34 .97 .28	1.53 .98 .25	1.25 .98 .24	.38 .99 .17	1.88 .98 .21	1.30 .97 .26	-.54 .98 .21	-1.52 .96 .30	.33 .94 .40	-.44 .95 .37
2.84 .97 .27	2.02 .97 .29	.55 .98 .25	-.19 .98 .19	.28 .98 .19	-.13 .98 .23	-1.62 .98 .21	-1.55 .96 .30	-1.61 .95 .35	-.91 .95 .36
1.47 .96 .32	.84 .97 .27	.97 .98 .24	-.37 .98 .18	-.57 .98 .21	-1.29 .98 .21	-2.06 .97 .25	-1.04 .96 .31	-1.04 .96 .32	-.61 .89 .52
.08 .96 .32	.42 .95 .35	.07 .97 .26	-.79 .98 .21	-1.37 .98 .22	-1.10 .97 .27	-.96 .98 .23	-.60 .95 .36	.02 .95 .37	-.95 .85 .61
-.49 .86 .60	.67 .93 .42	.21 .96 .31	-1.00 .97 .26	-.95 .97 .28	-.69 .97 .27	-.01 .97 .28	.73 .95 .36	-.86 .93 .41	-.54 .87 .54
	.87 .95 .40	.08 .93 .41	-.90 .96 .32	.02 .94 .38	.93 .94 .39	1.10 .95 .36	.19 .92 .43	-1.70 .93 .40	-1.62 .85 .57
		-.47 .65 .77	-1.25 .76 .75	.75 .89 .49	2.15 .78 .65	.15 .87 .56	-.62 .85 .57	-1.35 .85 .61	-1.21 .84 .64

35 KM

EXPLANATION:

- CONTOURS SHOWN ARE ZERO VELOCITY PERTURBATIONS
- IN EACH BLOCK, THE UPPER NUMBER IS VELOCITY PERTURBATION (%), THE MIDDLE NUMBER IS THE DIAGONAL ELEMENT OF THE RESOLUTION MATRIX, AND THE BOTTOM NUMBER IS THE STANDARD ERROR FOR THE BLOCK

Seismic velocity structure of the mantle (depth 131-231 km) from teleseismic P-wave residuals for the region of Death Valley groundwater system. From Monfort and Evans, 1982.

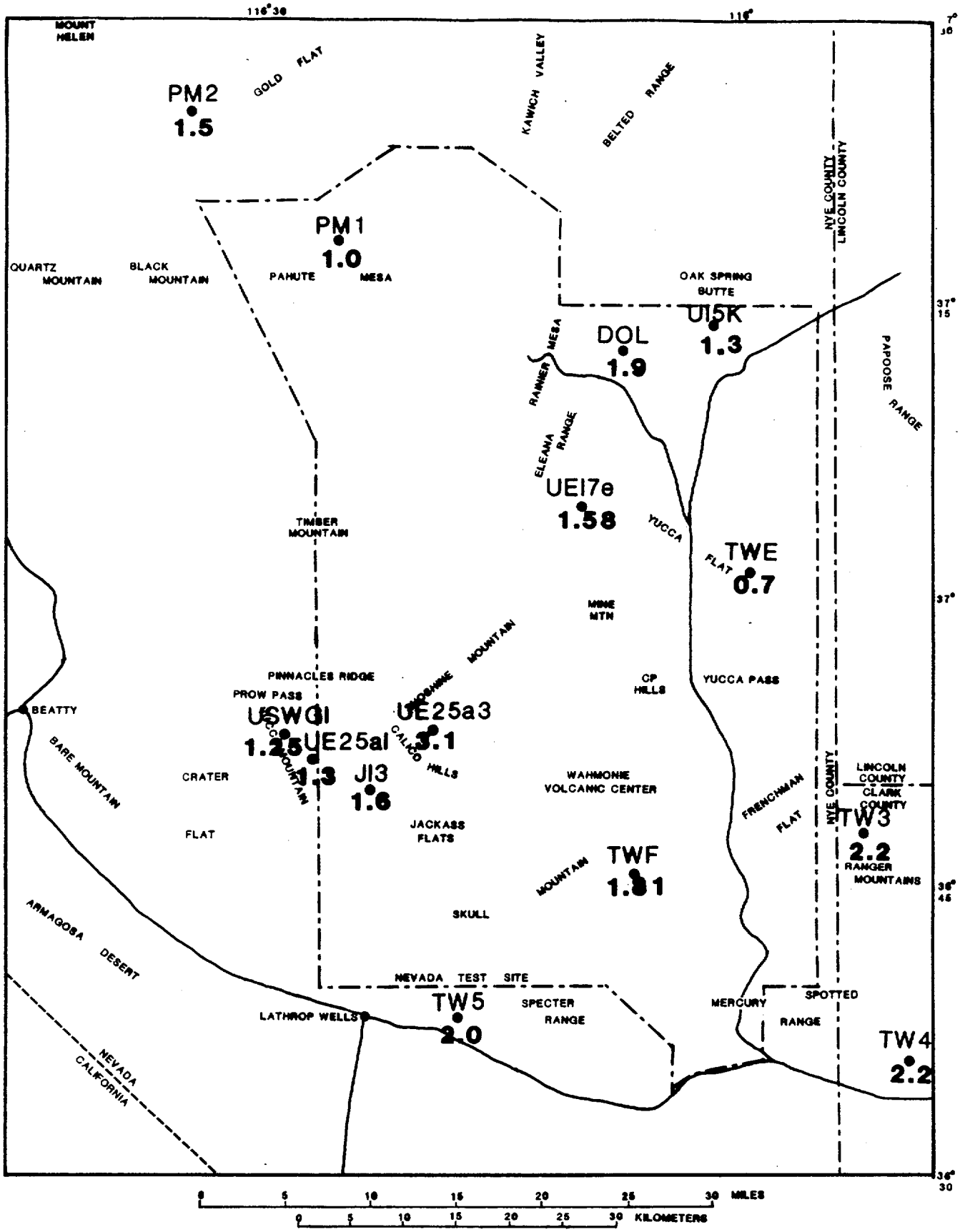

Regional heat-flow values within and adjacent to the Nevada Test Site. From Sass and Lachaenbruch, 1982.

Well	Heat flow		Reference
	mWm^{-2}	HFU	
PM2	63	1.5	Sass and others, 1971
PM1	42	1.0	Sass and others, 1971
DOL	80	1.9	Sass and others, 1971
U15K	56	1.3	USGS unpublished
Ue17e	66	1.58	USGS unpublished
TWE	29	0.7	Sass and others, 1971
J-13	67	1.6	Sass and others, 1971
Ue25a1	54	1.3	Sass and others, 1980
Ue25b1	47	1.1	USGS unpublished
Ue25a3	130	3.1	Sass and others, 1980
USWG1*	52	1.25	Table 2, this paper
TWF	76	1.81	Sass and others, 1971
TW3	92	2.2	Sass and others, 1971
TW5	84	2.0	Sass and others, 1971
TW4	91	2.2	Sass and others, 1971

*Average heat flow in lowermost ~600 m.

Intensities of heat flow at the Nevada Test Site. From Sass and Lachenbruch, 1982.

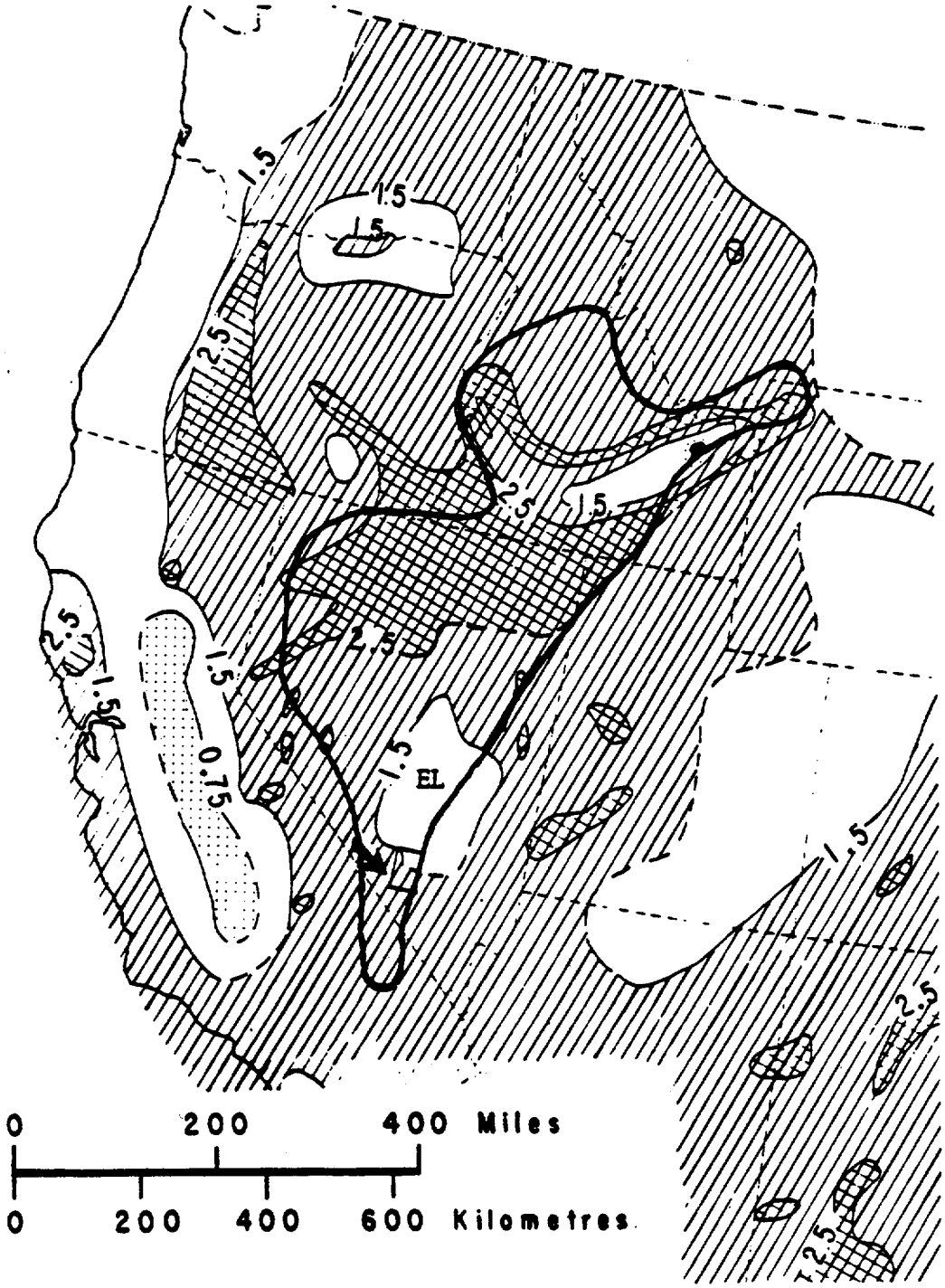

Explanation: (1) Contour lines are heat flow units (HFU); (2) EL is Eureke Low; (3) Arrow indicates outline of the Nevada Test Site; (4) Heavy line is 2.5 HFU contour (Swanberg and Morgan, 1978).

Map of western United States showing intensities of heat flow. From Sass and Lachenbruch, 1982.

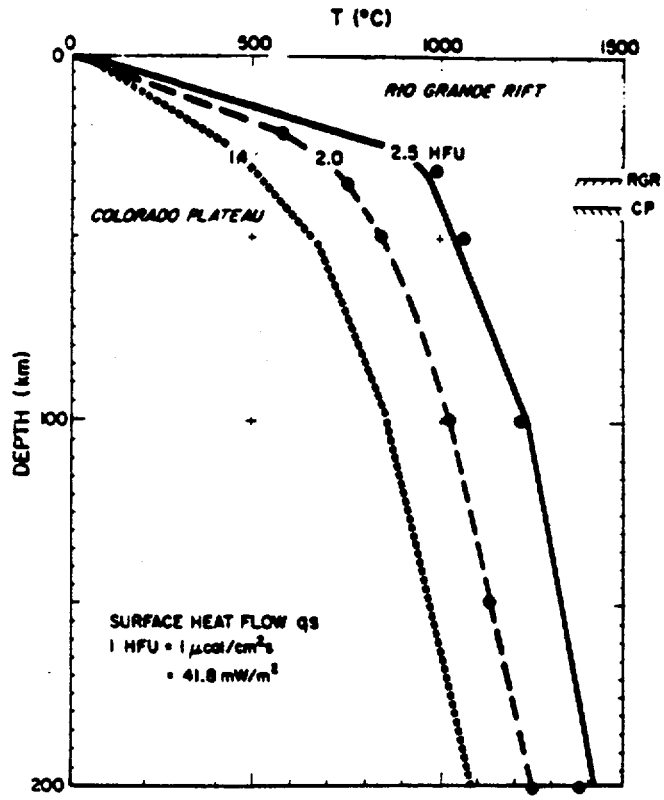

a) TERRESTRIAL TEMPERATURE AS A FUNCTION OF DEPTH AND INTENSITY OF FLUX OF TERRESTRIAL HEAT. FROM BRIDWELL AND POTZICK, 1981.

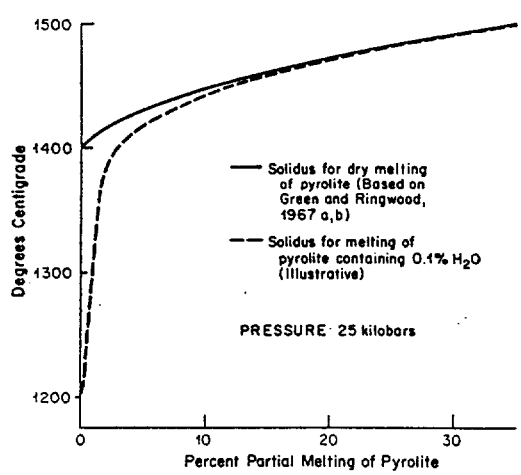

b) DEGREE OF MELTING AS A FUNCTION OF TEMPERATURE IN PYROLITE UNDER ANHYDROUS CONDITIONS AND IN THE PRESSURE OF 0.1% H_2O AT 25kb. FROM RINGWOOD, 1969.

Terrestrial temperature - a perspective.

Tectonic Zone	Number of Measure-ments	Arith-metic Mean, HFU	Range of Values, HFU
Precambrian folded regions	49	0.96	0.61–1.8
Shields	11	0.86	0.61–1.4
Platforms	38	0.99	0.70–1.4
Paleozoic folded regions	113	1.6	0.6 –2.6
Caledonian folded regions	11	1.1	0.8 –1.5
Hercynian folded regions	102	1.6	0.6 –2.6
Cis-Caucasus	32	1.6	0.91–2.6
Crimea	13	1.4	1.0 –1.8
Western Europe	57	1.7	0.60–2.6
Cenozoic folded regions	82	1.7	0.65–3.3
Foredeeps	33	1.2	0.65–1.9
Foredeeps, not including Cis-Alpine foredeep	30	1.12	
Folded mountain structures	28	1.8	1.2 –2.7
Cenozoic volcanic areas	21	2.1	1.4 –3.3

A) HEAT FLOW DATA FROM EURASIAN CONTINENT. FROM LUBIMOVA AND POLYAK, 1969.

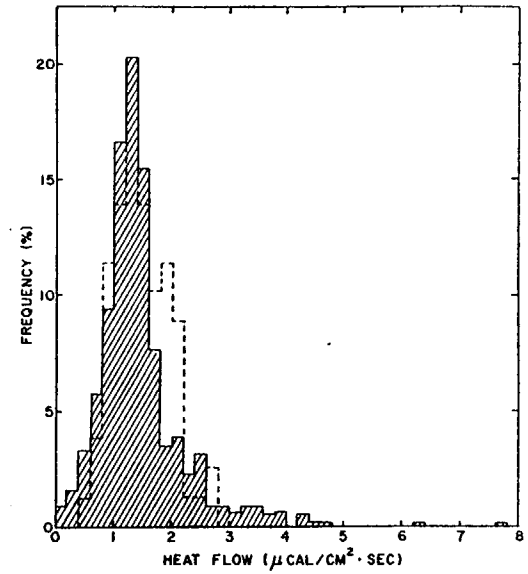

B) HISTOGRAM OF OCEANIC HEAT FLOW DATA. FROM VON HERZEN AND LEE, 1969.

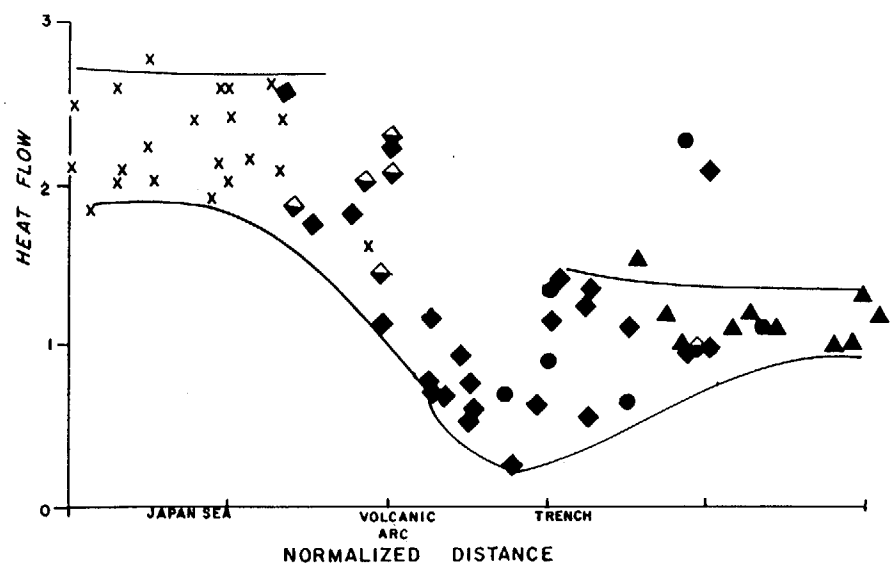

C) HEAT FLOW ACROSS THE JAPAN TRENCH. FROM ANDERSON, 1980.

Terrestrial heat flow - a perspective.